AD706865

MDC TR-70-11

AIR FORCE MISSILE DEVELOPMENT CENTER
TECHNICAL REPORT

DEVELOPMENT OF MEASURING TECHNIQUES FOR ROCKET SLEDS

William E. Baker
John C. Gustafson

Distribution of this document is unlimited.

DDC
RECEIVED
JUN 3 1970
C

APRIL 1970

HOLLOMAN AIR FORCE BASE
NEW MEXICO

Reproduced by the
CLEARINGHOUSE
for Federal Scientific & Technical
Information Springfield Va. 22151

This document has been approved for public release and sale; its distribution is unlimited.

170

MDC-TR-70-11

DEVELOPMENT OF MEASURING TECHNIQUES FOR ROCKET SLEDS

William E. Baker
and
John C. Gustafson

Department of Engineering
The University of New Mexico

TECHNICAL REPORT MDC-TR-70-11
APRIL 1970

Distribution of this document is unlimited.

Publication of this report does not constitute Air Force approval of the report's findings or conclusions. It is published only for the exchange and stimulation of ideas.

TYLER A. REDFIELD, Colonel, USAF
Director of Test Track

AIR FORCE MISSILE DEVELOPMENT CENTER
AIR FORCE SYSTEMS COMMAND
HOLLOMAN AIR FORCE BASE, NEW MEXICO

DISTRIBUTION

Defense Documentation Center Cameron Station Alexandria, Virginia 22314	20
Air University Library Maxwell AFB, Alabama 36112	1
ASD (ASMD) Wright-Patterson AFB, Ohio 45433	1
AFFTC (FTBPP-2) Edwards A. , California 93523	1
AFETR (ETLIG-3) Patrick AFB, Florida 32925	1
AFSWC (SWLPR) Kirtland AFB, New Mexico 87117	1
AEDC (AET) Arnold AF Station, Tennessee 37389	1
APGC (PGGT) Eglin AFB, Florida 32542	1
ESD (ESTI) L. G. Hanscom Field Bedford, Massachusetts 01730	1
SAMSO (SMSDI-STINFO) AF Unit Post Office Los Angeles, California 90045	1
HQ AFSC (SCAP)	1
RRD (Documents Service Center)	3
MDG	1
MDNH	1

TABLE OF CONTENTS

	Page
ABSTRACT	iii
LIST OF FIGURES	iv
LIST OF TABLES	vi
I INTRODUCTION	1
II FORCE MEASUREMENT ON THE CHAPARRAL SLED	2
1. PROBLEM STATEMENT	2
2. MODEL STUDY	8
2.1 Theory	9
2.2 Model Design and Construction	15
2.3 Model Test Set-Up	18
2.4 Model of Original Structure	22
2.5 Modified Model Studies	25
3. PROTOTYPE INSTRUMENTATION - FORCE MEASUREMENT	37
3.1 Description	37
3.2 Vertical Calibration	45
3.3 Off-Axis Loading	70
3.4 Comparison with Model Tests	77
4. PROTOTYPE INSTRUMENTATION - TEMPERATURE MEASUREMENT	78
4.1 Description	78
4.2 Calibration	82
5. CONCLUSIONS AND RECOMMENDATIONS	
III STUDY OF THE "TECH-2" SLED TRANSDUCERS	85

TABLE OF CONTENTS (continued)

		Page
IV	INSTRUMENTATION OF THE TRANSDUCER FOR THE MODULAR MONORAIL SLED	101
V	DYNAMIC RESPONSE OF A STRAIN-GAGED FORCE LINK	117
	1. INTRODUCTION	117
	2. THEORY	119
	3. PROCEDURE	125
	4. RESULTS	128
	5. CONCLUSIONS	143
VI	A NUMERICAL DIFFERENTIATION TECHNIQUE	145

ABSTRACT

Work is described which was undertaken to develop and improve techniques for measuring forces acting on rocket sleds. Several specific projects have been completed. The Chaparral sled was instrumented and appropriate calibration made for measurement of vertical forces acting on the sled by the slipper. Resistance thermometers were also applied for measurement of temperature in the vicinity of the gage. A study of the accuracy of the Tech-2 sled transducer was made, and revised instrumentation applied in order to improve the accuracy. A force measuring system utilizing strain gages was developed for the modular monorail force transducer. Analytical studies of the response of a simple strain-gaged force link were made in order to better understand the behavior of the sled transducers under dynamic loading. The last area of work described is that of a highly accurate technique of differentiating analog data.

LIST OF FIGURES

Figure		page
1	Front Slipper Assembly of Chaparral Sled	3
2	Sled During Run	5
3	Slipper Dimensions	7
4	Model Dimensions and Loads	19
5	Model Test Set-Up	20
6	Model Under Test	24
7	General State of Strain Induced in the Model	26
8	Two Through-Hole Models	28
9	Model of Final Design	32
10	Dimple Dimensions and Gage Locations	33
11	Schematic of Wiring Path	42
12	Instrumented Structure	43
13	Vertical Calibration	44
14	Response Curve	46
15	Second Loading Jig	51
16	Loading History for Final Calibration	52
17	Off-Axis Loading Frame	71
18	Off-Axis Load Definitions	72
19	Bridge Circuit	80
20	Temperature Circuit Calibration Curves	83
21	Tech-2 Transducer in Loading Fixture	89
22	Loading Conditions for the Tech-2 Transducer	90
23	Revised Strain Gage Instrumentation for One Unit of Tech-2 Transducer	96

LIST OF FIGURES (continued)

Figure		Page
24	Modular Monorail Force Transducer	103
25	Loading Fixture for Modular Monorail Transducer	104
26	Load Definitions for Modular Monorail Transducer Tests - Cross-track components and moment	105
27	Load Definitions for Modular Monorail Transducer Tests - Along-the-track components	106
28	Description of Force Link	120
29	Characteristic Plane	123
30	Ramp Function Pulse	126
31	Half Sine Pulse	126
32	Ramp Function Results: $\tau = 1.0\ \ell/c$	129
33	Ramp Function Results: $\tau = 5.0\ \ell/c$	130
34	Ramp Function Results: $\tau = 10.0\ \ell/c$	131
35	Half Sine Function Response: $\Gamma = 1.0\ \ell/c$	132
36	Half Sine Function Response: $\Gamma = 2.0\ \ell/c$	133
37	Half Sine Function Response: $\Gamma = 5.0\ \ell/c$	134
38	Half Sine Function Response: $\Gamma = 10.0\ \ell/c$	135
39	Half Sine Function Response: $\Gamma = 20.0\ \ell/c$	136
40	Harmonic Forcing Function Response: $\Gamma = 1.0\ \ell/c$	137
41	Harmonic Forcing Function Response: $\Gamma = 2.0\ \ell/c$	138
42	Harmonic Forcing Function Response: $\Gamma = 5.0\ \ell/c$	139
43	Harmonic Forcing Function Response: $\Gamma = 10.0\ \ell/c$	140
44	Harmonic Forcing Function Response: $\Gamma = 20.0\ \ell/c$	141

LIST OF TABLES

Table		Page
I	Failure Loads of Original Structure	25
II	Comparison of Modified and Unmodified Structure	34
III	Calibration for 20,000 Pound Maximum Force	54
IV	Calibration for 30,000 Pound Maximum Force	57
V	Calibration for 40,000 Pound Maximum Force	61
VI	Calibration for 50,000 Pound Maximum Force	64
VII	Summary of Vertical Calibration	67
VIII	System Calibration Data	68
IX	Results of Off-Axis Load Tests	73
X	Along-the Track Loading	76
XI	Calibration of the Temperature Measuring Circuitry	85
XII	Data and Results for Initial Tests on Tech-2 Transducer	88
XIII	Calibrate Resistor Data on Tech-2 Transducer - Initial Instrumentation	95
XIV	Data and Results for Tech-2 Transducer with Revised Instrumentation	97
XV	Calibrate Resistor Data on Tech-2 Transducer - Revised Instrumentation	100
XVI	Data Results of Load Tests on Modular Monorail Transducer	107
XVII	Calibrate Resistor Data on Modular Monorail Transducer	116
XVIII	Program to Find the First and Second Derivative of Digitized Graphical Data	147
XIX	Polytable for Curve Fitting	151

LIST OF TABLES (continued)

Table		Page
XX	Example 1 on Use of Numerical Differentiation Technique	153
XXI	Example 2 on Use of Numerical Differentiation Technique	155
XXII	Example 3 on Use of Numerical Differentiation Technique	157

BLANK PAGE

I INTRODUCTION

The objective of the work undertaken for this contract was to develop techniques for measuring forces acting on rocket sleds, either through instrumentation of the sled itself or through development of special force transducers, to improve data reduction techniques for data obtained from sled runs, and to conduct analytical studies as required in accomplishing the above. This objective has been accomplished through studies of special problems as considered appropriate by the contracting agency, and conduct of the necessary development work. Each of the following sections of this report covers one of the separate projects undertaken on this contract.

II FORCE MEASUREMENT ON THE CHAPARRAL SLED

1 - PROBLEM STATEMENT

The specific problem for this phase of the contract was to develop a method of instrumenting the front slipper support structure of the Chaparral rocket sled shown in Figure 1 to measure the vertical component of force transmitted by the slipper to the sled body during a test run. A knowledge of the source of the forces acting and their characteristics is helpful in understanding the scope of this problem.

The forces which act on the sled body through the slipper assembly are the result of the sled motion. The sled motion is predominately an along-the-track acceleration period followed by a deceleration period. The forces acting on the sled during a run include thrust forces, braking forces, aerodynamic forces, and forces exerted by the track on the sled. These forces contain oscillatory as well as sustained components; consequently, sled vibration occurs. Minor imperfections in the sled track, such as small dips, curves, and surface irregularities, combined with the high velocity of the sled contribute to the oscillatory forces.

The particular force component to be measured is the vertical component acting on the sled body at the front slipper. A study of Figure 1 shows that this will not necessarily be the force acting on the slipper by the track,

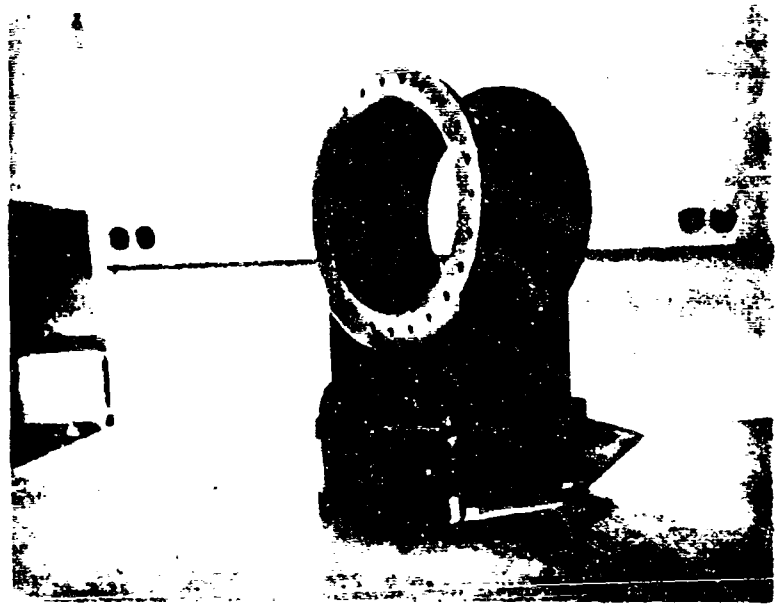

Figure 1. Front Slipper Assembly of Chaparral Sled.

since there will be a downward aerodynamic force on the wings of the slipper. The force transmitted to the sled body will be the vector sum of the track force and the aerodynamic force on the wings.

Another characteristic of the forces on the sled is that of side loads. These side loads on the sled body are caused by the air resistance, which may not be symmetrical, any bias due to the thrust load, and forces from the wind. The instrumentation applied to the structure to measure the vertical forces (in a sled-fixed coordinate system) should be insensitive to the side loads.

The friction between the slipper and track and between the air and sled causes considerable heat. Figure 2 illustrates the harsh environment to which the slipper and exposed frontal area of the sled components are subjected. However, due to the brevity of the sled run, the environment to which the instrumentation is subjected is somewhat less damaging, since there is a time lag for the heat to be conducted to the area instrumented. Preliminary tests indicate the maximum temperature to which the possible location of instrumentation will be subjected is 1100°F, but this temperature is reached after the run, and it is not required that the system be operable at this temperature. The temperature at which it must be operable is unknown but experience indicates that it should be designed for operation at the highest temperature possible.

Figure 2. Sled During Run.

The requirements for the instrumentation for this particular problem may be summarized as follows:

1. The instrumentation should give sufficient output for use with standard recording and telemetry systems currently in use by the appropriate test facility, for a maximum expected load of 50,000 lb.
2. The instrumentation should be insensitive to cross track and along-the-track components of force.
3. Any modification to the structure must not appreciably weaken it.
4. The instrumentation should be capable of withstanding temperature of 1100°F without damage.

Figure 3 shows the dimensions of the structure which are pertinent to this work.

This developmental work done in the course of this investigation included the following steps:

1. A model study to determine the most feasible method of instrumenting the assembly.
2. Instrumentation of the slipper assembly.
3. Static calibration and off-axis load tests.
4. Determination of error limits for the measurement method developed.
5. Development of temperature measuring technique for measuring the temperatures in the vicinity of the straingages.

The following sections of this report describe the work done on the above items.

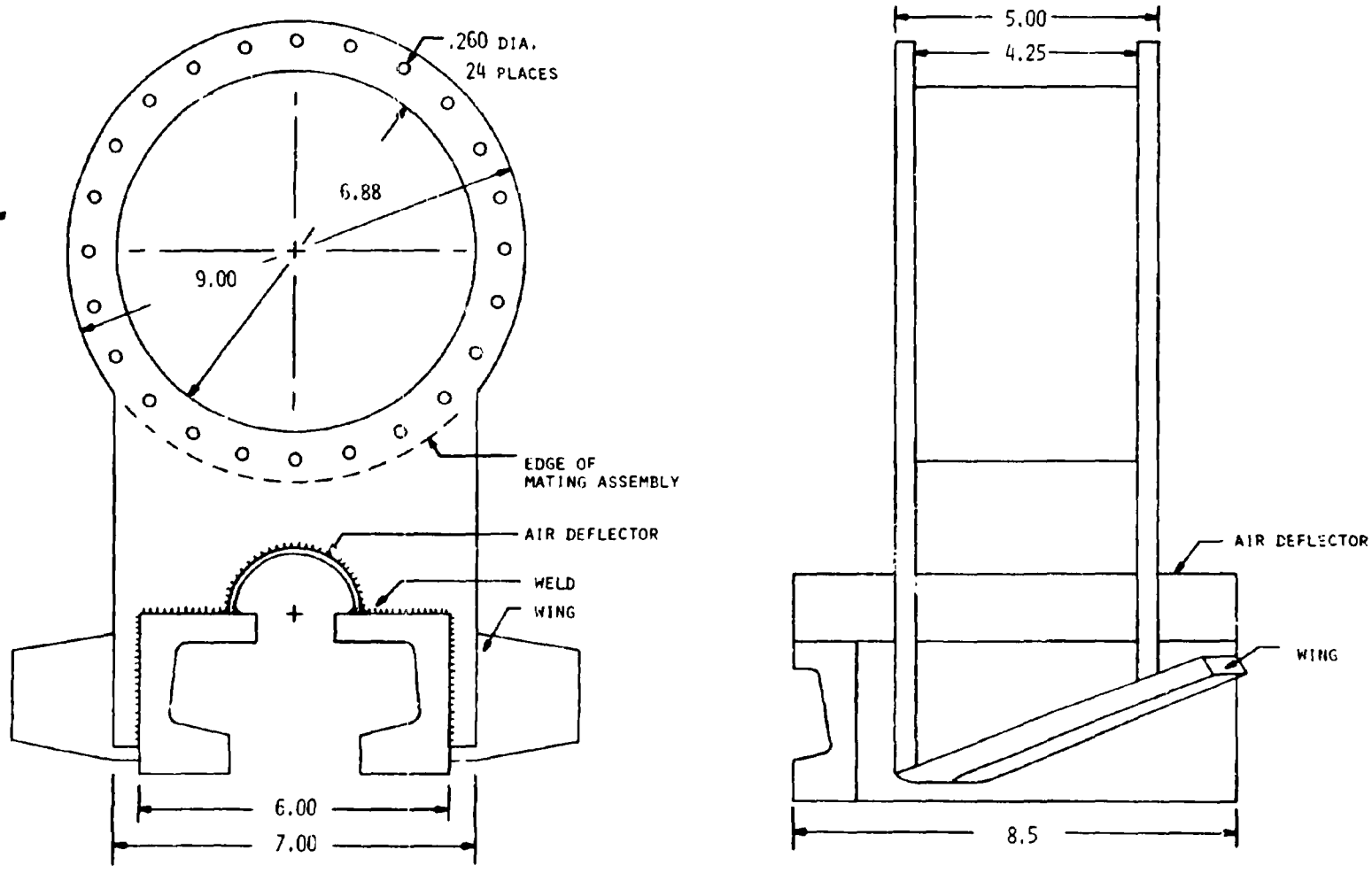

FIGURE 3 SLIPPER DIMENSIONS

2 - MODEL STUDY

A model study was used in the initial phase of the development work on this project. There were several reasons for this. The manner in which the load is imposed on the slipper assembly during use varies substantially in use. As seen in Figure 1, the slipper does not fit tightly over the sled track, causing the loading condition at the track to vary with the position of the slipper on the track. In use the slipper may slide as much as 3/16 inch from side to side and the slipper may also move 3/16 inch relative to the track in the vertical direction. If the slipper assembly itself were used in the development work, many physical and practical difficulties would be encountered. The size and weight of the unit make handling of it cumbersome. In addition, testing equipment needed would be equally cumbersome to handle. Any modifications to the slipper assembly; if unacceptable, would necessitate scraping the modified unit. The cost of fabricating one assembly is quite high, chiefly because of the amount of machining involved. The wide variation in the manner loads are imposed on the unit, due particularly to the fit of the track and the geometric complexity of the structure involved, indicates that a mathematical investigation of the problem would not be suitable. The type of information needed in development work indicated that photoelastic models would be the most useful.

The use of a model allows modifications of the structure to be easily produced and studied. Comparison of strengths of the modified and unmodified models is an easy matter.

Photoelasticity is a whole field method of study and the effect of any modification can be evaluated in terms of the entire structure not just the locations of the modification. If the modification proves to be unacceptable, the model must be scrapped but the cost involved here is small compared to the cost of scraping a prototype assembly. Equipment needed in a model study need not be as elaborate as would be needed in prototype studies.

After making needed simplifying assumptions a model was designed. A technique for building the model was developed and all the needed testing equipment constructed. A model of the original structure was thoroughly studied and information obtained in this work was used as a basis for modifications to the model. These modifications were made and studied to find a suitable method of instrumenting the structure to produce the desired transducer.

2.1 Theory

Since strain gages were to be used as sensors, a knowledge of the relationships between the strain and forces induced in the model and those of the prototype was needed. The significant variables involved and the symbols used to define them are as follows:

σ, the stress at any point in the structure

ε, the strain at any point in the structure

P, the applied load on the element of interest

t, a typical unit of length

E, the modulus of elasticity of the material

μ, Poissions ratio of the material

The relation between the independent and dependent variables may be written as follows:

$$\sigma = \phi_1(P,t,E,\mu)$$
$$\varepsilon = \phi_2(P,t,E,\mu) \qquad (2.1.1)$$

In non-dimensional form the above relationships are:

$$\left(\frac{\sigma}{E}\right) = \phi_3 \left(\frac{P}{Et^2}\right),\mu)$$
$$\varepsilon = \phi_4 \left(\frac{P}{Et^2}\right),\mu) \qquad (2.1.2)$$

The design or operating conditions are:

1. Geometric similarity
2. $\left(\frac{P}{Et^2}\right)_m = \left(\frac{P}{Et^2}\right)_p$ or

$$P_m = P_p\left(\frac{E_m t_m^2}{E_p t_p^2}\right) \qquad (2.1.3)$$

3. $\mu_m = \mu_p$ (2.1.4)

The subscripts m and p refer to the model and prototype respectively.

The prediction relationships between the model and prototype are:

1. $\sigma_p = \sigma_m \frac{E_p}{E_m}$ (2.1.5)
2. $\varepsilon_p = \varepsilon_m$ (2.1.6)

A model constructed using the above design conditions, particularly geometric similarity, would be difficult to make. It was desirable to simplify the construction of the model and still get reliable results. To do this, the following assumptions were made.

The aerodynamic loading induced by the wings on either side of the slipper, shown in Figure 1, was assumed to be transmitted to the sled body in an identical manner as the same magnitude of load would be transmitted if it were induced by the sled track. Consequently, the wings were eliminated from the model, and all force applied through the track.

The major assumption used in the design of the photoelastic model is that the behavior in the place of interest, i.e., a plane normal to the track, may be determined by a model of the support structure composed of only one vertical support plate rather than two as in the actual structure. This simplification of the model eliminates its use for along-the-track loads.

The effect of the slipper material away from the vertical support plate in the track direction has only a small effect on the strain induced in the plate. However, the length of the slipper would complicate model construction. Therefore, the length of the slipper which was considered to affect the strain field in one vertical plate was 3 inches.

It was necessary to further distort the model in the along-the-track direction because the thickest photoelastic plastic available from manufacturer stock is 0.250 inch and the model of the vertical plate was to be 0.375 inch. To compensate for

this distortion, it was only necessary for the applied load, P, to produce similar stresses. Further, this magnitude of applied load in the model must be such that the work was done in the elastic range of the photoelastic material.

In order to make the necessary correction, the prediction equation is placed in a different form by combining Equations 2.1.3 and 2.1.5. The result is

$$\sigma_p = \sigma_m \frac{P_p t^2_m}{P_m t^2_p} \qquad (2.1.7)$$

The primary purpose of this model is its response to tensile loading so the stress is dependent on the tensile area. This tensile area is the product (Lxh) where L is the typical length dimension in the place normal to the track (this requires complete geometric similarity in this plane), and h is the along-the-track dimension. The product (Lxh) replaces t^2 in Equation 2.1.7. The stress prediction equation for the simplified model now becomes:

$$\sigma_p = \sigma_m \frac{P_p h_m L_m}{P_m h_p L_p} \qquad (2.1.8)$$

A similar analysis of the strain prediction equation results in the predicted strain for the simplified model being

$$\varepsilon_p = \frac{\varepsilon_m P_p E_m h_m L_m}{P_m E_p h_p L_p} \qquad (2.1.9)$$

The model is full scale in the plane normal to the track so L_m/L_p is unity. The along-the-track scale factor is then

h_m/h_p, this factor must also be applied to the slipper section of the model.

The three inch dimension of the slipper (before scaling by h_m/h_p) was further scaled to make construction and handling of the model easier. This scaling was accomplished by the use of a more rigid material for the slipper section than that used for the vertical support plate. The scaling reproduced the rigidity in bending of the slipper by an appropriate length of the more rigid material. The resulting expression for the slipper length dimension, d, is

$$d_m = \frac{d_p E_m h_m}{E_s h_p} \qquad (2.1.10)$$

The third design condition ($\mu_m = \mu_p$) was neglected because the difference in the values μ's was small.

Needed relationships for the photoelastic study are

$$\sigma_1 - \sigma_2 = \frac{K_\sigma n}{h} \qquad (2.1.11)$$

$$\tau = \frac{K_\sigma n}{2h} \qquad (2.1.12)$$

$$\sigma_f = \frac{K_\sigma n}{h} \qquad (2.1.13)$$

$$n = (\sigma_1 - \sigma_2) \frac{h}{K_\sigma} \qquad (2.1.14)$$

where σ_1 and σ_2 are the principal stresses

τ is the maximum shearing stress

K_σ is the stress optical coefficient

n is the observed fringe order

h is the model thickness

σ_f is the stress value at a free boundary.

Equation 2.1.8 in terms of the shearing stress, τ, is

$$\tau_p = \tau_m \frac{P_p h_m L_m}{P_m h_m L_m} \qquad (2.1.15)$$

Substituting equation 2.1.15 into 2.1.12 the following relationship is obtained between the shearing stress of the prototype and the fringe order observed in the model

$$\tau_p = \frac{K_\sigma n}{2h_m} \frac{P_p}{P_m} \frac{h_m}{h_p} \frac{L_m}{L_p} \qquad (2.1.16)$$

For purposes of comparison of strength of the original and modified structures, it will be helpful to define what will be considered failure of the structure. The slipper structure is constructed of annealed 4130 steel; and this material will be assumed to yield according to the maximum shearing stress theory of failure. A shearing stress at any point greater than the yield of the material in pure shear will be considered as the failure point. Further, since the model has only two dimensional similarity and the method of investigation is photoelasticity, failure will be based on maximum shearing stress in the plane normal to the light field, i.e., the plane of geometric similarity.

2.2 Model Design and Construction

The photoelastic plastic must be selected such that when loaded the resultant model will produce a fringe order which will allow sufficient resolution for this application. The maximum load which can conveniently be applied to the resultant model with available equipment is about 350 pounds. Assuming the model of the unmodified assembly to be in a uniaxial state of strain under this load and using equation 2.1.9, the expected fringe order, n, is

$$n = \frac{350}{h\ W}\frac{h}{K_\sigma}$$

$$= \frac{350}{WK_\sigma} \qquad (2.2.1)$$

where W, the model width, is seven inches. The relationship between n and K_σ becomes

$$n = \frac{350}{7K_\sigma}$$

$$n = \frac{50}{K_\sigma} \qquad (2.2.2)$$

A fringe order of one would be acceptable in equation 2.2.2 because no allowance for stress concentrations has been made and this will increase the order, possibly greatly so. In view of this, a stress optical coefficient of 50 psi-in/fringe or less would be acceptable.

The photoelastic material selected should meet the above criteria as well as be sufficiently rigid that the deformations produced during model testing are not so great as to void the validity of the model. Also, it is desirable that the material be easily machined and that it exhibit a minimal time edge effect.

With these requirements in mind, the photoelastic material selected was PSM-1 plastic made by Photoelastic, Incorporated. It has a stress optical coefficient of 40 psi-in/fringe and a modulus of elasticity of 340,000 psi. The material thickness used was 0.250 inches. Other properties are given in the appendix. Equation 3.1.5 is used to determine some of the requirements of the model slipper material selected.

$$d_s = \frac{d_p E_m L_m}{E_s L_p} \qquad (2.1.5)$$

Substituting the parameter of the plastic selected and requiring that the resultant along-the-track slipper dimension be approximately 0.75 inches for convenience, this relationship becomes

$$0.75 = \frac{(3)(340,000)(0.25)}{E_s \; 0.375}$$

or

$$E_s = 9.08 \times 10^5 \text{ psi} \qquad (2.2.3)$$

The material selected for the slipper section of the model must have a modulus of elasticity of approximately $9X10^5$ psi. The port on of the model to be constructed from this material is geometrically complex as seen in Figure 3. This portion must also be bonded to the photoelastic material. Therefore, the material selected must either be easily cast to dimension or be easily machined to dimension because several models are needed.

Several different plastics and epoxies were investigated before the final selection was made. The material which was used for model construction was aluminum filled epoxy. This material has a modulus of elasticity of approximately 10^6 psi, is very easily machined and easy to cast to dimension for parts of this size. Further properties and details of the source are given in the Appendix A. Equation 2.1.5 requires a slipper length in the model for this material of 0.672 inch.

It was difficult to obtain an acceptable bond between the machined plastic portion of the model and the epoxy slipper section. Tests were conducted using scrap pieces of plastic and epoxy to develop a bonding method for these materials. The photoelastic plastic selected for use had a polyester base. Bonding of polyester based plastics to dissimilar materials is a problem the plastics industry has not, as yet, suitably solved. Plastic manufacturers had no recommendations of how to produce this bond.

Several different room cure epoxies were tested; all the resulting bonds were very strong in shear and all bonds failed at very low tensile stress values at the surface of the photo-

elastic plastic. Oven cure epoxies could not be used as the curing process introduced residual fringes in the plastic. Standard techniques to relieve these residual fringes proved unsuccessful in this case.

This difficulty in bonding was finally overcome by use of a bond having the cross-section of a vee-groove weld, and the use of a room cure epoxy. The bond was formed by beveling the flat edge of the part and filling the resulting groove with the bonding agent. When completed, the bonding agent at the interface of the plastic surface is subjected to predominately shear stresses. This was important since all bonding agents tested were found to be strongest in shear. The entire surface of the edge was roughened to further strengthen the bond. The epoxy used as a bonding agent was the aluminum filled epoxy used for the slipper section, with the oven cure hardener replaced by a room temperature cure hardener.

The dimensions of the unmodified model are shown in Figure 4. In later sections photographs of several of the models tested will be presented. The model thus fabricated was greatly simplified when compared to the actual slipper assembly, but was thought to be adequate for this study provided its limitations are kept in mind while interpreting the experimental results obtained from it.

2.3 Model Test Set-Up

Figure 5 shows the equipment used in the model testing. The circular polariscope has a 10 inch field. All photoelastic data was recorded using the Polaroid camera shown. Both the

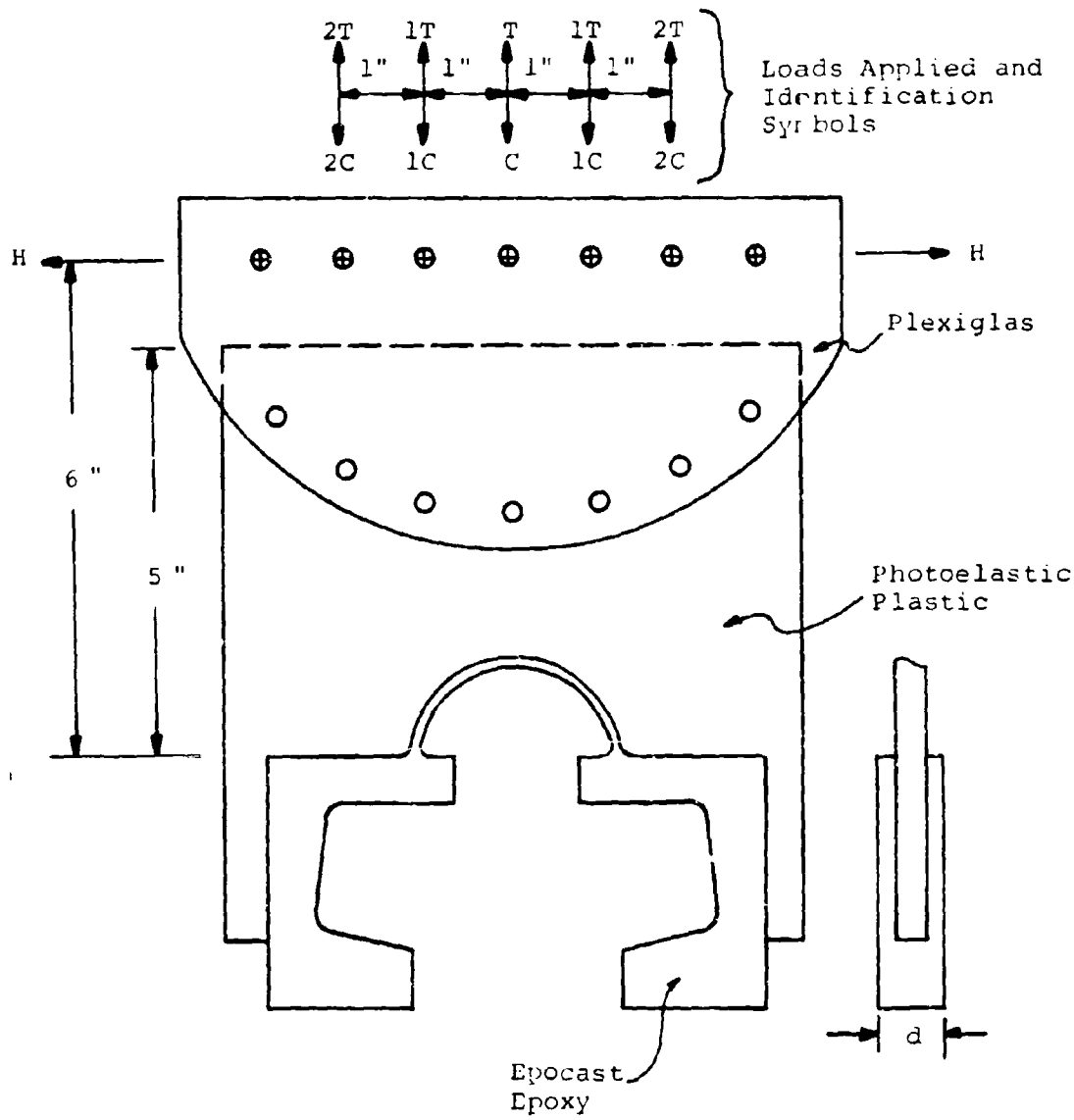

Figure 4 Model Dimensions and Loads

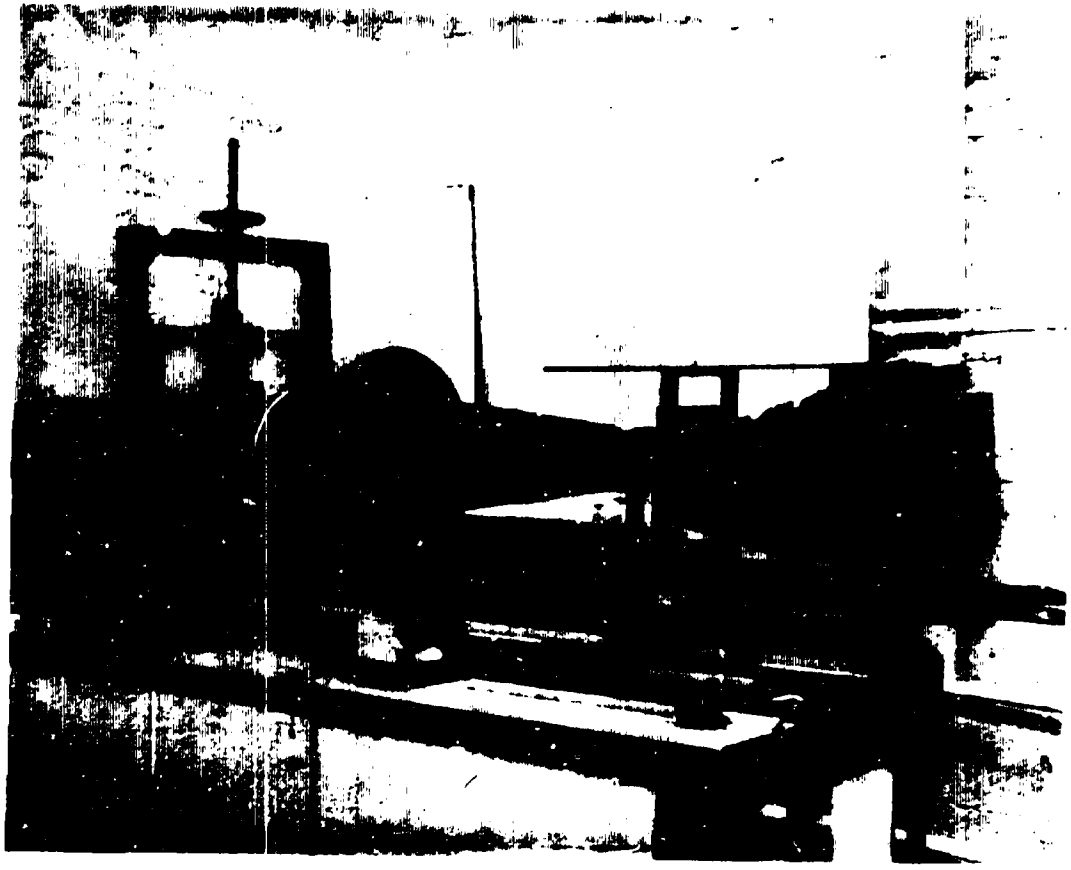

Figure 5. Model Test Set-Up.

horizontal and vertical loads applied to the model were produced using weights and a lever system. Figure 4 defines the loads applied to all models.

The loading at the lower end of the model was accomplished by the use of a short section of the actual sled track. The loading at the top of the model was accomplished at the beginning of this study, by sandwiching the plastic between two metal plates. Later, the sandwiching was done with metal plates using the same bolt circle as used to fasten the sled fore and aft bodies on. In the final stages of study, the metal plates were replaced with plexiglas plates which more closely models the rigidity of the sled parts.

Application of the compressive loads on the model caused trouble. In compression, the models tended to buckle and this introduced extraneous fringes. Several different methods of transmitting the load to the model were attempted. The best of these was transmission of the load to the model at two points approximately two inches apart in a manner similar to the standard technique used in applying a constant moment to a beam under test Along with this loading technique extreme care was needed in placing the model in the loading frame. Because of this difficulty, the compressive data was not as heavily weighted as the data obtained from the tensile loading.

The following section is a discussion of all the models studied with particular emphasis on the final design and the testing which lead to this design concept.

2.4 Model of Original Structure

As previously stated, the first step in this investigation was to thoroughly test the model of the original structure. There were two purposes for this series of tests. First: the original strength of the structure under various loads was needed so that the weakening caused by any stress raisers introduced could be evaluated. With this information it can be determined if requirement 3 of the resultant transducer is met, i.e., that any modifications to the original structure do not appreciably weaken it. Second: modifications to the structure were guided by the results of this first series of tests.

The first model constructed is shown in the loading frame in Figure 5. The fringe patterns produced during testing of this model indicated that bolt patterns of the mating fore and aft bodies of the sled and the rigidity of these parts could effect the stress distribution in the vertical plates of the slipper assembly. The model was then modified so that the bolt pattern of the sled assemblies was used in the loading of the model. The fringe patterns obtained from this model were significantly different from those obtained from the model of Figure 5. The dimensions of this model are given in Figure 4.

Both plexiglas and aluminum loading plates were used at the top of the model to transmit the load to the model. The aluminum plates were approximately 3 times more rigid than the plexiglas plates. There was not a significant difference in the fringe patterns obtained from the two different loading methods. This indicates that the rigidity of the fore and aft

bodies of the sled should not effect the sensitivity of the resultant instrumentation. Figure 6 is a photograph of the fringe pattern obtained when the model was loaded to 336 pounds in pure tension. The numbers on this photograph are the fringe orders observed at the location of the numbers. It is seen that the maximum fringe order is approximately four and is just left of the center in the photograph. This load condition will be used as an example of how the failure loads of the original structure were obtained.

To interpret this data equation 2.1.11 is used,

$$\tau_p = \frac{K_\sigma n\ P_p}{2\ h_m P_m} \frac{L_m h_m}{L_p h_p} \qquad (2.1.11)$$

Substituting values previously given one obtains

$$\tau_p = \frac{(40)(4)(P_p)(1)(.25)}{(1)(.25)(336)(1)(.375)}$$

$$\tau_p = 0.60\ P_p \qquad (2.4.1)$$

The yield stress of the slipper material is 130,000 psi. This is equivalent to a shearing yield stress of 65,000 psi. Using this value of shearing stress in equation 2.4.1, the maximum allowable force in the prototype, P_{pmax}, is obtained.

$$P_{pmax} = \frac{65,000}{.60}$$

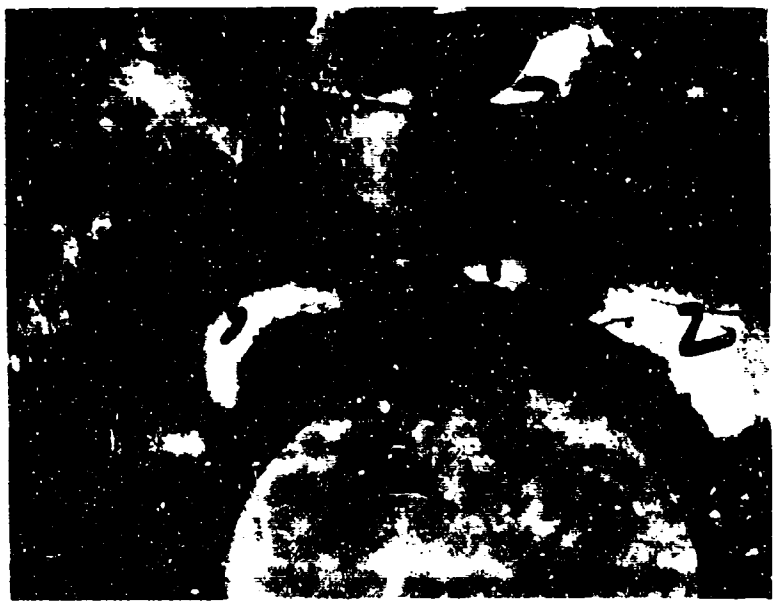

Figure 6. Model Under Test.

P_{pmax} = 108,000 pounds

This is the maximum vertical force that one of the two vertical supports plates can support before yield. If it is assumed that each of the two support plates will carry an equal portion of the load applied to the structure, the maximum allowable load is twice the above.

Using the above method of data reduction and the load definitions of Figure 4, the following table of failure loads of the original structure was obtained.

Table I. Failure Loads of Original Structure

Load Number	T	1T	2T	C	1C	2C	H
Failure Loads--Pounds	216K	214K	172K	214K	--	172K	34K

2.5 Modified Model Studies

Study of the original model indicated the strongest section for most loading conditions of the original structure was on the vertical axis of symmetry of the structure in the area directly above the air deflector (Figure 3). This study also showed the weakest section occurs at or very near the weld around the air deflector at two locations. These are located approximately at 45° from the vertical axis of symmetry, (Figure 6). It was desirable to instrument the weakest location of the structure with the strain sensors in order to produce the maximum possible signal from the resultant instrumentation for a given load. However, these locations were situated such that

that they could not be instrumented with sensors due to the physical limitations of the geometry at these locations. Therefore, it was necessary to consider other positions.

The original study also showed that the state of strain in the model with vertical and horizontal loads is approximately as indicated in Figure 7 below.

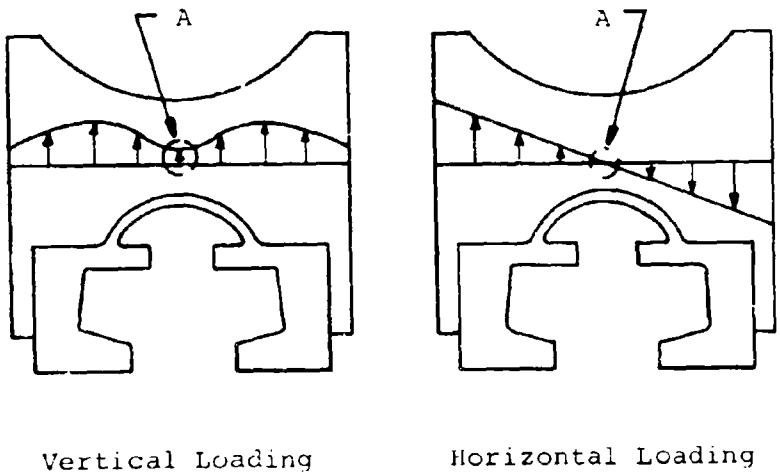

Figure 7 General State of Strain Induced in the Model

The first approach to the design of a stress raiser to meet the requirements was to use a through hole in the support structure. Point A of Figure 7 was selected as the first location to modify for installation of the sensors. This location was chosen for four reasons. First, it was the strongest section of the structure; therefore, modification to this region would have a minimal effect on the strength of the structure. Second, for vertical loading the strain induced in this location was linear with the applied vertical load. Third, for sensors symmetrically located in this area, the signal due to horizontal loading would be cancelled when these sensors were connected in an appropriate bridge circuit. Fianlly, if the sensors could have been located here, the distance between the sensors would be minimized. This would minimize the problem of temperature compensation since proper temperature compensation in a bridge circuit requires that adjacent gages of a bridge be at the same temperature.

The second through seventh models were constructed with modifications to this area. These models consisted of a single hole through the structure and the strain field at these stress raisers was studied using photoelastic techniques. These holes had various shapes, but all of these holes were symmetric about the vertical line of symmetry as well as being symmetric about a horizontal axis approximately three-quarters of an inch above the air deflector. The geometry of these holes varied from circular configuration of various diameters to elongated holes. Figure 8 shows two of these models.

Figure 8. Two Through-Hole Models.

Each of these six models had certain characteristics which were considered undesirable. Among the most important of these were cross sensitivity, excessive nonlinearity of sensitivity due to eccentric vertical loads, and excessive weakening effect on the structure. The later designs tested did not exhibit these undesirable characteristics to the extent of the first; however, their effect was considered to be excessive.

Due to the lack of success with this design concept of a single through hole, this approach was abandoned. The eighth photoelastic model consisted of two circular through holes removed from the vertical axis of symmetry. A photoelastic study of this model again showed excessive weakening of the structure but not to the extent of previous models. Cross sensitivity and the nonlinearity exhibited by the previous models were not significantly present in this model. At this time it was decided to discontinue the through-hole approach to achieve a usable strain field because of the severe weakening caused by this type of stress raiser.

The second approach to the stress raiser design was to partially penetrate the structure to form an indentation or dimple which would then be instrumented. Using this concept and the knowledge gained from the eight photoelastic models already discussed, a two dimple design was investigated. The dimples were formed by partially penetrating the model material with a ball mill, advancing the tool a small horizontal distance and withdrawing the ball mill. The resultant dimple has a spherical contour at both ends with a cylindrical contour

at the center section. The purpose of the cylindrical section is to allow the mounting of the strain gages on a two-dimensional rather than a three-dimensional surface. Three-dimensional surfaces are difficult to mount strain gages on since a gage is essentially a plane and may not be easily formed to a three-dimensional surface.

Photoelastic study of models with a changing thickness in the direction parallel to the light of the polariscope is difficult. Interpretation of the fringe order observed is dependent on the thickness of the model, and complications are introduced since the surface of the dimple is not perpendicular to the light rays except in the bottom of the cylindrical portion of the dimple. Refraction of the light rays under those conditions complicates data reduction.

Because of these difficulties, two types of models were used in the investigation of this design. A plexiglas model was made and instrumented with strain gages in order to determine the suitability of the resulting force-signal relation. Also, a photoelastic model was constructed to investigate the weakening effect of the discontinuities introduced.

The models instrumented with strain gages were designed using the same techniques as for the photoelastic models. The plastic of the photoelastic models was replaced with plexiglas 3/8 inch thick, which was the same thickness as the vertical support plates of the support structure. The only scaled dimension was the length of the epoxy slipper which was computed to be 1.30 inches.

In all, three plexiglas models were constructed based upon this type of stress raiser, instrumented with foil strain gages, and evaluated in a manner similar to that of the photoelastic models. These three models had different horizontal spacing of the dimples and different dimple depths. The model from which the final design was taken is shown in Figure 9. The dimensions and strain gage locations and orientations are shown in Figure 10. This dimple was produced with a one inch ball mill; i.e., a mill cutter with a one inch diameter spherical cutting end. Strain gages were mounted on both sides of the plastic, to help eliminate bending effects during testing. The eight gages were connected in a 240 Ω bridge.

During the study of models with this type of stress raiser no allowance for the reinforcing effect of the foil strain gages was made. When using foil strain gages to measure strain in plastics this reinforcing effect may be significant. The addition of the strain gage along with its backing and bonding agent has the effect of locally reinforcing the area where it is mounted. If, as in this case, the thickness of the plastic is large compared to the gage and backing thickness and the plastic has a modulus of elasticity of the same order of magnitude as the gage material this reinforcing effect is small. The effect would not significantly influence the results which are desired from this study and was not further considered.

These models were subjected to the same loading conditions that the photoelastic models were subjected to. The loading directions are defined in Figure 4. The output of the 240 Ω

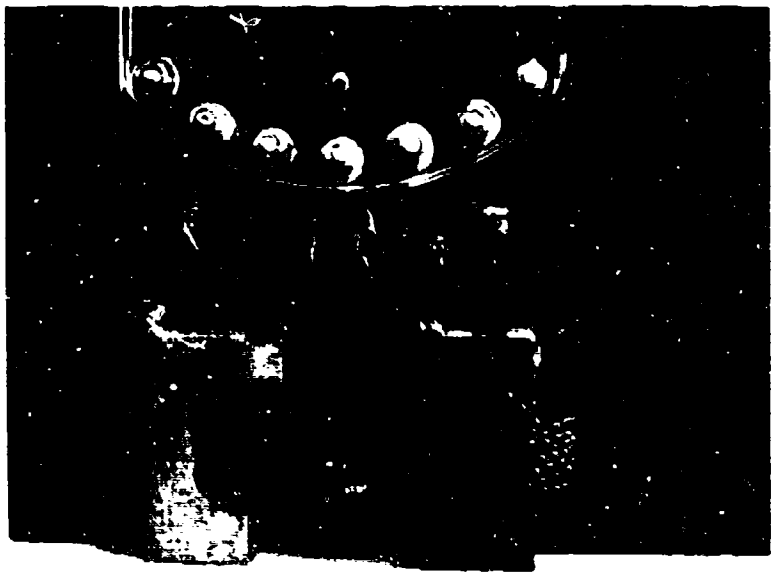

Figure 9. Model of Final Design.

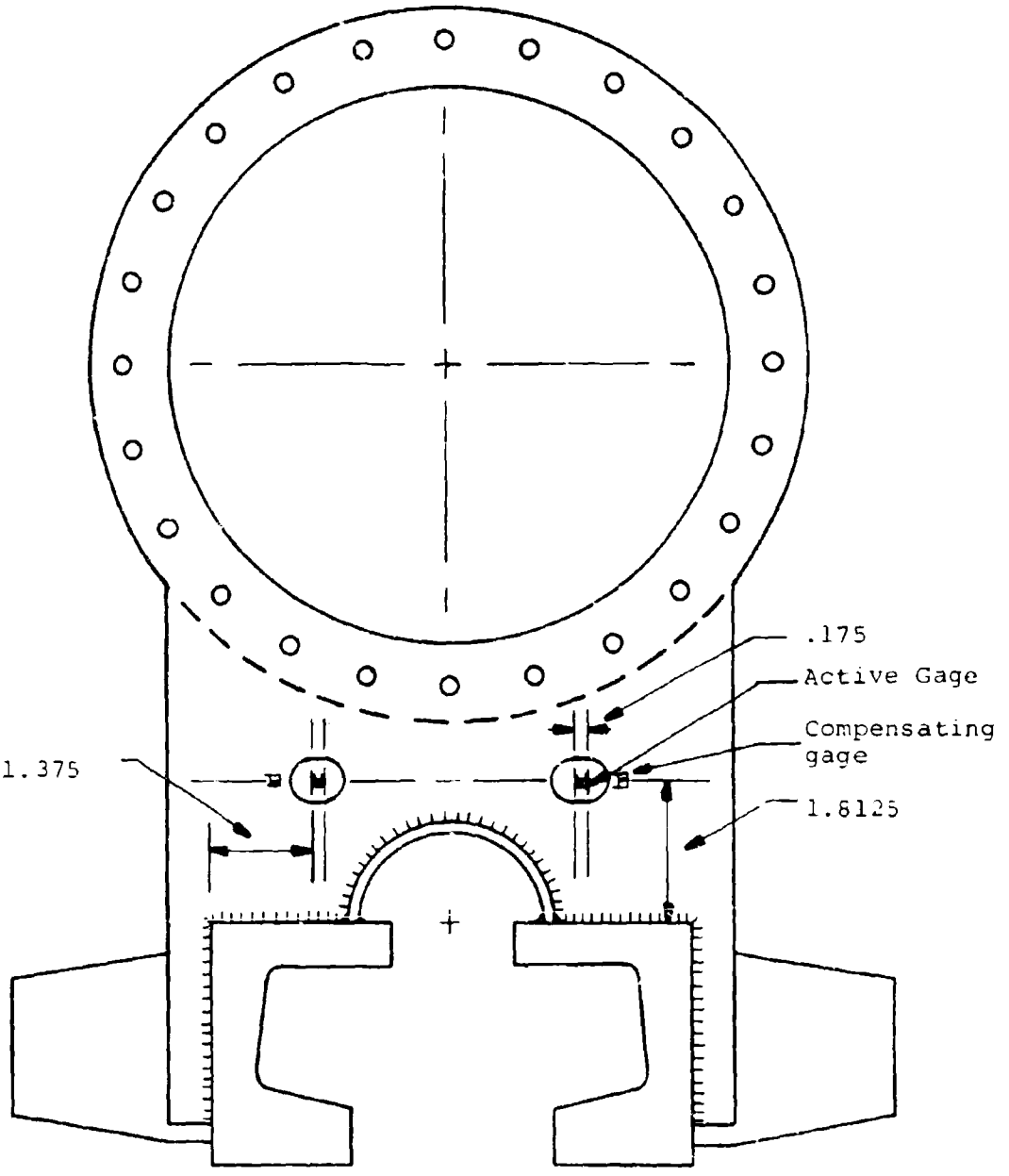

Dimples are produced using a 1 inch ball mill, penetrating 0.135 inch, traveling 0.175 inch and withdrawing the mill cutter.

Figure 10 Dimple Dimensions and Gage Location

bridge was measured with a Budd strain indicator. This instrument is calibrated in $\mu\varepsilon$; however, in this case the indicator deflection was not strain at a particular point. The deflection was a measure of the net strain induced in all the strain gages, i.e., the sum of strain induced in all the eight strain gages. Througnout the remainder of this paper, the terms, units of indicator deflection and net strain are used in this sense.

When a vertical load of 336 pounds was applied to the model of Figure 9, the indicator deflection was approximately 1300 $\mu\varepsilon$. The response of the instrumentation was essentially linear with the magnitude of the vertical load applied. The sensitivity of the instrumentation on the model to vertical load was then 336/1300, or .258 lb/$\mu\varepsilon$.

Additional information obtained from this model was that concerning the cross talk introduced in the vertical force instrumentation due to a horizontal load. The horizontal loading of the gaged plexiglas model produced a false output of the vertical instrumentation equivalent to 15% or less of the horizontally applied load. Measurements on other rocket sleds have shown the magnitude of the horizontal loads encountered during a test run are generally 1/3 or less of the magnitude of the vertical loads encountered. Considering the relative magnitude of loads expected, the false signal due to horizontal loading will not be significant.

The photoelastic model of this dimple design was made in order to determine the amount of weakening caused by the dimples

and was not geometrically similar to the modeled prototype. The thickness of the model was .250 inch as determined by the thickness of photoelastic plastic commercially available. The modeled structure had a thickness of 0.375 inches. The distortion was introduced by the scaling of the dimple to account for this different thickness.

Due to the distortion in the thickness of the model, the depth of the dimple in the photoelastic model could not be the same as in the plexiglas model. The depth in the photoelastic model was computed in order to keep the stress concentration factor in the dimple area the same for both the plastic model and the photoelastic model. This computation was based on stress concentration factors for a rectangular tensile specimen with a cylindrical groove across the perpendicular to the applied load. Using the appropriate parameters and the Handbook of Stress and Strength, (Reference 4), the dimple depth in the photoelastic model was found to be 0.090 inch.

The dimpled photoelastic model was studied in an identical manner as previous models. However, no attempt was made to interpret the fringe values within the dimple area except at the line of constant model thickness in the bottom of the cylindrical section of the dimples, for reasons previously stated. Table II shows a comparison of the prototype yield strength obtained from the studies of the unmodified model, and the photoelastic model of the two dimple design.

Table II Comparison of Modified and

Unmodified Structure Strength

Load Location	Yield Strength of Prototype Pounds: Original Model	Photoelastic Model	% of Strength
T	216K	264K	115
1T	214K	176K	82
2T	172K	132K	78
H	34K	38K	111
C	214K	172K	80
2C	172K	152K	88

The percentages greater than 100% are understandable when it is considered that the modifications to the structure changed the state of strain in the entire structure. Also, the position of the epoxy slipper section of the model on the track has some effect on the induced strain, and this position varied from one test to another.

The results of these tests indicated that this design would be satisfactory from the standpoint of bridge linearity and response to horizontal loads and strength of the structure. An additional factor to be checked from the results of the model study was that of adequate bridge out for the prototype. In making this check, use must be made of the following facts. The single plexiglas plate models both of the vertical plates of the prototype, and the instrumentation is on both sides of the plexiglas, instead of only one side, as will be the case for the two vertical plates of the slipper

assembly Since the gages on the side of the model that does not have the dimple are not subjected to as high of strain as the ones in the dimple, the output from the model bridge is slightly reduced from the value it would be if all the vertical gages were mounted in dimples. When loaded, this model in effect models both vertical plates of the prototype and the model load is applied to both of the modeled plates resulting in the equivalent force on the prototype being twice that used in the strain relationship of Equation 2.1.4.

The calculations made to determine if there would be enough strain in the prototype under the expected loads for a signal of sufficient strength for recording purposes follows. The strain in the prototype is

$$\varepsilon_p = \frac{E_m \varepsilon_m P_p h_m L_m}{E_p P_m h_p L_p} \qquad (2.1.4)$$

$$\varepsilon_p = \frac{(4.5\times10^5)(1200)(2500)(1)(.375)}{(3\times10^7)(336)(1)(.375)}$$

This shows that the net strain in the prototype when subject to a vertical load of 50,000 pounds is approximately 1400 με.

The output voltage for an initially balanced strain gage bridge which has been unbalanced by inducing strain in the gages is

$$E_o = \frac{F\ E_s\ \varepsilon_{net}}{4} \qquad (2.5.1)$$

where

E_o is the output voltage

E_s is the bridge voltage

F is the gage factor of the gages

ε_{net} is the net strain induced in the bridge due to the loading

Using the above value of strain and equation 2.1.5, the output voltage in terms of the supply voltage when a load of 50,000 pounds is applied to the structure may be found. The gage factor of the sensors selected was 2.14, so

$$E_o = \frac{2.14E_s(1400)}{4}$$

or, in terms of a voltage ratio

$$\frac{E_o}{E_s} = 7.5\text{x}10^{-4} \text{ per } 50,000 \text{ pounds.}$$

It was concluded that instrumentation of the prototype in the manner just discussed would produce the needed transducer. The modifications to the existing structure would not appreciably weaken the structure, the instrumentation would have sufficient sensitivity, it would give a linear output with the applied vertical load, and it would be essentially insensitive to components of load other than the desired vertical component.

3 - PROTOTYPE INSTRUMENTATION - FORCE MEASUREMENT

3.1 Description

The electrical resistance strain gage selected for this application was the HT-212-2A free-filament wire grid gage produced by BLH Electronics. The selection of this sensor was based on both the physical and electrical properties of the sensor. The resistance of these gages is given as 120 $\pm$ 1.0 ohms and gage factor is 2.14. The physical dimensions are 1/8 inch gage length by 1/16 inch grid width. It is only 3/32 inch wide at the leads. These dimensions are small enough to allow the easy placement of the gages in the cylindrical section of the dimples.

Either a ceramic adhesive or the Rokide flame spray bonding technique could have been used to install the free filament wire gages. Electrical properties of ceramic adhesives deteriorate with increased temperature and the maximum operating temperature is 1000°F. The Rokide bonding is usable to above 1500°F and its electrical properties are stable to this temperature. Also, the Rokide bonding has superior dynamic characteristics compared to those of the ceramic bonding technique and the installation procedure using Rokide is less complicated than with the ceramic bonding technique. For these reasons the Rokide flame spray bonding technique was selected for installation of the sensors. The physical installation of the sensor was performed at Holloman Air Force Base by their instrumentation group.

After installation each gage was then separately tested under load to insure that all were functioning properly. This resulted in replacement of three of the eight sensors. The sensors were then connected in a wheatstone bridge using nichrome wire. This wire is usable to a maximum of 1700°F. The physical connection of the wire to the ribbons of the sensor was accomplished by spot welding. The insulation used was fiberglass sleeving. This sleeving is stable to about 500°F. To the authors knowledge, this is the best insulation available for this type of application. The sleeving was slipped over the wire and ribbon to the point where the ribbon comes out of the Rokide bond. At locations where taping was necessary, a thermo setting glass tape manufactured by Minnesota Mining Company was used.

The Rokide bond is very pourous and will absorb moisture from the atmosphere. This could cause an electrical shorting of the gages to the metal to which they are bonded. To avoid this the installation must be waterproofed. The waterproofing selected and recommended by BLH was their "Barrier H." It is a thermo setting barrier which is stable to 800°F and is oil resistant. In this application, waterproofing required that the mounted gages first be heated to 250°F to drive off all moisture. Then the liquid waterproofing was applied and oven cured at 600°F for several hours.

The final lead connection was accomplished by first spot welding constantan ribbon to the four nichrome wire leads from the wheatstone bridge. Standard shielded four conductor wire

was then soldered to the constantan ribbon. The solder used had a melting temperature of 450°F, but these solder joints were located in the cylindrical section of the slipper assembly where the temperature was not expected to be very high. The constantan ribbon was used for ease of soldering. Nichrome does not solder well, and screw fasteners could not be used in the electrical circuit since they tend to vibrate loose and cause electrical noise.

A schematic of the strain gage circuit and wire path is shown in Figure 11. As is seen in the figure there is an equal length of wire in each leg of the bridge and that for every inch of wire in an active leg there is an inch of wire in a compensating leg along side it. This physical placement of the wire in constructing the circuit is required to minimize temperature induced signal from the instrumentation. The wiring is held in place by both the cover plates and thermo-setting tape.

The along-the-track loading signal will be cancelled due to the symmetrical locations of the strain sensors of the front and rear support plates. When the structure is loaded in the along-the-track direction, the active gages on one of the vertical plates will be subjected to tensile strains while the gages on the second vertical plate will be subjected to compressive strains.

Figure 12 is a photograph of the completed transducer with the front cover plate lying in the foreground.

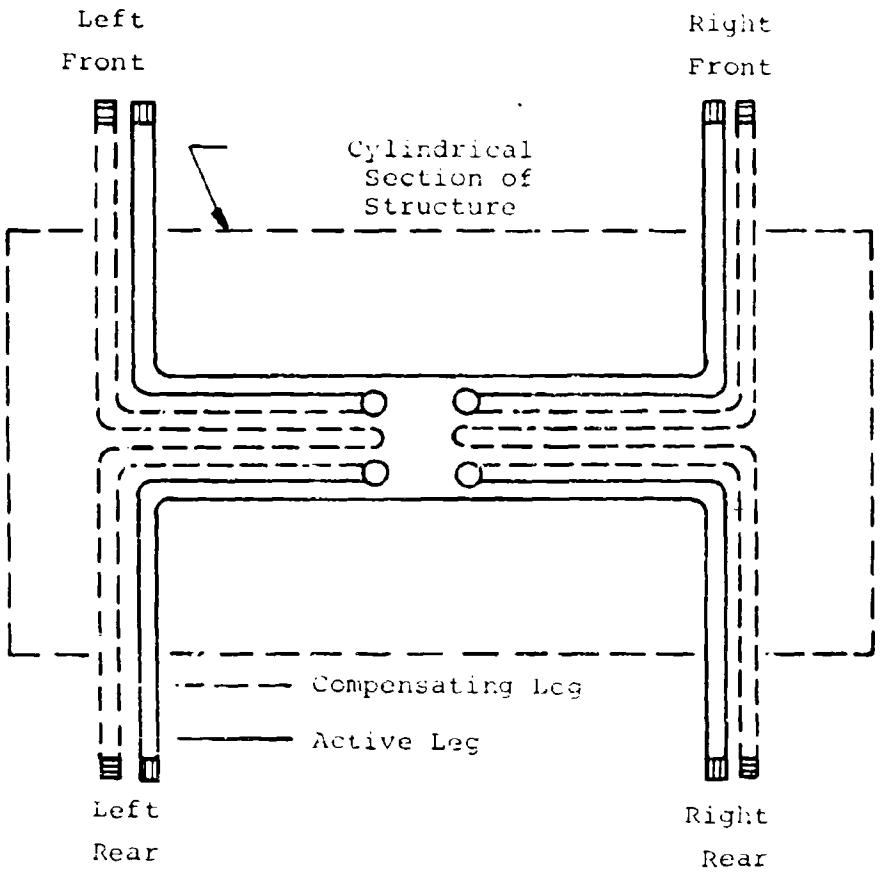

Figure 11 Schematic of Wiring Path

Figure 12. Instrumented Structure.

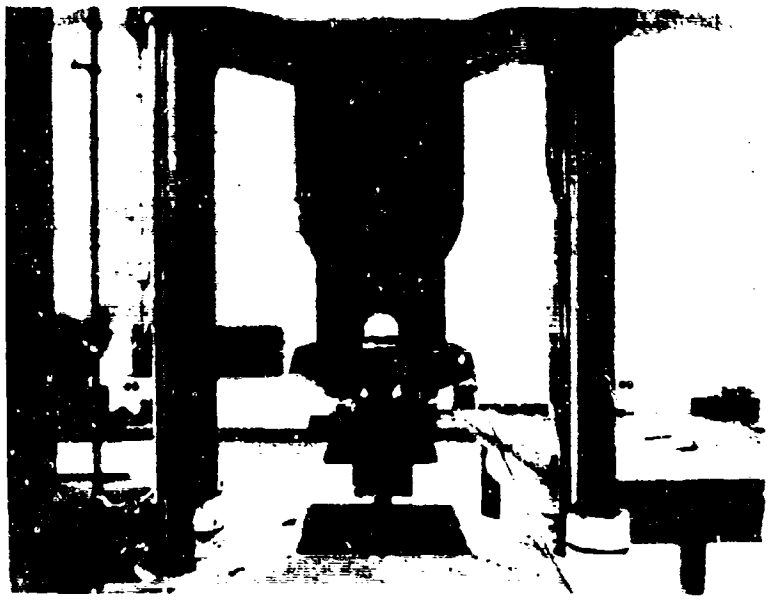

Figure 13. Vertical Calibration.

3.2 Vertical Calibration

The load on the prototype at the bottom of the structure was applied by use of a section of the sled track in a manner similar to that used in the model tests. The load at the top of the structure was applied to the assembly by using the bolt circle normally used for attaching the fore and aft bodies of the sled to the structure. Both tensile and compressive loads were applied in this manner. Two different loading jigs were constructed and used in the vertical calibration. The reasons for this will be discussed later. All vertical testing was conducted using a 60,000 pound universal testing machine. Figure 13 shows photographs of the unit under tension and compression testing. The loading jig in these two photographs was the first of the two constructed. It consisted of two vertical 1/2 inch steel plates with a 3/4 inch plate welded between them, through which the load was transmitted.

This jig was bolted to the structure using grade 9 bolts having a yield strength of 130,000 psi. The bolts go through the loading jig, the cover plates, and the instrumented structure. Bolts were tightened to a torque of 15 foot pounds or more prior to all tests.

The initial vertical testing indicated that for cyclic tensile-compressive loading above 20,000 pounds, the signal from the instrumentation produced an applied force-signal curve resembling the typical hysteresis loop. A sketch of this response is given in Figure 14.

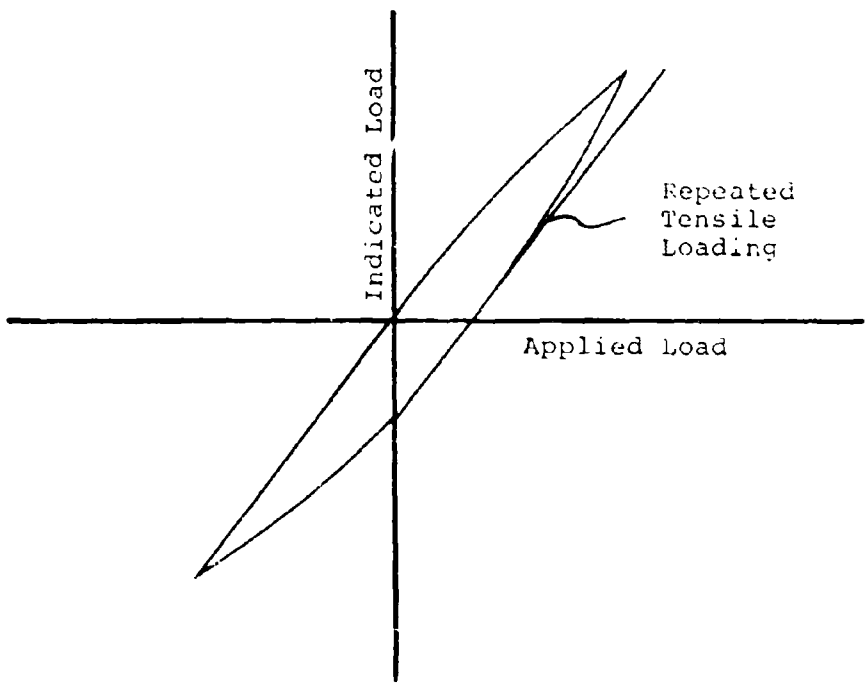

Figure 14 Response Curve

The testing procedure used to determine this curve was as follows:

1. The loading jig was bolted to the slipper assembly using 48 grade 9 bolts.
2. The indicator was zeroed.
3. A tensile load of 50,000 pounds was applied as shown in Figure 13 in increments of 10,000 pounds, the indicator reading recorded at each of these increments.

Numerical values will be stated in order to clarify this behavior. A 50,000 pound tensile load produces 1400 units of response. After removing the load, the indicator read -350 units. Application of a compressive load of 50,000 pounds gave an indicator reading of -1750 units. After removal of the load, the indicator returned to the original zero.

If the load following the application and removal of the initial tensile load had been another tensile load, the indicator reading at 50,000 pounds would have been 1400 again. Upon returning to no load, the zero position of the reading would have again been -350. The applied load-indicator reading relation is very close to linear for the second and all succeeding tensile loads as long as no compressive loads are applied. The above response is reversed if the loading sequence is reversed.

This type of curve is indicative of the behavior for all magnitudes of load from 20,000 to 50,000 pounds. The amount of hysteresis is dependent of the magnitude of the maximum

load applied and the curve does collapse to an approximate straight line below maximum loads of 20,000 pounds. Information showing the degree of this hysteresis will be given later.

Considerable effort was expended in an effort to understand this phenomenon and correct the response to a straight line relationship. It was learned that the zero shift in the reading was also associated with a change of the across the track dimension of the slipper, i.e., the slipper tended to spread as a tensile load was applied. This change of dimension was reversible by reversing the load which suggested that either the slipper assembly or the loading jig was yielding. Several additional studies were made in order to understand this phenomenon.

The loading jig was reinforced and tests conducted. This did not produce any change in the response of the unit.

A slipper assembly made of Vascomax 300 (an alloy with a yield strength of 300,000 psi) was studied under load. It behaved as the instrumented structure. The prototype was coated with stress coat and the points of high strain were located. Twenty of these high strain locations were instrumented with foil strain gages. Under a load of 50,000 pounds none of these locations was strained to beyond 40% of the yield strain of the material. However, most of these locations did show that after returning the structure to the no load condition that strain in these locations was still present. In some locations the strain was of opposite sign to that induced by the

applied load. However, due to the low values of strain at the points believed to be high strain points, it was concluded that the failure of the strain gage instrumentation to return to the original zero was not due to yield of the structure.

Impact testing was then initiated to determine if the behavior under dynamic loads would be the same as for static loads. The slipper assembly was bolted to the loading jig and and entire assembly cyclicly loaded in tension only. Then a 37 pound weight was dropped on the assembly from a height of 14 feet. The indicated force applied was approximately 50,000 pounds with a pulse duration of 0.7 milliseconds. This impact load resulted in a zero shift equivalent to +11,000 pounds which was approximately the zero shift encountered in static testing when a 50,000 pound load was applied. This result made further study necessary.

Further consideration of the character of this problem led to the belief that the difficulty was relative motion between the loading fixture and the slipper assembly. No slippage would occur at low peak loads, and the calibration curve for these conditions would return to zero. At sufficiently large loads, slippage would occur. Then, after removal of the load, both the slipper assembly and loading jig would not allow one another to return to their original state of strain. This belief was verified by recording the indicator deflection before mounting the loading jig, assembling the jig and slipper, loading the unit once, removing the jig and noting that the indicator deflection returned to its original position.

and the load is applied through this pin. Extensive testing was conducted using this new loading jig. The results of this testing were essentially the same as those obtained with the use of the first jig.

Although this testing did not result in any change of the transducer's response another important parameter of the system was investigated. This parameter was the effect of the rigidity of the mating parts on the sensitivity of the strain gage instrumentation. The fore and aft bodies are slightly less rigid than the second loading jig. But a factor of two in the rigidity of the two loading jigs did not alter the response characteristics of the instrumentation, so it can be expected that the instrumentation will respond with the fore and aft bodies mounted in the same manner as with the loading fixture attached.

Since the difficulties encountered with the instrumentation as indicated by the presence of the hysteresis loop, were the result of the sled design and not the instrumentation, the calibration procedure taken was one to include a study of the effect of load reversal and load magnitude on accuracy. This procedure is described below.

The loading jig of Figure 15 was installed using new grade 9 bolts with 15 foot-pounds of torque. The loading history shown in Figure 16 was applied to the unit. This loading history is given in terms of the maximum peak load applied. This loading was applied for peak loads of 20,000; 30,000; 40,000; and 50,000 pounds. The indicator deflection was recorded at

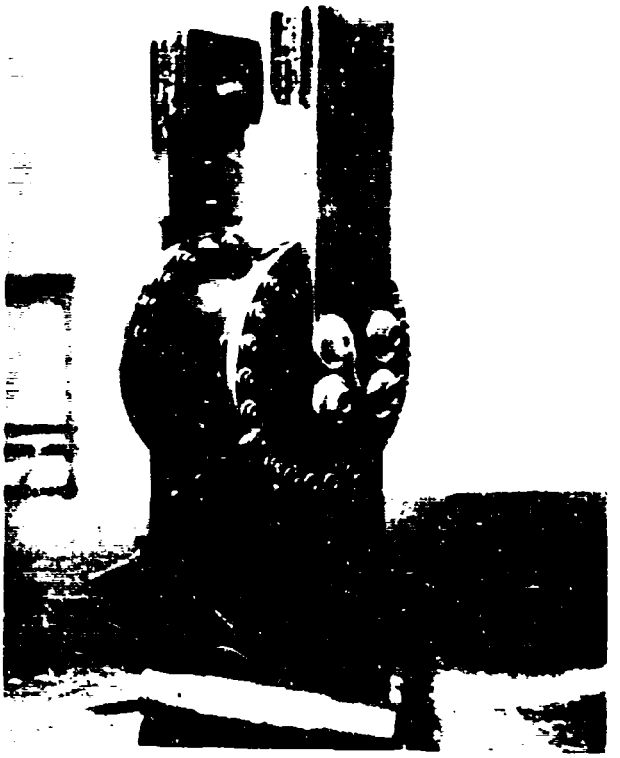

Figure 15. Second Loading Jig

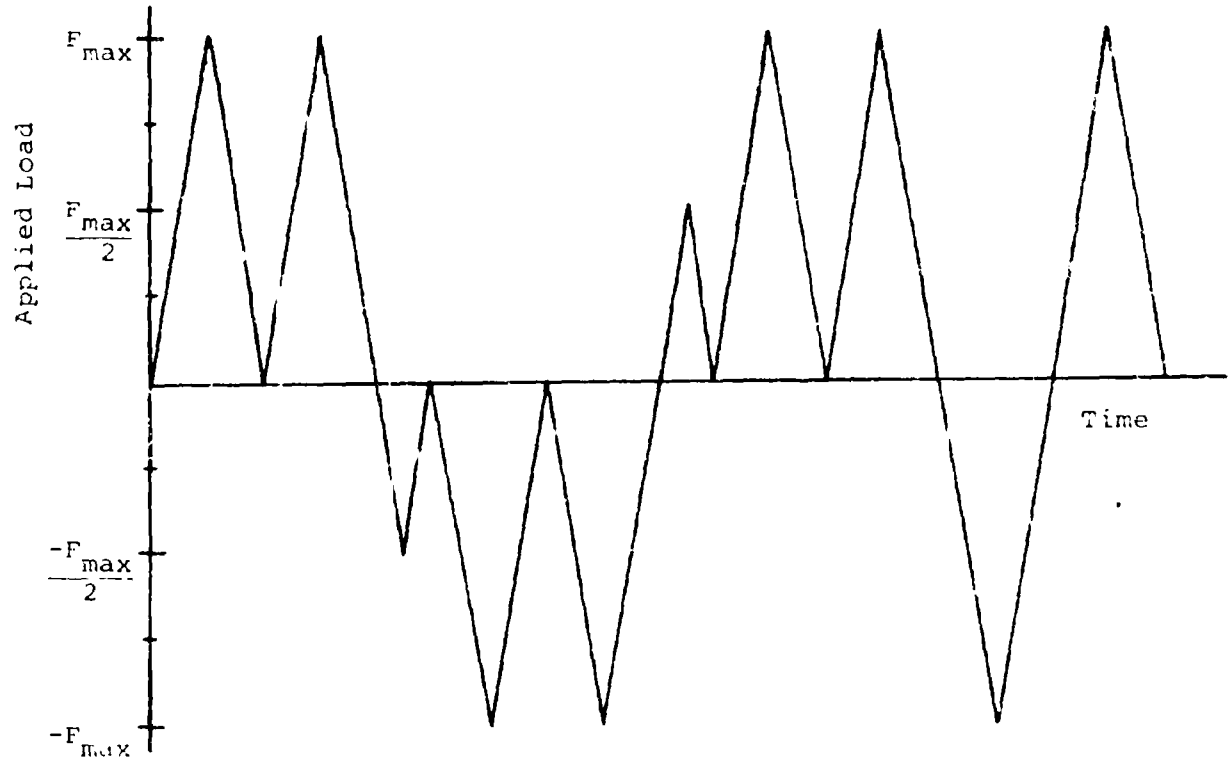

Figure 16 Loading History for Final Calibration

intervals of load not greater than 10,000 pounds. The data obtained was then reduced in the manner previously discussed.

Since the amount of hysteresis increased as the peak load was increased, it was necessary to use a different sensitivity factor for the different peak loads. These sensitivity factors were chosen such that the errors in the measured load would be small at or near the peak loads.

The data obtained from this calibration procedure is given in Tables III through VI. Included in these tables are the indicator deflection, the sensitivity factor, the measured load, the magnitude of the error in the measured load the the percent error of the measured load.

Table VII is a summary of Tables III through VI. The errors shown in Table VII are the maximum that occurred throughout the loading sequence. With these tables and Figure 16, the error at any position in the data obtained from this transducer may be more closely bounded than Table III suggests. This would be done by comparing the loading history of the data with a similar history of Figure 16. In Table VII, the percent error in many cases are quite high; however, the magnitude of error relative to the maximum load applied is usually small.

Table VIII gives the calibrate resistor information for this strain gage bridge in order that appropriate scales may be placed on the data when the unit is used in a sled run. The calibrate resistor used for calibration should have a tolerance of 1% or better.

In addition to vertical calibration, the unit was subjected to off-axis loading in the plane perpendicular to the sled track and along-the-track loading.

Table III Calibration for 20,000 Pound Maximum Force

Sensitivity Factor = 27 Pounds/Unit of Indicator-Deflection

Force Applied Pounds (x1000)	Indicator-Deflection	Measured Force Pounds	Error Pounds	% Error
-5	-140	-3780	-1220	-24
-10	-380	-10500	+500	+5
-15	-570	-15400	+400	+2.7
-20	-750	-20200	+200	+1
-15	-550	-14850	-150	-1
-10	-360	-9700	-300	-3
-5	-150	-4050	-950	-19
0	+40	+1080	+1080	---
-5	-150	-4050	-950	-19
-10	-350	-9450	-550	-5.5
-15	-550	-14850	-150	-1
-20	-740	-20000	0	0
-15	-560	-15100	+100	+1
-10	-360	-9700	-300	-3
-5	-150	-4050	-950	-19
0	+40	+1080	+1080	---
5	+240	+6450	+1450	+29
10	+420	+11350	+1350	+13.5
5	+240	+6450	+1450	+29
0	+40	+1080	+1080	---
5	+230	+6250	+1200	+24
10	+410	+11080	+1080	+10.8
15	+570	+15400	+400	+2.7
20	+710	+19200	-800	-4
15	+550	+14850	-150	-1
10	+370	+10000	0	0
5	+180	+4860	-140	-2.8
0	-30	-810	-810	---
5	+150	+4050	-950	-19
10	+330	+8900	-100	-1.0

Table III - Continued

Force Applied Pounds (x1000)	Indicator-Deflection	Measured Force Pounds	Error Pounds	% Error
15	+520	+14050	-950	-6.3
20	+700	+18900	-1100	-5.5
15	+540	+14600	-400	-2.7
10	+370	+10000	0	0
5	+180	+4860	-140	-2.8
0	-30	-810	-810	---
-5	-230	-6200	+1200	+24
-10	-410	-11080	+1080	+10.8
-5	-210	-5670	+670	+13.4
0	-30	-810	-810	---
-5	-210	-5670	+670	+13.4
-10	-410	-11080	+1080	+10.8
-15	-590	-15900	+900	+6
-20	-760	-20500	+500	+2.5
-15	-570	-15400	-400	-2.7
-10	-370	-10000	0	0
-5	-170	-4590	-410	-8.2
0	+30	+810	+810	---
-5	-150	-4050	-950	-19
-10	-360	-9700	-300	-3
-15	-550	-14850	-150	-1
-20	-750	-20200	+300	+1.5
-15	-270	-15400	+400	+2.7
-10	-370	-10000	0	0
-5	-160	-4320	-680	-13.6
0	+30	+810	+810	---
5	+220	+5940	+940	+18.8
10	+410	+11050	+1050	+10.5
15	+580	+15650	+650	+4.3
20	+730	+19700	-300	-1.5
15	+550	+14850	-150	-1

Table IV - Continued

Force Applied Pounds (x1000)	Indicator-Deflection	Measured Force Pounds	Error Pounds	% Error
0	-80	+2480	+2480	---
-5	-270	-8370	+3370	+66
-10	-470	-14600	+4600	+46
-15	-660	-20450	+5450	+36
-20	-810	-25100	+5100	+26
-25	-930	-28800	+3800	+15
-30	-1050	-32500	+2500	+8.3
-25	-860	-26600	+1600	+6.4
-20	-670	-20800	+800	+4
-15	-470	-14600	-400	-2.6
-10	-270	-8370	-1630	-16
-5	-80	-2480	-2520	-50
0	+100	+3100	+3100	---
-5	-90	-2790	-2210	-44
-10	-290	-9000	-1000	-10
-15	-480	-14900	-100	-1
-20	-680	-21000	+1000	+5
-25	-880	-27300	+2300	+9.2
-30	-1060	-32800	+2800	+9.3
-25	-860	-25700	+700	+2.8
-20	-660	-20500	+500	+2.5
-15	-470	-14500	-500	-3.3
-10	-270	-8370	-1630	-16
-5	-70	-2170	-2830	-56
0	+100	+3100	+3100	---
5	+290	+9000	+4000	+80
10	+440	+13600	+3600	+36
15	+570	+17700	+2700	+18
10	+380	+11800	+1800	+18
5	+190	+5900	+900	+18
0	-20	-620	-620	---

Table IV - Continued

Force Applied Pounds (x1000)	Indicator-Deflection	Measured Force Pounds	Error Pounds	% Error
5	+180	+5570	+570	+11.4
10	+370	+11500	+1500	+15
15	+560	+17300	+2300	+15
20	+680	+21100	+1100	+5.5
25	+800	+24800	-200	-1
30	+910	+28200	-1800	-6
25	+740	+23000	-2000	-8
20	+570	+17700	-2300	-11.5
15	+390	+12100	2900	-19
10	+200	+6200	-3800	-38
5	-10	-310	-4690	-94
0	-200	-6200	-6200	---
-5	-360	-11100	+6100	+120
-10	-520	-16100	+6100	+61
-15	-600	-18600	+3600	+24
-20	-800	-24800	+4800	+24
-25	-930	-28800	+3800	+15
-30	-1060	-32900	+2900	+9.7
-25	-870	-27000	+2000	+8
-20	-670	-20800	+800	+4
-15	-480	-14900	-100	-1
-10	-290	-9000	-1000	-10
-5	-80	-2480	-2520	-50
0	+90	+2790	+2790	---
5	+280	+8680	+3680	+73
10	+430	+13300	+3300	+33
15	+560	+17300	+2300	+15
20	+670	+20800	+800	+4
25	+790	+24500	-500	-2
30	+900	+27900	-2100	-7
25	+730	+22700	-2300	-9

Table IV - Continued

Force Applied Pounds (x1000)	Indicator-Deflection	Measured Force Pounds	Error Pounds	% Error
20	+560	+17300	-2700	-14
15	+380	+11800	-3200	-21
10	+180	+5510	-4430	-44
5	-20	-620	-4380	-86
0	-200	-6200	-6200	---

Table V Calibration for 40,000 Pound Maximum Force

Sensitivity Factor = 32 Pounds/Unit of Indicator Deflection

Force Applied Pounds (x1000)	Indicator-Deflection	Measured Force Pounds	Error Pounds	% Error
10	+400	+12800	+2800	+28
20	+720	+23000	+3000	+15
30	+970	+31000	+1000	+3
40	+1190	+38100	-1900	-5
30	+580	+27200	-2800	-9
20	+500	+16000	-4000	-20
10	+120	+3840	-6160	-61
0	-210	-6700	-6700	---
10	+180	+5750	-4250	-42
20	+550	+17600	-2400	-12
30	+890	+28500	-1500	-5
40	+1180	+37800	-2200	-5.5
30	+840	+27900	-2100	-7
20	+490	+15700	-4300	-21
10	+120	+3840	-6160	-62
0	-210	-6720	-6720	---
-10	-510	-16300	+6300	+63
-20	-780	-25000	+5000	+25
-10	-400	-12800	+2800	+28
0	+40	+1280	+1280	---
-10	-390	-12500	+2500	+25
-20	-780	-25000	+5000	+25
-30	-1030	-33000	+3000	+10
-40	-1280	-41000	+1000	+2.5
-30	-900	-28800	-1200	-4
-20	-490	-15700	-4300	-21
-10	110	-3520	-6480	-65
0	+190	+6080	+6080	---
-10	-190	-6080	-3920	-39

Table V · Continued

Force Applied Pounds (x1000)	Indicator-Deflection	Measured Force Pounds	Error Pounds	% Error
-20	-580	-18600	-1450	-7
-30	-950	-30400	+400	+1
-40	-1280	-41000	+1000	+2.5
-30	-880	-28200	-1800	-6
-20	-480	-15350	-4650	-23
-10	-90	-2880	-7120	-71
0	+200	+6400	+6400	---
10	+480	+15350	+5350	+53
20	+730	+23400	+3400	+17
10	+350	+11200	+1200	+12
0	-50	-1600	-1600	---
10	+340	+10900	+900	+9
20	+720	+23000	+3000	+15
30	+960	+30700	+700	+2.3
40	+1190	+38100	-1900	-4.4
30	+850	+27200	-2800	-9.3
20	+500	+16000	-4000	-20
10	+120	+3840	-6160	-61
0	-210	-6720	-6720	---
-10	-480	-15350	+5350	+53
-20	-750	-24000	+4000	+20
-30	-1000	-30000	0	0
-40	-1270	-40600	+600	+1.5
-30	-810	-27800	-2150	-7.2
-20	-480	-15350	-4650	-23
-10	-100	-3200	-6800	-68
0	+200	+6400	+6400	---
10	+470	+15050	+5050	+50
20	+720	+23000	+3000	+15
30	+960	+30700	+700	+2.3
40	+1200	+38400	-1600	-4

Table V - Continued

Force Applied Pounds (x1000)	Indicator-Deflection	Measured Force Pounds	Error Pounds	% Errors
30	+860	+27700	-2300	-7.7
20	+520	+16650	-3350	-17
10	+130	+4150	-5850	-58
0	-200	-6400	-6400	---

Table VI Calibration for 50,000 Pound Maximum Force

Sensitivity Factor = 35 Pounds/Unit of Indicator Deflection

Force Applied Pounds (x1000)	Indicator-Deflection	Measured Force Pounds	Error Pounds	% Error
10	+400	+14000	+4000	+40
20	+720	+25200	+5200	+26
30	+970	+33900	+3900	+13
40	+1200	+42000	+2000	+5
50	+1360	+47600	-2400	-4.8
40	+1020	+35700	-4300	-11
30	+680	+23800	-6200	-21
20	+320	+11200	-8800	-44
10	0	0	-10000	---
0	-300	-10500	-10500	---
10	+90	+3150	-6850	-68
20	+450	+15750	-4250	-21
30	+800	+28000	-2000	-7
40	+1080	+37800	-2200	-5.5
50	+1350	+47200	-2800	-5.6
40	+1010	+35300	-4700	-12
30	+680	+23800	-6200	-21
20	+340	+11900	-8100	-41
10	+10	+350	-9650	-96
0	-290	-10150	-10150	---
-10	-580	-20300	+10300	+100
-20	-830	-29000	+9000	+45
-25	-950	-33300	+8300	+33
-20	-760	-26600	+6600	+33
-10	-360	-12600	+2600	+26
0	+30	+1050	+1050	---
-10	-350	-12250	+2250	+22
-20	-750	-26200	+6200	+31
-30	-1060	-37100	+7100	+24

Table VI - Continued

Force Applied Pounds (x1000)	Indicator-Deflection	Measured Force Pounds	Error Pounds	% Error
-40	-1300	-45500	+5500	+14
-50	-1550	-54200	+4200	+8.2
-40	-1160	-40600	+600	+2
-30	-760	-26600	-3400	-11
-20	-370	-12950	-7050	-35
-10	-30	-1050	-8950	-89
0	+230	+8050	+8050	---
-10	-160	-5600	-4400	-44
-20	-560	-19600	-400	-2
-30	-920	-32200	+2200	+7
-40	-1240	-43400	+3400	+9
-50	-1540	-5400	+4000	+8
-40	-1150	-40200	+200	+0.5
-30	-750	-26200	-3800	-13
-20	-360	-12600	-7400	-37
-10	-30	-1050	-8950	-89
0	+230	+8050	+8050	---
10	+500	+17500	+7500	+75
20	+720	+25200	+5200	+26
25	+820	+28700	+3700	+14.8
20	+640	+22400	+2400	+12
10	+260	+9100	-900	-9
0	-120	-4200	-4200	---
10	+270	+9450	-550	-5.5
20	+640	+22400	+2400	+12
30	+920	+32200	+2200	+7.4
40	+1130	+39500	-500	-1.3
50	+1330	+46500	-3500	-7
40	+1000	+25000	-5000	-12.5
30	+660	+23[illegible]00	-6900	-23
20	+320	+11[illegible]00	-8800	-44

Table VI- Continued

Force Applied Pounds (x1000)	Indicator-Deflection	Measured Force Pounds	Error Pounds	% Error
10	-10	-350	-9650	-96
0	-290	-10150	-10150	---
-10	-560	-19600	+9650	+96
-20	-790	-27700	+7700	+38
-30	-1020	-35700	+5700	+19
-40	-1240	-43400	+3400	+8.5
-50	-1510	-52800	+2800	+5.6
-40	-1120	-39200	-800	-2
-30	-730	-25600	-4400	-15
-20	-340	-17200	-2800	-14
-10	-20	-700	-9300	-93
0	+230	+8050	+8050	---
10	+490	+17150	+7150	+71
20	+690	+24200	+4200	+21
30	+890	+31200	+1200	+4
40	+1110	+38800	-1200	-3
50	+1320	+46200	-3800	-7
40	+980	+34300	-5700	-14
30	+650	+23800	-6200	-21
20	+310	+10850	-9150	-46
10	-20	-700	-9300	-93
0	-290	-10150	-10150	---

Table VII Summary of Vertical Calibration

Maximum Load Pounds	Load Pounds	Magnitude of Error Pounds Low	High	% Error
± 20K	0	-810	1080	---
	±5K	-1220	1450	-24 +29
	±10K	-550	1350	-5.5 +13.5
	±15K	-950	900	-6.3 +6
	±20K	-1100	500	-5.5 +2.5
± 30K	0	-6200	2800	---
	±10K	-4400	6100	-44 +61
	±20K	-2650	5100	-13 +25
	±30K	-2100	2900	-7 +9.7
± 40K	0	-6700	6400	---
	±10K	-7120	5300	-71 +53
	±20K	-4650	5000	-23 +25
	±30K	-2800	3000	-9.3 +10
	±40K	-2200	1000	-5.5 +2.5
± 50K	0	-10150	8050	---
	±10K	-10000	10000	-100 +100
	+20K	-8800	9000	-44 +45
	±30K	-6900	7100	-23 +24
	±40K	-5700	5500	-14 +14
	±50K	-3500	4200	-7 +8.4

Table VIII. System Calibration Data

Maximum Load Pounds	R_{cal} ohms	Across Leads	Indicator-Deflection	Indicated Force Pounds
20,000	1Meg	Red	130	3510
	500K	and	262	7060
	200K	White	653	17600
	1Meg	Red	-130	-3510
	500K	and	-262	-7060
	200K	Black	-653	-17600
30,000	1Meg	Red	130	4030
	500K	and	262	8120
	200K	White	653	20600
	100K		1304	40400
	1Meg	Red	-130	-4030
	500K	and	-262	-8120
	200K	Black	-653	-20600
	100K		-1304	-40400
40,000	1Meg	Red	130	4160
	500K	and	262	8375
	200K	White	653	20900
	100K		1304	41700
	1Meg	Red	-130	-4160
	500K	and	-262	-8375
	200K	Black	-653	-20900
	100K		-1304	-41700
50,000	1Meg	Red	130	4550
	500K	and	262	9175
	200K	White	653	22850
	100K		1304	45600

Table VIII. (continued)

Maximum Load Pounds	R_{cal} ohms	Across Leads	Indicator-Deflection	Indicated Force Pounds
50,000	1Meg	Red	-130	-4550
	500K	and	-262	-9175
	200K	Black	-653	-22850
	100K		-1304	-45600

3.3 Off-Axis Loading

A loading frame was constructed to apply off-axis and along-the-track loads to the unit. Figure 17 is a photograph of this loading frame in use. This loading frame has a capacity of 20,000 pounds in both tension and compression. The load is produced using a push-pull hydraulic cylinder and is monitored by a strain gage instrumented force line constructed for this application. The load is applied at the top of the unit using the first loading jig constructed. At the bottom of the unit, the load is transmitted through a section of sled track, as in the vertical calibration.

The magnitude of loads applied in this phase of calibration were not large enough to produce the hysteresis effect encountered in the vertical calibration phase. Figure 18 defines the loads applied to the slipper assembly using the loading frame. Only one along-the-track loading direction was applied as only one direction of this load will be encountered in use. This load would be directed toward the rear of the sled and applied at the slipper by both friction between the slipper and the track and by the aerodynamic drag on the wings of the slipper.

The sensitivity used for all data reduction in this section is that used for the 20,000 pound vertical calibration. Due to the simplicity of the data reduction, the indicator deflections are not given. Table IX is a summary of the off-axis calibration. The errors given here are due only to the horizontal components applied, as the magnitude of loads applied were not

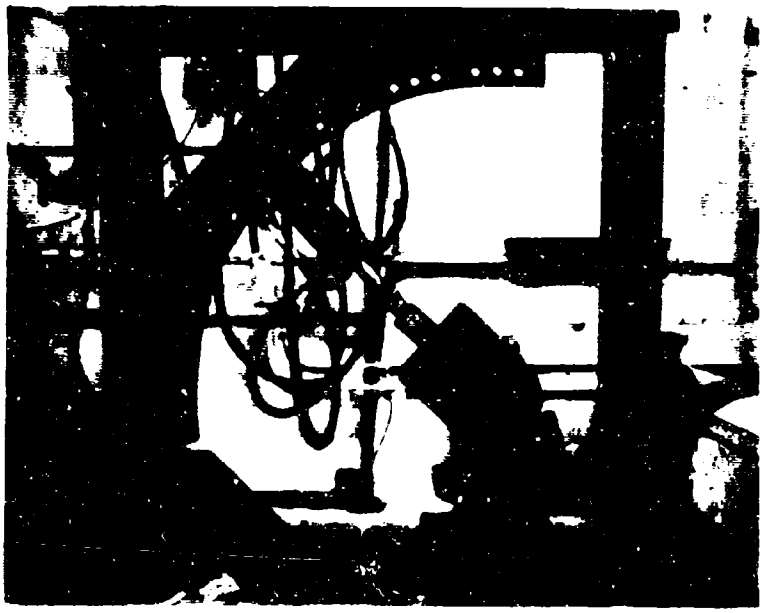

Figure 17. Off-Axis Loading Frame.

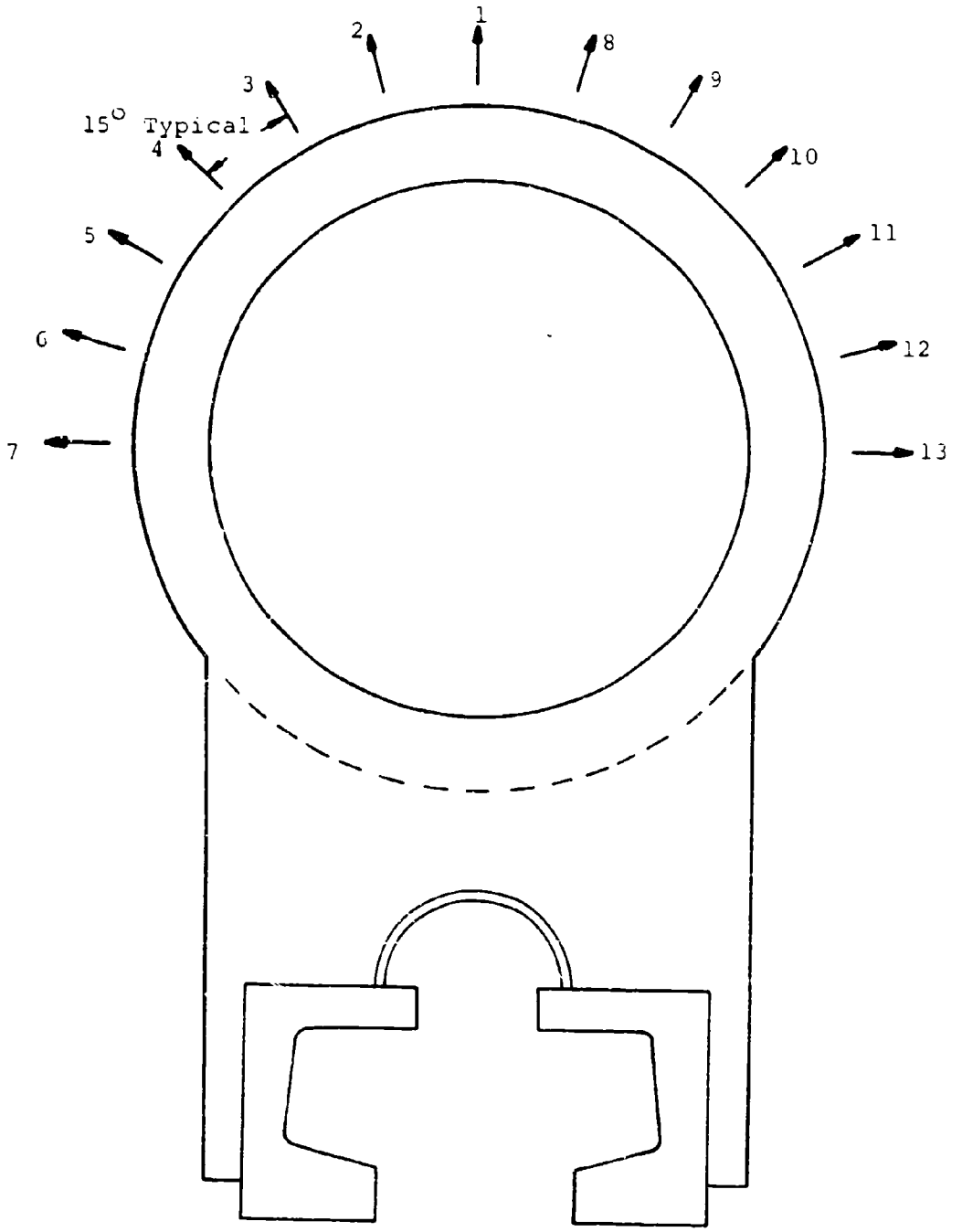

Figure 18 Off Axis Load Definitions

Table IX Results of Off-Axis Load Tests

Load Number	Load Applied Pounds	Components-Pounds Horizontal	Components-Pounds Vertical	Vertical Measured Pounds	% Error
8	5K	-1280	4830	5290	9.5
	10K	-2560	9660	10600	9.7
	15K	-3840	14490	15300	5.5
	20K	-5120	19320	19600	1.5
	-5K	1280	-4830	-4650	-3.7
	-10K	2560	-9660	-9450	-2.2
	-15K	3840	-14490	-13700	-5.4
	-20K	5120	-19320	-18100	-6.2
2	5K	1280	4830	5120	6
	10K	2560	9660	10100	4.8
	15K	3840	14490	15100	4.2
	20K	5120	19320	19600	1.4
	-5K	-1280	-4830	-4210	-12.7
	-10K	-2560	-9660	-8460	-12.5
	-15K	-3840	-14490	-12700	-12.5
	-20K	-5120	-19320	-17150	-11
9	5K	2500	4330	4550	5
	10K	5000	8660	9550	10
	15K	7500	12990	13900	7
	-5K	-2500	-4330	-4550	5
	-10K	-5000	-8660	-8700	0
	-15K	-7500	-12990	-12650	-2.7
3	5K	2500	4330	4750	9.7
	10K	5000	8660	9270	7
	15K	7500	12990	13150	1.2
	-5K	-2500	-4330	-4070	-6
	-10K	-5000	-8660	-8200	-5.3
	-15K	-7500	-12990	-12150	-6.4

Table IX Results of Off-Axis Load Tests (continued)

Load Number	Load Applied Pounds	Components-Pounds Horizontal	Vertical	Vertical Measured Pounds	% Error
10	5K	-3535	3535	4000	13
	10K	-7070	7070	7600	7.5
	-5K	3535	-3535	-4000	13
	-10K	7070	-7070	-7800	10.5
4	5K	3535	3535	4000	13
	10K	7070	7070	8200	16
	-5K	-3535	-3535	-3940	11
	-10K	-7070	-7070	-7450	5.4
13	1K	1K	0	0	
	2K	2K	0	0	
	3K	3K	0	87	
	4K	4K	0	145	
	5K	5K	0	174	
	6K	6K	0	174	
	7K	7K	0	0	
7	1K	1K	0	-145	
	2K	2K	0	82	
	3K	3K	0	82	
	4K	4K	0	435	
	5K	5K	0	435	
	6K	6K	0	720	
	7K	7K	0	720	

large enough to produce the hysteresis effect. Negative applied loads signifies that the force link attached to the hydraulic cylinder is in compression.

It is seen in Table IX with the exception of load 2, that when the vertical component of force applied is greater than 10,000 pounds and less than 20,000 pounds, the maximum error in the measured force is 6.2%. The false signal produced by a pure horizontal load (loads 7 and 13) is 7.3% or less of the applied horizontal load. Compared to the hysteresis effect present, these errors are small. Also, when the vertical component is large, the horizontal component must be a small fraction of the vertical or the sled would twist off the track, which at times it has done. For these reasons, the error induced in the signal due to horizontal components of force will not be significant and will not be discussed further.

Table X shows the false vertical force signal from the instrumentation due to the along-the-track loading. On first loading the along-the-track did produce a false signal equal to about 40% of the applied load, with a large zero shift after the load was removed. The second loading in this direction produced a false signal of only 12% of the applied load. In use the along-the-track force will vary, but it will always be in one direction. Also, it will be applied simultaneously with vertical and horizontal components of load. Due to the lack of knowledge of the magnitudes of this load component in use, the effect of this behavior cannot be evaluated.

Table X Along-the-Track Loading

Applied Load Pounds	False Vertical Force Indicated - Pounds	
	First Loading	Second Loading*
500	0	0
1000	30	120
1500	250	210
2000	460	---
2500	650	350
3000	860	---
3500	1080	---
4000	1350	400
4500	1500	---
5000	1650	590
4000	1600	480
3000	1450	270
2000	1400	270
1000	1350	270
0	1350	270

*Immediately applied after first loading sequence and after the indicator was re-zeroed.

3.4 Comparison with Model Tests

The model study predicted that the bridge circuit in the prototype would give an indicator deflection of 1400 με when the prototype is subjected to a 50,000 pound vertical load. When the prototype was subjected to 50,000 pounds, the indicator deflection was approximately 1350 με. Table X shows these values. It is noted that when the load was -50,000 pounds, the indicator deflection was approximately -1550 με. However, these values do not include the effect of the zero shift since this was not encountered in the model studies. When this is included, a 50,000 pound load is associated with an indicator deflection of approximately 1700 με. The model prediction of the sensitivity of the instrumentation should then be compared to this higher value of net strain. On this basis the model study was accurate to 83%.

This close agreement between the predicted sensitivity of the resultant instrumentation and the actual sensitivity verifies the validity of the model. This then indicates that the failure loads for the slipper assembly obtained from the model study as given in Table I, are also representative of the prototype behavior.

The model was also designed to predict prototype behavior for cross-track loads. Comparisons between model and prototype behavior were made for these conditions. The model predicted a false signal for pure horizontal loading equal to 16% of the applied load. Corresponding values for the prototype from Table IX, loads 7 and 13 are 7.2%.

4 - PROTOTYPE INSTRUMENTATION - TEMPERATURE MEASUREMENT

4.1 Description

It was decided to measure the temperature in the vicinity of each dimple, in order to better understand the temperature history of the gages and the possible effect on the bridge output. The sensor selected for use was a resistance thermometer manufactured by BLH Electronics, their part number RTP-28F-5.

This sensor has the same general appearance as the strain gage being used, in that it is a free-filament type. However, it was larger, the grid size being 9/32" x 1/4", and the filament was made of platinum. The resistance at 70°F was 50.8 ± .1 ohms. Two of these resistance thermometers were mounted on the front plate of the slipper assembly, one each immediately above each dimple. The mounting technique used was the Rokide process.

Measurement of temperature with these sensors required a knowledge of how the resistance changed with time. Two channels were available in the sled instrument package for making these measurements, and each had a fixed amplification factor of 10. It was necessary that the circuitry used with the resistance thermometer have an output within the range -250mv to +250mv for the temperature range 70°F to 1000°F, so the output of the system would be within the range ± 2.5v as required for the telemetry system.

Bridge circuits were used with the sensors to accomplish this. One leg of each bridge was a sensor, and the resistances in the other legs were selected to satisfy two requirements: 1) the bridge unbalance in voltage be within the required limits for the temperature range of interest, and 2) the bridge output be linear with respect to temperature over the required range.

Figure 19 defines the quantities used in the equations required in the development of a circuit to satisfy the above requirements. The equation for the output voltage e_o, for an initially balanced bridge is given by

$$\frac{e_o}{E} = \frac{R_1\Delta R_2 - R_2\Delta R_1}{(R_1+R_2)^2+(R_1+R_2)(\Delta R_1+\Delta R_2)} + \frac{R_3\Delta R_4 - R_4\Delta R_3}{(R_3+R_4)^2+(R_3+R_4)(\Delta R_3+\Delta R_4)}.$$

For this temperature circuit, R_1 will be the resistance thermometer, and R_2, R_3, and R_4 will be fixed resistors. The above equation then reduces to

$$\frac{e_o}{E} = \frac{-R_2\Delta R_1}{(R_1+R_2)^2+(R_1+R_2)\Delta R_1}$$

since $\Delta R_2 = \Delta R_3 = \Delta R_4 = 0$.

If $\frac{R_2}{R_1}$ is large, say 100, then the equation may be put in the form

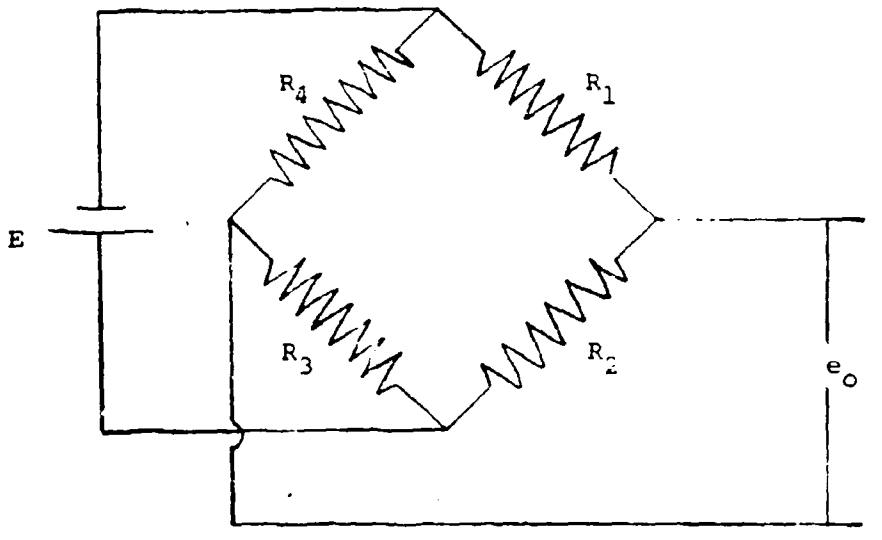

Figure 19. Bridge Circuit

$$\frac{e_o}{E} = \frac{-\Delta R_1/R_1}{102+1.01\frac{\Delta R_1}{R_1}}$$

The second term in the denominator is the one which makes the circuit nonlinear. For the resistance thermometer selected, the ratio of resistance at 1000°F to that at 70°F is 2.743, so $\frac{R}{R_1}$ at 1000°F would be 1.74. Computation then shows that neglecting the nonlinear term will introduce an error of about 1.5% in the results, and this was considered an acceptable value. Since the resistance thermometer is 50.8 ohms at 70°F, a value of 5000Ω was selected for R_2. R_4 would be 50Ω from the condition for an initially balanced bridge.

In order to utilize the full range of the telemetry system during the run, it was necessary that the bridge output be approximately -250mv at ambient temperature, and +250mv at the maximum expected temperature. The value of R_3 computed so the output would be about -240mv at 70°F was 2462Ω for 24 volts excitation. Computation also showed that the bridge output would be approximately +200mv for a temperature of 1000°F. These values for output satisfied the first requirement previously mentioned for the bridge.

Therefore, the nominal values of the parameter selected for use were as follows:

R_1 = 50.8Ω (the resistance thermometer)

R_2 = 5000Ω

R_3 = 2500Ω

$R_1 = 50\Omega$

$E = 24$ volts.

When the actual resistors were selected for use in the bridges, these nominal values for R_2 and R_3 were not easily found. The actual value of these resistances used in the circuit were 4960Ω for R_2 and 2410Ω for R_3.

In the construction of the actual bridges, the resistances other than the sensors were potted in epoxy in a phenolic mounting board. This was done to minimize the possibility of damage for the circuit from the vibration environment at the slipper. This mounting board was bolted to the front plate on the slipper, and may be seen in Figure 12 at the top of the large circular opening

4.2 Calibration

When the bridges were constructed, it was not possible to use nominal values of resistances given above. Calibration curves were run by heating the unit slowly and measuring the bridge outputs and temperature. This procedure also made it possible to check the manufacturers' resistance-temperature function, to eliminate the error introduced in the circuit due to lead resistance, and to eliminate the error introduced by the loading effect of the amplifiers into which the bridge output looks.

The initial temperature for the calibration test was $79^{\circ}F$ and the final temperature was $390^{\circ}F$. Figure 20 shows plots of the data obtained.

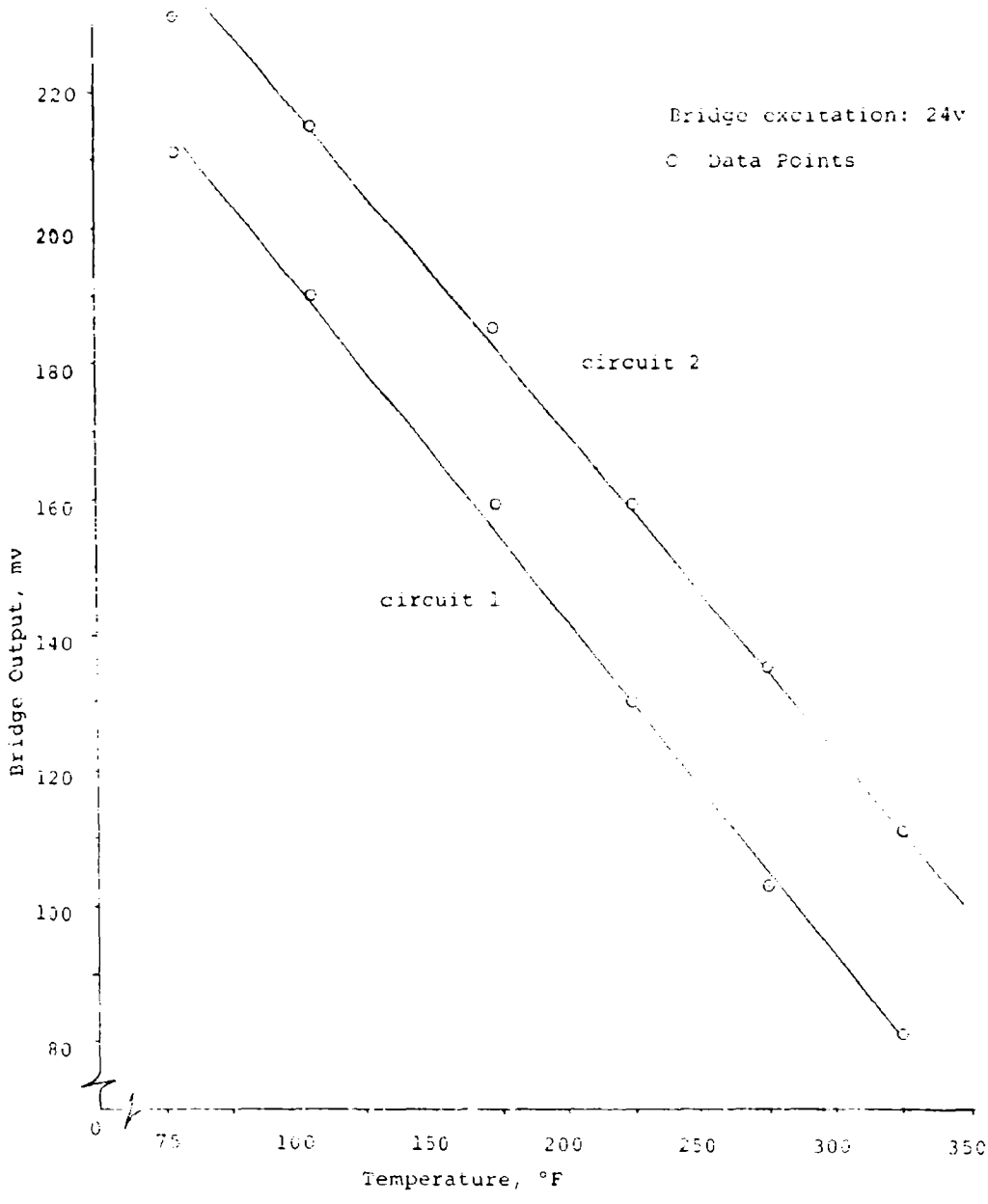

Figure 20. Temperature Circuit Calibration Curves.

Calibration of the circuitry and data records may be done with calibrate resistors, in a manner similar to that used for strain-gage circuits. Table XI gives this information.

Table XI. Calibration of Temperature Measuring Circuits

Calibrate Resistor,[1] - ohms	Output, volts T_1	Output, volts T_2	Change in Output, volts T_1 and	Change in Output, volts T_2	Temperature Change, °F
∞	-.231	-.208	.0		Reference[2]
20 K	-.161	-.139	.070		147
10 K	-.093	-.070	.138		291
5 K	.045	.067	.275		579
4 K	.110	.132	.341		717
3 K	.222	.245	.453		955
2 K	.442	.463	.671		1410

[1]The calibrate resistor is to be placed across the black and red leads.

[2]The reference temperature for this calibration table is 79°F. The temperature during calibration should be recorded. If it is not 79°F the ΔT for the R_{cal} should be added to the actual temperature.

5 - CONCLUSIONS AND RECOMMENDATIONS

The feasibility of measuring force transmitted by a component of a vehicle has been investigated by development of a technique for measuring vertical force on the front slipper of the Chaparral rocket sled. The conclusions from this work are as follows:

1. It was possible to develop a method of measuring a particular force component transmitted by the structure used in this work through instrumentation of the structure itself with electrical resistance strain gages, and meet the specified requirements.
2. The error limits of the measured force are significantly greater than those obtainable with commercial transducers.
3. The bolted joint which is loaded in shear and located in the vicinity of the strain gage location significantly lowers the accuracy of the measurement due to relative motion at the joint causing a zero shift in the circuit.
4. The accuracy of the system due to a zero shift depends on the maximum previous load applied, the magnitude of load of interest, and the recent past load history.
5. If the system is subjected to only a uni-directional force, the accuracy is greatly increased.

Conclusion five will be clarified by an example. If the maximum load previously applied is +35,000 pounds all the succeeding applied loads are greater than zero but less than +35,000 pounds, the accuracy of the measured load will be ± 8% at any magnitude, not just for the peak load.

There is one topic regarding this problem which is not discussed in this section. This concerns the frequency response characteristics of the resulting system. Throughout this development work, static loads have been used, but the unit will be used to measure varying loads. The question arises as to what will be the upper frequency limit on this instrumentation. Theoretical studies have been conducted on this particular problem. Since it is common to essentially all of the force measuring systems developed under this contract and the preceeding ones, the discussion of this work is given in a separate section of this report.

There is one significant recommendation which can be made as a result of this work. In the event other sleds are designed for which there will be a requirement to measure vertical force at the slipper in a manner similar to the Chaparral sled, an effort should be made to avoid transmitting the load from the sled body to the slipper through bolted joints loaded in shear.

III STUDY OF THE "TECH-2" SLED TRANSDUCERS

The purpose of the work done on the Tech-2 sled transducers was to investigate the accuracy of the units as furnished, and to modify the strain gage installation as required to improve the accuracy if this was considered desirable. These transducers, which were designed and constructed by a different agency, were designed to measure vertical load and roll moment when used as a pair. The testing work done involved calibration of the vertical force instrumentation and a check of the accuracy of this channel when the unit is subjected to off-axis loads.

Prior to loading the transducer, it was necessary to design and construct a loading fixture. Figure 21 shows two units of the transducer assembled in the loading fixture.

This unit was loaded to ±20,000 lb. in the vertical direction, ±7,000 lb. in the cross-track direction, and to ±4,000 lb. in the along-the-track direction. In addition, it was subjected to a wide range of combined loads. Figure 22 defines the various loads which were applied. Table XII gives the data obtained and the results. The readings were taken using a Budd Type 350 strain indicator. The applied force values were computed using a sensitivity factor which was determined from the data of load E.

A study of the errors in the measured force indicates that the strain gage instrumentation as originally applied gives results for which the accuracy is significantly less

Figure 21. Tech-2 Transducer in Loading Fixture.

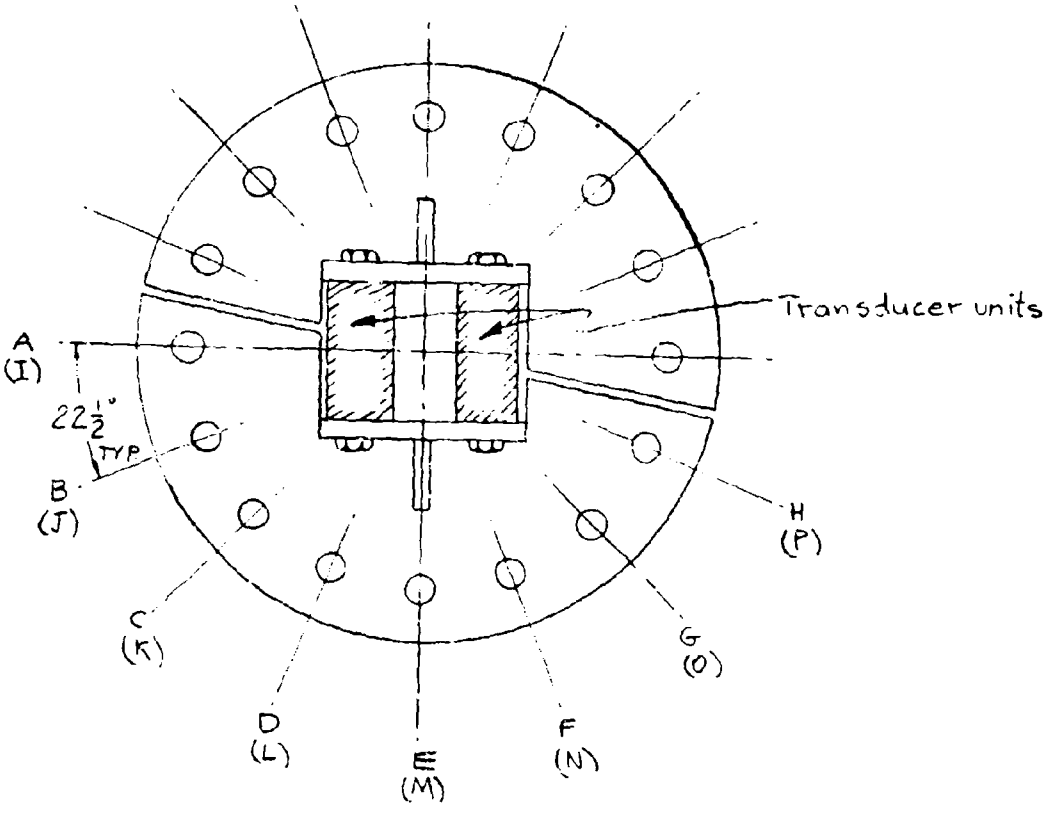

Note:
1. Letter identifies the loading condition.
2. The loading condition with the letter in parentheses is run with the two transducer units notated in the fixture 90° from that shown.

Figure 22. Loading conditions for the Tech-2 Transducer

Table XII. Data and Results for Initial Tests on Tech-2 Transducer

	Load	Reading A	Reading B	Indicated Force A	Indicated Force B	Vertical Force Meas.	Vertical Force Applied	% Error
A	2000	-47	5	-144	15.3	-128.7	0	---
	4000	-74	32	-226	98	-128	0	---
	6000	-94	65	-228	199	-89	0	---
	7000	-109	74	-334	226	-108	0	---
	-2000	47	5	175	18.6	193.6	0	---
	-4000	97	14	360	52	412	0	---
	-6000	142	24	530	85.6	615.6	0	---
	-7000	162	34	605	127	732	0	---
B	2000	54	92	165	282	447	765	-41.5
	4000	137	220	420	675	1095	1530	-28.4
	6000	233	352	715	1080	1795	2300	-22.0
	8000	338	505	1030	1540	2570	3060	-16.0
	-2000	-52	095	-194	-354	-548	-765	-28.4
	-4000	-117	-190	-435	-706	-1141	-1530	-25.2
	-6000	-189	-294	-705	-1095	-1800	-2300	-21.8
	-8000	-265	-410	-985	-1530	-2516	-3060	-17.8
C	2000	148	184	452	562	1014	1410	-28.1
	4000	325	400	995	1220	22[illegible]	2830	-21.8
	6000	510	631	1560	1930	3[illegible]	4240	-17.7
	8000	715	876	2190	2680	48[illegible]	5650	-13.8
	9500	885	1073	2900	3280	6180	6720	-8.0
	-2000	-142	-171	-528	-636	-1164	-1410	-17.4
	-4000	-305	-350	-1160	-1300	-2460	-2830	-13.2
	-6000	-477	-537	-1770	-2000	-3770	-4240	-11.1
	-8000	-643	-736	-2390	-2780	-5770	-5650	-8.5
	-9500	-787	-890	-2930	-3310	-6240	-6720	-7.15
D	3000	341	370	1040	1130	2170	2770	-21.6
	6000	722	790	2210	2420	4630	5550	-16.6
	9000	1132	1232	3460	3760	7220	8310	-13.2
	12000	1580	1716	4840	5250	10090	11100	-9.1
	13500	1822	1974	5570	6050	11620	12500	-7.0
	-3000	-323	-340	-1200	-1265	-2465	-2770	-11.0
	-6000	-674	-707	-2500	-2620	-5120	-5550	-7.75
	-9000	-1032	-1070	-3840	-3990	-7820	-8310	-5.9
	-12000	-1402	-1452	-5200	-5400	-10600	-11100	-4.5
	-13500	-1582	-1638	-5900	-6110	-12000	-12500	-4.0
E	5000	668	659	2040	2010	4050	5000	-1.0
	10000	1480	1470	4525	4500	9025	10000	-.9
	15000	2355	2347	7200	7180	14380	15000	-.4
	20000	3272	3272	10000	10000	20000	20000	0
	-5000	-628	-619	-2340	-2300	-4640	-5000	-7.2
	-10000	-1320	-1273	-4880	-4740	-9620	-10000	-3.8
	-15000	-2030	-1970	-7550	-7450	-15000	-15000	0
	-19000	-2600	-2525	-9650	-9400	-19050	-19000	+2.6

Table XII. (Continued)

	Load	Reading A	Reading B	Indicated Force A	Indicated Force B	Vertical Force Meas.	Vertical Force Applied	% Error
F	3000	392	365	1200	1117	2317	2770	-16.4
	6000	802	755	2460	2310	4770	5550	-14.0
	9000	1277	1182	3900	3620	7520	8310	-9.5
	12000	1680	1800	5150	5500	10650	11100	-4.0
	13500	2080	1936	6350	5920	12270	12500	-1.8
	-3000	-366	-326	-1360	-1210	-2570	-2770	-7.2
	-6000	-738	-636	-2750	-2480	-5230	-5550	-5.75
	-9000	-1150	-1030	-4280	-3840	-8120	-8310	-2.3
	-12000	-1615	-1432	-6000	-5340	-11340	-11100	+2.14
	-13500	-1835	-1645	-6825	-6125	-12950	-12500	+3.60
G	2000	201	175	615	535	1150	1410	-18.4
	4000	418	375	1280	1145	2425	2830	-14.5
	6000	658	590	2020	1800	3820	4240	-9.9
	8000	925	825	2830	2520	5350	5650	-5.3
	9500	1145	1016	3500	3100	6600	6720	-1.8
	-2000	-200	-162	-745	-605	-1350	-1410	-4.25
	-4000	-400	-325	-1490	-1210	-2700	-2830	-4.6
	-6000	-608	-500	-2260	-1860	-4120	-4240	-2.84
	-8000	-840	-695	-3120	-2580	-5700	-5650	+.89
	-9500	-1060	-872	-3940	-3250	-7190	-6720	+7.0
H	2000	124	85	380	324	704	765	-8.0
	4000	264	195	810	595	1405	1530	-8.2
	6000	430	323	1320	995	2315	2300	+1.65
	8000	608	440	1860	1345	3205	3060	+4.7
	-2000	-122	-81	-460	-302	-752	-765	-1.7
	-4000	-244	-160	-910	-595	-1505	-1530	-1.6
	-6000	-364	-238	-1355	-885	-2240	-2300	-1.1
	-8000	-545	-350	-2625	-1300	-3325	-3060	+8.65
I	1000	6	4	78.4	12.3	30.7	0	---
	2000	13	8	39.8	24.5	64.3	0	---
	3000	22	17	67	52	119	0	---
	4000	16	19	49	58	107	0	---
	-1000	-11	+11	-41	41	0	0	---
	-2000	-12	+16	-44.6	59.5	14.5	0	---
	-3000	-12	+16	-44.6	59.5	14.5	0	---
	-4000	-10	+18	-37.2	67	29.8	0	---
J	1000	50	54	153	165	318	380	-16.3%
	2000	98	104	300	318	618	765	-19.3%
	3000	150	158	460	485	945	1150	-18.7
	4500	230	244	705	746	1451	1720	-15.6
	-1000	-44	-46	-164	-173	-337	-380	-11.3
	-2000	-86	-92	-320	-343	-663	-765	-13.4
	-3000	-128	-136	-476	-505	-981	-1150	-14.7
	-4500	-190	-210	-706	-782	-1488	-1720	-13.5

Table XII. (Continued)

	Load	Reading A	Reading B	Indicated Force A	Indicated Force B	Vertical Force Meas.	Vertical Force Applied	% Error
K	2000	158	184	484	564	1048	1410	-25.6
	4000	322	380	985	1160	2145	2830	-24.2
	5500	460	546	1410	1670	3080	3890	-20.8
	-2000	-170	-168	-634	-625	-1259	-1410	-21.4
	-4000	-322	-338	-1200	-1260	-2460	-2830	-13.2
	-5500	-444	-475	-1650	-1770	-3420	-3890	-12.2
L	2000	213	233	652	713	1365	1850	-26.2
	4000	432	469	1320	1430	2756	3700	-25.6
	6000	664	730	2000	2240	4240	5550	-23.6
	8000	928	1015	2840	3100	5940	7400	-19.7
	-2000	-210	-224	-780	-835	-1615	-1850	-12.7
	-4000	-414	-440	-1540	-1640	-3180	-3700	-14.0
	-6000	-622	-662	-2320	-2460	-4780	-5550	-13.9
	-8000	-832	-896	-3100	-3315	-6415	-7400	-13.3
M	5000	580	646	1780	1980	3760	5000	-24.8
	10000	1288	1394	3980	4260	8240	10000	-17.6
	15000	2090	2296	6400	7000	13400	15000	-10.7
	20000	2940	3090	9000	9450	18450	20000	-7.75
	-5000	-556	-598	-2060	-2220	-4280	-5000	-14.4
	-10000	-1126	-1214	-4180	-4525	-8705	-10000	-12.95
	-15000	-1728	-1844	-6425	-6860	-13285	-15000	-11.4
	-19000	-2224	-2356	-8300	-8750	-17050	-19000	-10.3
N	2000	204	236	625	723	1347	1850	-27.2
	4000	418	476	1280	1460	2740	3700	-25.9
	6000	660	732	2020	2040	8260	5550	-23.3
	8000	936	1016	2860	3100	5960	7400	-19.5
	-2000	-207	-210	-770	-780	-1550	-1850	-16.2
	-4000	-420	-418	-1560	-1558	-3118	-3700	-15.7
	-6000	-636	-624	-2370	-2320	-4690	-5550	-15.5
	-8000	-876	-860	-3260	-3200	-6460	-7400	-12.7
O	1000	84	84	257	257	514	707	-27.3
	2000	164	166	507	504	1006	1410	-28.7
	4000	336	342	1030	1048	2078	2830	-26.6
	5500	484	488	1480	1490	2970	3890	-23.6
	-1000	-78	-86	-290	-320	-610	-707	-13.7
	-2000	-152	-168	-565	-625	-1190	-1410	-15.6
	-4000	-300	-322	-1120	-1200	-2320	-2830	-18.0
	-5500	-432	-452	-1610	-1680	-3290	-3890	-15.4
P	1000	42	50	128	153	281	380	-26.0
	2000	83	102	254	132	566	765	-26.0
	3000	128	154	392	470	862	1150	-25.0
	4000	176	204	537	625	1162	1490	-21.0
	4500	198	229	605	700	1305	1720	-24.2
	-1000	-44	-44	-164	-164	-328	-380	-13.7
	-2000	-86	-86	-320	-320	-640	-765	-16.4
	-3000	-124	-126	-460	-470	-930	-1150	-19.2
	-4500	-186	-182	-690	-680	-1370	-1720	-20.2

than desirable. However, in the event it becomes necessary to use a set of transducers instrumented in this way, calibrate resistor information was taken, and this is given in Table XIII.

Since the errors in the initial design were excessive, it was considered necessary to redesign the strain gage installations. Figure 23 describes the revised instrumentation for one of the units of the transducer.

This unit was then retested in a manner identical to that used previously, and the data similarly reduced. The results of these tests are given in Table XIV. Comparison of the errors for the initial and revised design shows some improvement. Specifically, for the combined loads involving a cross-track component, the revised design shows improvement when the cross track component is small, but some loss of accuracy is observed for loads having large cross-track components. For the load conditions involving along-the-track components, there is significant improvement for all but one geometry, and this is the one having no vertical component.

While the improvement in the accuracy of the transducer was not obtained for each loading condition, overall improvement was obtained. Conditions for which there was no improvement were the ones for which the vertical component was small and errors for these conditions are not as important.

The calibrate resistor information for the transducer with the revised instrumentation design is given in Table XV.

Table XIII. Calibrate Resistor Data on Tech-2 Transducer - Initial Instrumentation. Strain Gage Bridge Design.

Unit	R_{cal} ohms	Location[1]	Equivalent Force[2]
A	30,000	BE and A	- 7,500
	20,000	BE and A	-11,100
	10,000	BE and A	-22,200
	30,000	BE and F	+ 6,000
	20,000	BE and F	+ 9,000
	10,000	BE and F	+18,000
B	30,000	G and HL	- 7,500
	20,000	G and HL	-11,100
	10,000	G and HL	-22,200
	30,000	G and KL	+ 6,000
	20,000	G and KL	+ 9,000
	10,000	G and KL	+18,000

[1]The location of the calibrate resistor is specified in terms of the lead wire identification code given on Goodyear Aerospace Corp. drawing number 345N-110.

[2]Positive force indicates tension; negative indicates compression.

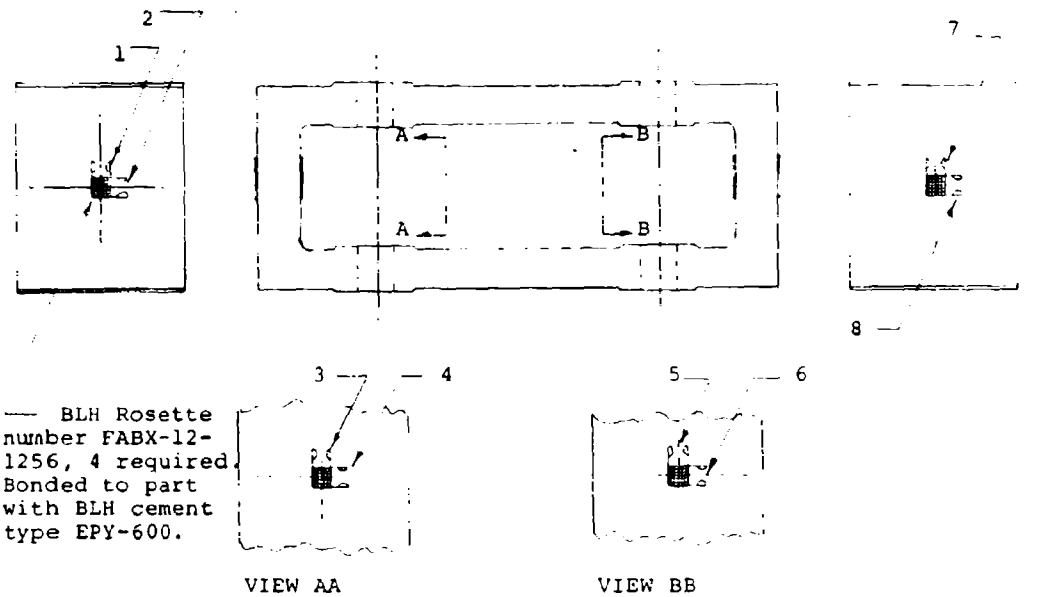

a. Gage installation information

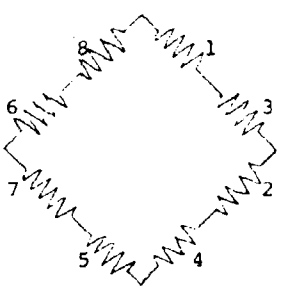

b. Bridge design

Figure 23. Revised Strain Gage Instrumentation for One Unit of Tech-2 Transducer.

Table XIV. Data and Results for Tech-2 Transducer with Revised Instrumentation

	Load	Reading A	Reading B	Indicated Force A	Indicated Force B	Vertical Force Meas.	Vertical Force Applied	% Error
A	2000	-18	-10	-193	-107	-300	0	---
	4000	-30	-20	-320	-214	-534	0	---
	6000	-40	-18	-430	-300	-730	0	---
	7000	-46	-32	-490	-343	-833	0	---
	-2000	16	16	175	175	350	0	---
	-4000	34	22	374	242	616	0	---
	-6000	62	21	680	352	1032	0	---
	-7000	76	30	835	330	1165	0	---
B	2000	26	26	277	277	558	765	-27
	4000	50	50	535	535	1070	1500	-30
	6000	76	82	815	880	1695	2300	-26
	8000	102	102	1090	2180	2180	3060	-29
	-2000	-10	-14	-110	-154	-264	-765	-65
	-4000	-30	-38	-330	-417	-747	-1530	-51
	-6000	-46	-54	-505	-590	-1095	-2300	-52
	-8000	-62	-70	-650	-770	-1450	-3060	-52
C	2000	64	64	685	685	1370	1414	-3
	4000	122	122	1310	1310	2620	2818	-7
	6000	176	176	1880	1880	3760	4242	-13.7
	8000	240	240	2570	2570	5140	5656	-9
	9500	282	282	30200	30200	6040	6720	-10
	-2000	-54	-54	-594	-594	-1188	-1414	-16
	-4000	-112	-112	-1230	-1230	-2460	-2828	-13
	-6000	-158	-158	-1740	-1740	-3480	-4242	-18
	-8000	-210	-210	-2310	-2310	-4620	-5656	-18
	-9500	-248	-248	-2730	-2730	-5460	-6720	-19
D	3000	132	132	1410	1410	2820	2750	2.5
	6000	254	254	2720	2720	5440	5500	1.1
	9000	364	364	3900	3900	7800	8250	5.5
	12000	516	516	5520	5520	11040	11000	.36
	13500	558	558	5970	5970	11940	12400	-3.7
	-3000	-124	-122	-1370	-1340	-2710	-2750	-1.4
	-6000	-248	-238	-2730	-2620	-5350	-5500	-2.7
	-9000	-352	-340	-3870	-3740	-7610	-8250	-8
	-12000	-476	-460	-5240	-5060	-10300	-11000	-6.3
	-13500	-530	-512	-5840	-5650	-11490	-12400	-7.3
E	5000	246	239	2630	2460	5090	5000	1.8
	10000	478	460	5120	4930	10050	10000	0.5
	15000	724	690	7750	7390	15140	15000	1
	20000	958	912	10650	9750	20000	20000	0
	-5000	-256	-236	-2770	-2480	-5250	-5000	-5
	-10000	-476	-446	-5200	-4900	-10100	-10000	-1
	-15000	-696	-664	-7660	-7300	-14960	-15000	≈0
	-20000	-934	-896	-10300	-9800	-20100	-20000	-0.5

	Load	Reading A	Reading B	Indicated Force A	Indicated Force B	Vertical Force Meas.	Vertical Force Applied	% Error
F	3000	150	142	1600	1520	3120	2750	13
	6000	294	274	3140	2930	6070	5500	10
	9000	426	394	4550	4210	8760	8250	6.2
	12000	574	528	6140	5650	11790	11000	7.2
	13500	650	600	6950	6420	13370	12400	9.1
	-3000	-138	-132	-1520	-1450	-2970	-2750	8
	-6000	-274	-262	-3020	-2880	-5900	-5500	7.3
	-9000	-412	-390	-4550	-4300	-8850	-8250	7.2
	-12000	-542	-518	-5970	-5700	-11670	-11000	6
	-13500	-610	-576	-6700	-6340	-13040	-12400	5
G	2000	84	82	900	877	1777	1414	25
	4000	164	154	1750	1650	3400	2828	20
	6000	246	226	2630	2420	5050	4242	19
	8000	324	298	3470	3180	6650	5656	18
	9500	388	350	4150	3740	7890	6720	17
	-2000	-80	-74	-880	-815	-1695	-1414	20
	-4000	-152	-142	-1670	-1560	-3230	-2828	15
	-6000	-222	-208	-2440	-2290	-4730	-4730	12
	-8000	-296	-276	-3220	-3040	-6260	-5656	11
	-9500	-344	-322	-3790	-3550	-7340	-6720	9
H	2000	50	44	535	470	1005	765	31
	4000	108	88	1150	940	2090	1530	37
	6000	164	134	1750	1430	3180	2300	38
	8000	214	180	2290	1930	4220	3060	38
	-2000	-52	-38	-570	-417	-987	-765	29
	-4000	-102	-84	-1125	-922	-2042	-1530	33
	-6000	-144	-122	-1570	-1340	-2930	-2350	27
	-8000	-184	-160	-2050	-1760	-3810	-3060	25
I	1000	0	0	0	0	0	0	0
	2000	2	-6	21	-64	-40	0	---
	3000	6	-12	64	-128	-64	0	---
	4000	12	-12	128	-128	0	0	0
	-1000	-4	10	-44	110	56	0	---
	-2000	-10	21	-110	230	120	0	---
	-3000	-16	30	-176	330	150	0	---
	-4000	-20	36	-220	400	180	0	---
J	1000	18	12	193	127	320	380	-15.7
	2000	42	24	450	257	707	765	-5.8
	3000	62	40	665	430	1095	1150	-3.9
	4500	92	76	1020	810	1830	1720	6.4
	-1000	-16	-8	-176	-88	-264	-380	-30
	-2000	-36	-20	-400	-220	-620	-765	-19
	-3000	-56	-30	-615	-330	-945	-1150	-17.7
	-4500	-86	-46	-945	-505	-1450	-1720	-15.7

Table XIV. (Continued)

	Load	Reading A	Reading B	Indicated Force A	Indicated Force B	Vertical Force Meas.	Vertical Force Applied	% Error
K	2000	72	56	770	600	1370	1414	-0.3
	4000	142	112	1520	1200	2750	2828	-0.3
	5500	200	152	2140	1630	3770	3890	-0.3
	-2000	-72	-56	-790	-615	-1405	-1414	0
	-4000	-146	-144	-1540	-1210	-2750	-2828	-3
	-5500	-194	-144	-2140	-1580	-3720	-3890	-4.5
L	2000	86	86	920	920	1840	1850	0
	4000	170	160	1820	1710	3530	3700	-4.6
	6000	262	240	1800	2560	5360	5550	-3.4
	8000	346	324	3700	3460	7160	7400	-3.2
	-2000	-84	-84	-925	-925	-1850	-1850	0
	-4000	-166	-166	-1820	-1820	-3640	-3700	-1.6
	-6000	-250	-242	-2750	-2660	-5410	-5550	-2.5
	-8000	-336	-314	-3450	-3700	-7150	-7400	-3.4
M	5000	234	220	2510	2360	4870	5000	-2.6
	10000	474	442	5080	4740	9820	10000	-1.8
	15000	716	674	7620	7200	14820	15000	-1.2
	20000	750	898	10200	9620	19820	20000	-0.9
	-5000	-208	-230	-2290	-2530	-4820	-5000	-3.6
	-10000	-414	-450	-4550	-4950	-9500	-10000	-5
	-15000	-622	-668	-6850	-7350	-14200	-15000	-5.5
	-20000	-838	-880	-9200	-9700	-18900	-20000	-5.5
N	2000	80	88	855	940	1795	1850	-3
	4000	160	172	1710	1840	3550	3700	-4
	6000	240	260	2570	2780	5350	5550	-4
	8000	320	350	3420	3740	7160	7400	-3
	-2000	-86	-86	-945	-945	-1890	-1850	-2
	-4000	-160	-168	-1760	-1850	-3610	-3700	-2.4
	-6000	-236	-250	-2600	-2750	-5350	-5550	-3.6
	-8000	-314	-326	-3450	-3590	-7040	-7400	-5
O	2000	54	70	575	750	1325	1414	-0.6
	4000	110	140	1180	1500	2680	2828	-0.5
	5500	152	192	1620	2050	3670	3890	-0.6
	-2000	-52	-66	-570	-725	-1295	-1414	-8.5
	-4000	-104	-134	-1150	-1480	-2630	-2828	-7
	-5500	-142	-182	-1560	-2000	-3560	-3890	-8.5
P	1000	10	20	110	220	330	380	-15.7
	2000	22	40	236	430	666	765	-12.9
	3000	36	60	385	642	1027	1150	-10.7
	4500	56	92	600	985	1585	1720	-7.9
	-1000						-380	
	-2000						-765	
	-3000						-1150	
	-4500						-1720	

Table XV Calibrate Resistor Data On Tech-2 Transducer--Revised Instrumentation

R_{cal} Ohms	Across Colors	Indicator Deflection	Indicated Force Pounds
1Meg	Green	+123	+1320
500K	and	+242	+2590
200K	Red	+605	+6475
100K		+1205	+12900
50K		+2420	+25900
1Meg	Green	-123	-1350
500K	and	-242	-2660
200K	White	-605	-6650
100K		-1205	-1325
50K		-2420	_26600

IV INSTRUMENTATION OF THE TRANSDUCER FOR THE MODULAR MONORAIL SLED

The hardware for the modular monorail sled transducer was furnished to the contractor for instrumentation in a manner to permit measurement of vertical force and roll moment. The work involved on this problem involved placement of strain gages, wiring of the bridge circuits, calibration, and testing under combined load conditions.

The strain gages which were mounted on this unit were BLH biaxial rosettes type FAB-25-12S6. A total of eight of these rosettes were used, two on each of the four legs of the hardware. Each rosette was mounted so it was centered on the large edge of each leg, with one gage of the rosette aligned with the vertical load axis of the unit. The cement used for bonding was BLH cement type EPY600. This cement was reported to be useful for temperatures to 600°F.

The bridge design was similar to that used in previous transducers. Two bridges were used. One involved all the strain gages on the two legs which were on one side of the track, and the other including the gages on the legs on the other side of the track. Each bridge was wired to measure the vertical force on its side of the track. Gages along the vertical axis were in opposite legs (2 in each leg), and gages in the transverse direction were in opposite legs. This method gave two bridges, each having a resistance across corners of 240Ω. The vector sum of the forces as

measured by the two bridges gives the total vertical force acting; and the vector difference multiplied by the effective distance between the two forces gives the roll moment. Figure 24 shows the completed unit.

Loading of this unit, both for calibration and for the combined load tests was accomplished using a loading fixture which was furnished. It is shown in Figure 25. Figures 26 and 27 describe the various loads which were applied to the transducer using this fixture. Load conditions A and AA correspond to the calibration loads. The others are tests, involving the application of more than one component of force.

The data and results of these tests are shown in Table XVI. The output of the bridges was read with a Budd P-350 strain indicator, as on other transducer tests. The measured force was computed from the indicator reading using a sensitivity factor of 180lb/unit of deflection, for both bridge 1 and 2. The value for "measured moment" and "false moment" was computed using 1.75" as the distance between F_1 and F_2. A review of the errors in vertical force obtained with this unit show that the accuracy of force measurement possible with this unit are very good.

Table XVII gives the calibration data required to calibrate the circuits during use. This calibration information may be stated in terms of the output voltage. This value for the sensitivity is 0.0279mv out/volt for each 1000 lb of force.

Figure 24. Modular Monorail Force Transducer.

Figure 25. Loading Fixture for Modular Monorail Transducer.

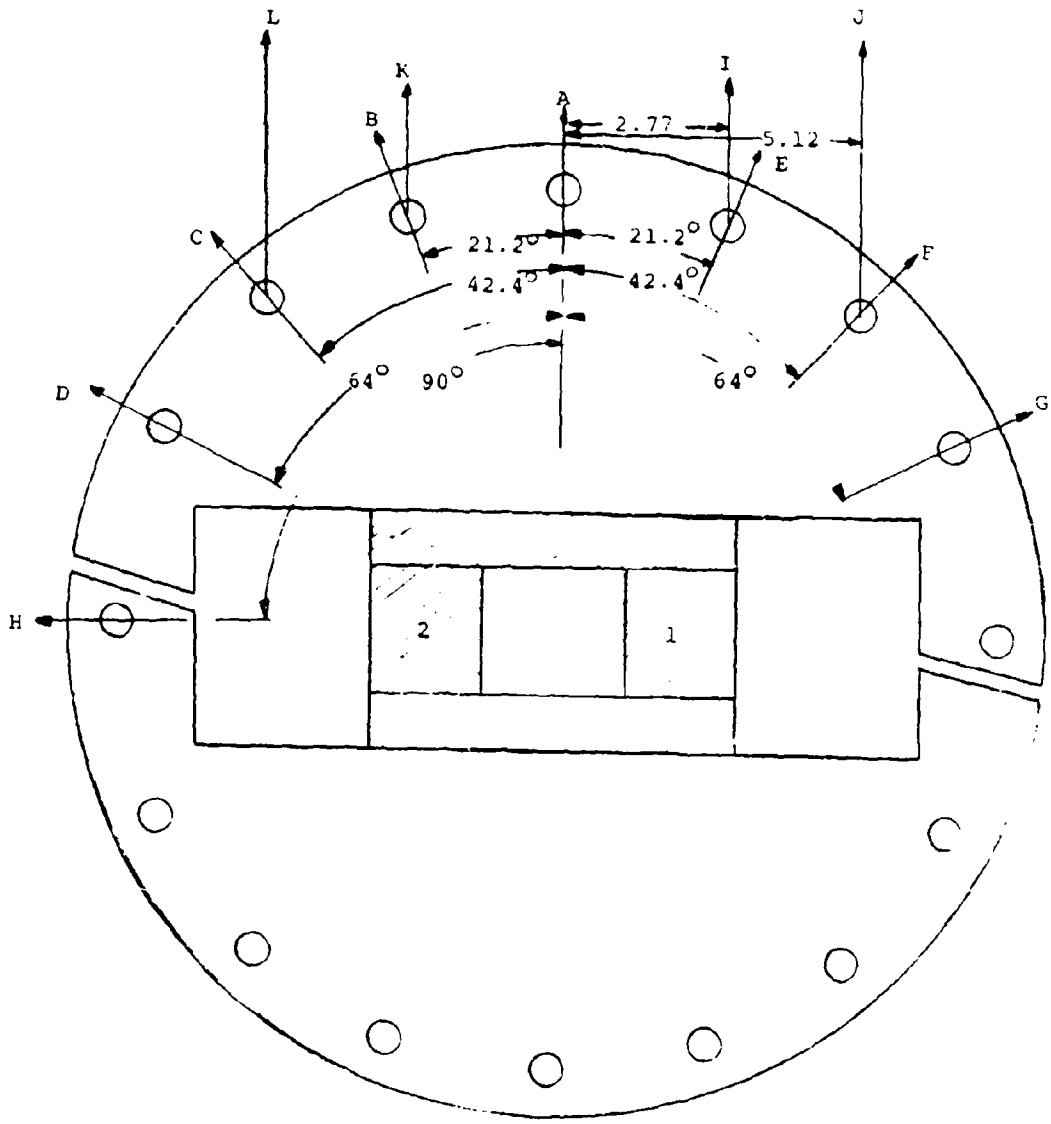

Figure 26. Load Definitions for Modular Monorail Transducer Tests - Cross-track components and moment.

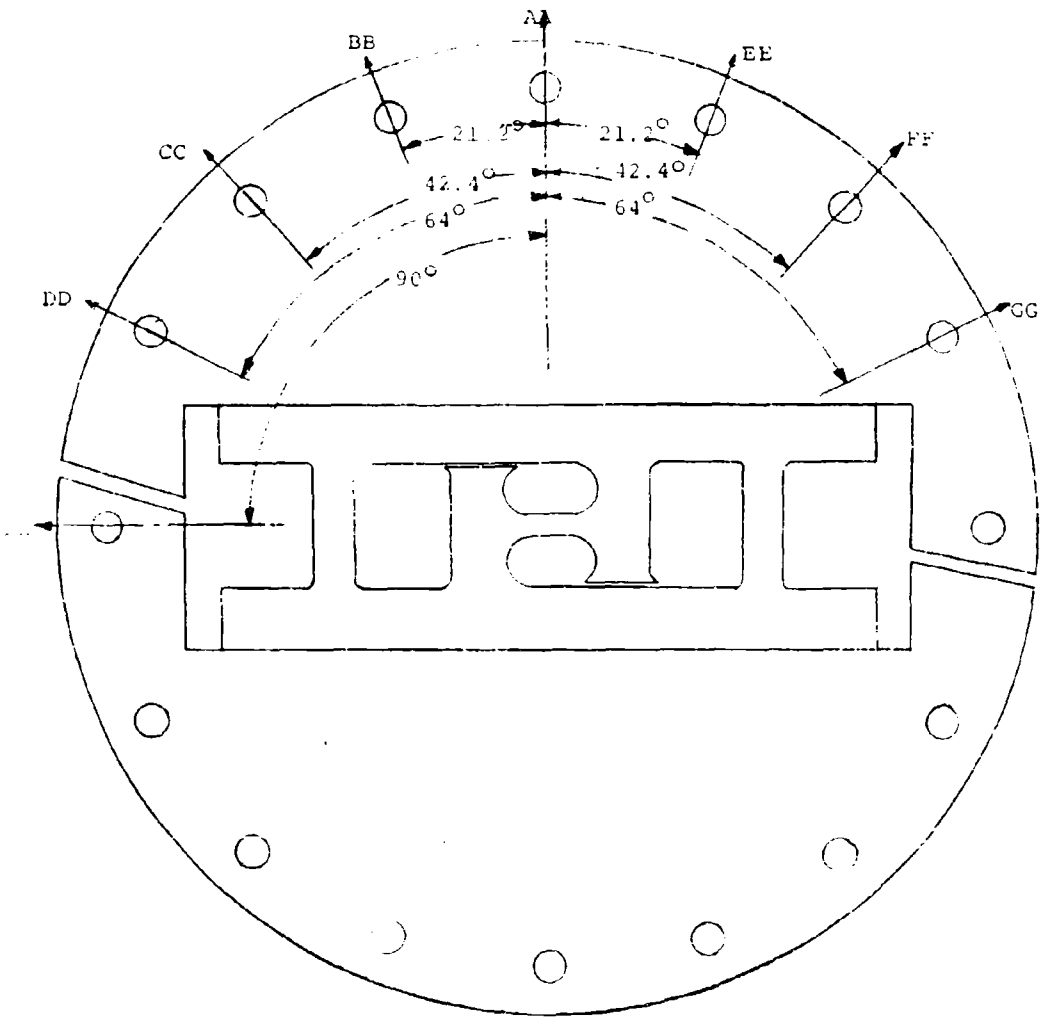

Figure 27. Load Definitions for Modular Monorail Transducer Tests - Along-the-track components.

Table XVI. Data and Results of Load Tests on Modular Monorail Transducer

Load Number	Load Pounds	Indicator Deflection F_1	Indicator Deflection F_2	Measured Force Pounds F_1	Measured Force Pounds F_2	False Moment Inch Pounds	Vertical Force Applied	Vertical Force Measured	Error Pounds	% Error
A	10K	280	250	5040	5040	0	10K	1080	+80	+.8
	20K	544	558	9780	10100	-560	20K	19880	-120	-.6
	30K	830	844	14920	15200	-490	30K	30120	+120	+.4
	40K	1100	1130	19800	20200	-700	40K	40K	0	0
	50K	1390	1410	2500	25400	-700	50K	50400	+400	+.8
	-10K	-275	-285	-4950	-5140	+300	-10K	-10090	+90	+1
	-20K	-540	-565	-9725	-10200	+830	-20K	-19925	-75	-0.4
	-30K	-820	-840	-14750	-15100	+610	-30K	-29850	-150	-0.5
	-40K	-1070	-1115	-19300	-20100	+1400	-40K	-39400	-600	-1.5
	-50K	-1325	-1380	-23900	-24850	+1650	-50K	-48750	-1250	-2.5
B	10K	240	275	525	4950	-1100	9320	9275	-45	-.5
	20K	490	530	8825	9550	-1260	18640	18375	-265	-1.4
	30K	760	810	13700	14600	-1570	27960	28300	+340	+1.2
	40K	1025	1080	18450	19400	-1650	37280	37850	+470	+1.3
	-10K	-240	-270	-4320	-4860	+950	-9320	-9275	+45	+0.5
	-20K	-470	-540	-8450	-9720	+2200	-18640	-18375	+265	+1.4
	-30K	-705	-805	-12700	-14500	+3150	-27960	-28300	+340	+1.2
	-40K	-930	-1070	-16730	-19250	+4400	-37280	-37850	+570	+1.5

Table XVI (continued)

Load Number	Load Pounds	Indicator Deflection F_1	F_2	Measured Force Pounds F_1	F_2	False Moment Inch Pounds	Vertical Force Applied	Measured	Error Pounds	% Error
C	5K	90	105	1620	1890	-470	3710	3510	-200	-5.5
	10K	185	215	3330	3860	-925	7420	7190	-230	-3.1
	15K	285	320	5140	5750	-1070	11130	10890	-240	-2.2
	20K	380	425	6850	7650	-1400	14840	14500	-340	-2.3
	-5K	-90	-115	-1620	-2070	+790	-3710	-3690	-20	-0.6
	-10K	-175	-220	-3150	-3950	+1400	-7420	-7100	-320	-4.4
	-15K	-260	-325	-4675	-5850	+2100	-11130	-10525	-600	-5.4
	-20K	-340	-430	-6120	-7740	+2800	-14840	-13860	-980	-6.6
D	5K	48	70	865	1260	-700	2190	2025	-165	-7.5
	10K	100	135	1800	2430	-1100	4380	4230	-150	-3.4
	15K	155	200	2790	3600	-1420	6570	6390	-180	-2.8
	20K	220	265	3950	4760	-1420	8760	8710	-50	-.6
	-5K	-45	-70	-810	-1260	+790	-2190	-2070	-120	-5.5
	-10K	-85	-140	-1530	-2520	+1750	-4380	-4050	-330	-7.5
	-15K	-120	-200	-2160	-3600	+2500	-6570	-5760	-810	-12
	-20K	-160	-265	-2880	-4760	+3300	-8760	-7640	-1120	-13
E	10K	265	265	4775	4775	0	9320	9550	+230	+2.4
	20K	530	525	9450	9550	-175	18640	19000	+360	+1.9
	30K	780	800	14050	14400	-610	27960	28450	+490	+1.7

Table XVI (continued)

Load Number	Load Pounds	Indicator Deflection F_1	Indicator Deflection F_2	Measured Force Pounds F_1	Measured Force Pounds F_2	False Moment Inch Pounds	Vertical Force Applied	Vertical Force Measured	Error Pounds	% Error
E	40K	1050	1080	18900	19450	-960	37380	38350	+970	+2.5
	-10K	-270	-255	-4850	-4600	-440	-9320	-9450	+130	+1.4
	-20K	-535	-500	-9620	-9000	-1080	-18640	-18620	-20	≈0
	-30K	-795	-750	-14300	-13500	-1400	-27960	-27800	-160	-0.6
	-40K	-1050	-990	-18900	-17700	-2100	-37380	-36600	-780	-2.1
F	5K	115	100	2070	1800	+470	3710	3870	+160	+4.3
	10K	230	205	4140	3690	+960	7420	7830	+450	+5.5
	15K	330	310	5940	5580	+630	11130	11520	+390	+3.5
	20K	445	410	8000	7390	+1070	14840	15390	+530	+3.6
	-5K	-115	-95	-2070	-1710	-630	-3710	-3780	+70	+1.9
	-10K	-230	-190	-4140	-3420	-1220	-7420	-7560	+140	+1.9
	-15K	-340	-385	-6120	-5120	-1750	-11130	-11240	-90	-0.8
	-20K	-450	-370	-8100	-6650	-2540	-14840	-14750	-90	-0.6
G	5K	75	60	1350	1080	+470	2190	2430	+240	-11
	10K	155	120	2790	2160	+1100	4380	4950	+570	-13
	15K	230	185	4140	3330	+1400	6570	7470	+1100	-17
	20K	310	245	5570	4400	+2020	8760	9970	+1320	-13

Table XVI (continued)

Load Number	Load Pounds	Indicator Deflection F_1	Indicator Deflection F_2	Measured Force Pounds F_1	Measured Force Pounds F_2	False Moment Inch Pounds	Vertical Force Applied	Vertical Force Measured	Error Pounds	% Error
G	-5K	-75	-45	-1350	-810	-1300	-2190	-2160	-30	-1.5
	-10K	-150	-95	-2700	-2700	-3000	-4380	-4410	+30	+0.8
	-15K	-220	-145	-3950	-2610	-4100	-6570	-6560	0	0
	-20K	-280	-190	-5050	-3420	-2850	-8760	-8470	-300	-3.5
H	5K	20	-8	360	144	+1050	0	216	216	---
	10K	45	-10	810	-180	+1730	0	630	630	---
	15K	65	-12	1170	216	+2450	0	950	950	---
	20K	95	-6	1710	-108	+3200	0	1600	1600	---
	-5K	-25	+8	-450	+140	-1030	0	-310	-310	---
	-10K	-50	+9	-900	+160	-1850	0	-740	-740	---
	-15K	-45	+35	-810	+630	-2520	0	-180	-180	---
	-20K	-35	+70	-630	+1260	-3300	0	-630	-630	---
AA	10K	275	295	4950	5300	-610	10K	10250	+250	+2.5
	20K	560	580	10100	10450	-610	20K	20550	+550	+2.7
	30K	840	880	15100	15800	-1220	30K	30900	+900	+3
	40K	1130	1170	20300	21100	-1400	40K	41400	+1400	+3.5
	50K	1410	1460	25400	26300	-1580	50K	51700	+1700	+3.4

Table XVI (continued)

Load Number	Load Pounds	Indicator Deflection F_1	Indicator Deflection F_2	Measured Force Pounds F_1	Measured Force Pounds F_2	False Moment Inch Pounds	Vertical Force Applied	Vertical Force Measured	Error Pounds	% Error
AA	-10K	-310	-265	-5570	-4770	-1440	-10K	-10340	+340	+3.4
	-20K	-605	-535	-10900	-9620	-2250	-20K	-20520	+520	+2.6
	-30K	-890	-810	-16000	-14600	-2450	-30K	-30600	+600	+2
	-40K	-1180	-1090	-21200	-19600	-2800	-40K	-41800	+1800	+4.2
	-50K	-1460	-1370	-26300	-24700	-3000	-50K	-51000	+1000	+2
BB	10K	270	270	4850	4850	0	9320	9700	+380	+4
	20K	540	540	9720	9720	0	18640	19440	+800	+4.2
	30K	820	820	14750	14750	0	27960	29500	+1540	+5.5
	40K	1100	1100	19800	19800	0	37280	39600	+2320	+6.2
	-10K	-280	-265	-5050	-4760	-500	-9320	-9810	+490	+5.3
	-20K	-550	-530	-9900	-9550	-610	-18640	-19450	+810	+4.3
	-30K	-825	-800	-14850	-14400	-790	-27960	-29250	+1290	+4.6
	-40K	-1090	-1060	-19600	-19100	-870	-37280	-38700	+1420	+3.8
CC	5K	100	120	1800	2160	-630	3710	3960	+250	+6.7
	10K	200	230	3600	4140	-950	7420	7740	+280	+3.8
	15K	300	350	5400	6300	-1570	11130	11700	+570	+5.1
	20K	405	465	7300	8360	-1650	14840	15660	+820	+5.5
	-5K	-110	-110	-1980	-1980	0	-3710	-3960	+250	+6.7
	-10K	-220	-220	-3960	-3960	0	-7420	-7920	+500	+6.7

Table XVI (continued)

Load Number	Load Pounds	Indicator Deflection F_1	F_2	Measured Force Pounds F_1	F_2	False Moment Inch Pounds	Vertical Force Applied	Measured	Error Pounds	% Error
CC	-15K	-330	-330	-5840	-5840	0	-11130	-11680	+550	+4.7
	-20K	-430	-430	-7740	-7740	0	-14840	-15480	+640	+4.2
DD	5K	60	70	1080	1260	-310	2190	2340	+150	+6.8
	10K	140	140	2160	2520	-630	4380	4680	+300	+6.8
	15K	185	210	3330	3780	-780	6570	7110	+540	+8.2
	20K	250	285	4500	5140	-1110	8760	9640	+880	+10
	-5K	-70	-70	-1260	-1260	0	-2190	-2320	+130	+5.9
	-10K	-130	-130	-2340	-2340	0	-4380	-4680	+300	+6.8
	-15K	-190	-200	-3420	-3600	+310	-6570	-7020	+450	+6.8
	-20K	-260	-270	-4675	-4860	+320	-8760	-9535	+775	+9
EE	10K	255	275	4700	4950	-440	9320	9650	+330	+3.5
	20K	510	540	9170	9700	-930	18640	18970	+330	+1.8
	30K	770	805	13850	14000	-260	27960	27850	-110	-0.4
	40K	1030	1070	18500	19300	-1400	37280	37800	+520	+1.4
	-10K	-295	-230	-5300	-4140	-2000	-9320	-9440	+120	+1.3
	-20K	-570	-470	-10250	-8550	-3000	-18640	-18800	+160	+0.9
	-30K	-845	-710	-15200	-12800	-4200	-27960	-27960	+40	0
	-40K	-1110	-965	-20000	-17500	-4400	-37280	-37500	+220	+0.6

Table XVI (continued)

Load Number	Load Pounds	Indicator Deflection F_1	Indicator Deflection F_2	Measured Force Pounds F_1	Measured Force Pounds F_2	False Moment Inch Pounds	Vertical Force Applied	Vertical Force Measured	Error Pounds	% Error
FF	5K	100	105	1800	1890	-150	3710	3690	-20	-0.6
	10K	200	205	3600	3690	-150	7420	7290	-130	-1.8
	15K	300	310	5400	5570	-300	11130	10970	-160	-1.5
	20K	400	410	7200	7400	-350	14840	14600	-240	-1.6
	-5K	-120	-85	-2160	-1530	-1100	-3710	-3690	-20	-0.6
	-10K	-235	-170	-4050	-3060	-1800	-7420	-7110	-310	-4.2
	-15K	-345	-260	-6200	-4680	-2640	-11130	-10880	-250	-2.3
	-20K	-455	-350	-8200	-6300	-3300	-14840	-14500	-340	-2.3
GG	5K	60	55	1070	990	+140	2190	2060	-130	-5.9
	10K	125	110	2250	1980	+470	4380	4230	-150	-3.4
	15K	185	160	3330	2880	+790	6570	6210	-360	-5.5
	20K	250	215	4500	3870	+1100	8760	8370	-390	-4.5
	-5K	-70	-50	-1260	-900	-630	-2190	-2160	-30	-1.5
	-10K	-140	-90	-2520	-1620	-1570	-4380	-4140	-240	-5.5
	-15K	-210	-140	-3780	-2520	-2200	-6570	-6300	-270	-4.1
	-20K	-275	-190	-4950	-3420	-2650	-8760	-8370	-390	-4.5

Table XVI (continued)

Load Number	Load Pounds	Indicator Deflection F_1	Indicator Deflection F_2	Measured Force Pounds F_1	Measured Force Pounds F_2	False Moment Inch Pounds	Vertical Force Applied	Vertical Force Measured	Error Pounds	% Error
III	5K	-5	-20	-90	-360	+470	0	-450	-450	---
	10K	-8	-35	-144	-630	+840	0	-774	-774	---
	15K	-5	-50	-90	-900	+1410	0	-990	-990	---
	20K	0	-60	0	-1080	+1900	0	-1080	-1080	---
	-5K	+5	+10	+90	+180	-160	0	+270	+270	---
	-10K	+10	+33	+180	+580	-700	0	+760	+760	---
	-15K	+15	+40	+270	+720	-790	0	+990	+990	---
	-20K	+20	+50	+360	+900	-950	0	+1260	+1260	---

Table XVI (continued)

Load Number	Vertical Force	Moment Applied	Indicator Deflection F_1	F_2	Force Measured F_1	F_2	Vertical Pounds	Error Pounds	% Error	Moment Measured	Error Inch Pounds	% Error
I	2K	5540	138	-30	2485	-540	1945	-55	-2.7	5300	-240	-4.2
	4K	11080	275	-54	4950	-970	3980	-20	-0.5	10350	-730	-6.6
	6K	16620	406	-78	7300	-1400	5900	-100	-1.7	15200	-1420	-8.5
	8K	22160	545	-104	9820	-1870	7950	-50	-0.6	20450	-1710	-7.8
J	2K	10240	196	-97	3520	-1750	1770	-230	-11	9250	-990	-9.8
	4K	20480	405	-192	7300	-3460	3840	-160	-4	18900	-1580	-7.7
	5K	25600	512	-238	9225	-4275	4950	-50	-1	23800	-1800	-7
K	2K	-5540	-30	140	-540	2520	1980	-20	-1	-5350	-190	-3.4
	4K	-11080	-58	278	-1040	5000	3960	-40	-1	-10600	-480	-4.3
	6K	-16620	-80	410	-1440	7380	5940	-60	-1	-17200	-580	-3.5
	8K	-22160	-106	545	-1910	9800	7890	-110	-1.3	-20500	-1660	-7.5
L	2K	-10240	-98	210	-1770	3780	2010	+10	+0.5	-9720	-520	-5.1
	4K	-20480	-190	415	-3420	7450	4030	+30	+0.8	-19000	-1480	-9.2
	6K	-25600	-235	520	-4240	9350	5110	+110	+2.2	-23800	-1800	-7.0

Table XVII. Calibrate Resistor Data on Modular Monorail Transducer

Calibrate Resistor, Ω	Indicator Deflection	Equivalent Force
1,000,000	123	2,200
500,000	243	4,350
200,000	596	10,500
100,000	1198	21,500
50,000	2395	43,000

Note: 1. Resistors having a tolerance of 1% or less should be used.

2. On Side 1, the calibrate resistor across black and green is equivalent to a compressive force.

3. On Side 2, the calibrate resistor across white and green is equivalent to a compressive force.

V DYNAMIC RESPONSE OF A STRAIN-GAGED FORCE LINK

1 - INTRODUCTION

In many problems involving force measurement, a commonly used solution is to place strain gages on a link which transmits the load in simple tension or compression. The strain gage readings are related to the applied forces through a calibration curve obtained under static conditions. When these force-links are used to measure dynamic loads, it is then necessary to consider the conditions under which the static calibration curve may be used for reduction of dynamic data.

If the load on the link is static, the strain (and hence the strain reading) is a function of the applied load only, and accurate measurements would be obtainable with the force-link. However, if the load is dynamic, the strain in the link is a function of position and time due to the finite wave propagation velocity of the strain wave, as well as the applied load. Under these conditions, there will be a time lag between the applied pulse and the strain in the gages. In addition, there will be reflections of the strain wave from the other end of the force link, which is usually fixed. These reflected waves will be superimposed on the wave of the applied load. Each of the above factors will cause a distortion of the measured force when the frequency content of the applied force is too high.

The purpose of the work undertaken for this section of the report was to investigate the degree of distortion of impulsive forces when measured by a force-link of this type using wave propagation theory. Since the instrumentation of the Chaparral sled and force transducers developed for sled use are based upon the same principle as force links of the nature discussed above, the results of this work are directly applicable to these units.

This investigation is based upon wave propagation theory, since the frequency response limit is caused by the time delays due to a finite wave propagation velocity. The appropriate differential equation was solved with the desired boundary and initial conditions using a numerical technique.

2 - THEORY

The theory upon which this study is based is that of the one-dimensional wave equation. The form of the equation used for this study applies to the propagation of elastic waves in a rod. When the dependent variable is the strain in the bar, it may be written as:

$$\frac{\partial^2 \varepsilon}{\partial x^2} = \frac{E}{\rho} \frac{\partial^2 \varepsilon}{\partial t^2} \qquad (5.2.1)$$

where ε = longitudinal strain in the bar

x = position coordinate of the particle of interest

t = time

E = modulus of elasticity of the bar material

ρ = density of the bar material.

The travelling wave solution to this equation may be used to show that $\sqrt{\frac{E}{\rho}}$ is the propagation velocity of the strain wave and c will be used to represent this quantity.

The assumptions used in deriving this equation are as follows:

1. Strain is one-dimensional.
2. Material is linearly elastic.
3. Stress is uniformly distributed across cross-sectional area.

Figure 28 shows a sketch of the system to which this equation will be applied. This sketch represents a force link fixed at one end with the forcing function to be

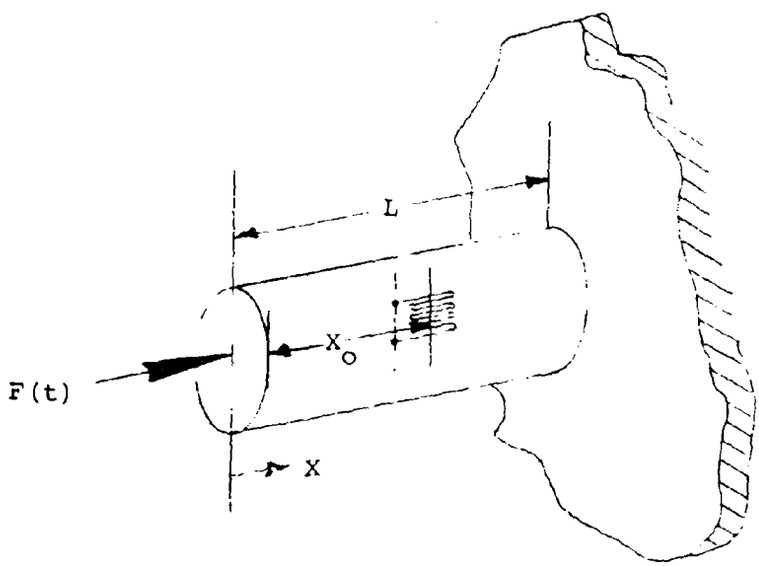

Figure 28. Description of Force Link

measured, (Ft), applied at the other end. The cross section of the link is not restricted to being circular. Strain gages are normally mounted on the surface of the link at some position, and force measurement is based upon their signal.

To determine the pulse signature which would be obtianed from the gages for a given forcing function applied at the free end, the governing equation must be solved for $\varepsilon(x_o,t)$. The required initial and boundary conditions are as follows:

$$\varepsilon(x,0) = 0 \tag{5.2.2}$$

$$\frac{\partial U}{\partial t}(x,0) = 0 \tag{5.2.3}$$

$$\frac{\partial U}{\partial t}(L,t) = 0 \tag{5.2.4}$$

$$\varepsilon(0,t) = \frac{F(t)}{AE} \tag{5.2.5}$$

where U is particle displacement and $\frac{\partial U}{\partial t}$ is particle velocity.

The technique used for solving this problem was that of characteristics. This method of solving partial differential equations of this type has been well discussed in the literature, for example, in Crandall[1]; and the description here will be limited to how it was applied to this problem.

[1]Crandall, S. H., "Engineering Analysis," McGraw-Hill Book Co., Inc., 1956.

The plane of interest is the x - t plane, as shown in Figure 27. The dependent variable σ must be calculated at each grid point in a manner such that equations 1 through 5 are satisfied. The difference equations for making these calculations take on three separate forms for the three regions, i.e., the boundary at x = 0, an interior point, and the boundary at x = L. These difference equations are:

$$x = 0 \quad (\sigma_P - \sigma_S) + \rho c(v_P - v_S) = 0, \text{ along } -c \qquad (5.2.6)$$

$$\sigma_P = \frac{F(t_o)}{A}, \text{ from the boundary condition} \qquad (5.2.7)$$

$$0<x<L \quad (\sigma_P - \sigma_Q) - \rho c(v_P - v_Q) = 0, \text{ along } +c \qquad (5.2.8)$$

$$(\sigma_P - \sigma_S) + \rho c(v_P - v_S) = 0, \text{ along } -c \qquad (5.2.9)$$

$$x = L \quad (\sigma_P - \sigma_Q) - \rho c(v_P - v_Q) = 0, \text{ along } +c \qquad (5.2.10)$$

$$v_Q = 0, \text{ from the boundary condition} \qquad (5.2.11)$$

In these equations, σ, v and A are the stress, particle velocity and bar area respectively, and the subscripts P, Q and S identify the corresponding point in the (x,t) plane. The points for each set of equations are identified in Figure 29. The point P identifies the node at which the variables are being computed. Subscripts Q and S identify points for which the variables have been determined from previous calculations, or were known from the boundary and initial conditions. These equations were solved for the desired dependent variable at each point and evaluation of the resulting equations in the appropriate order was done

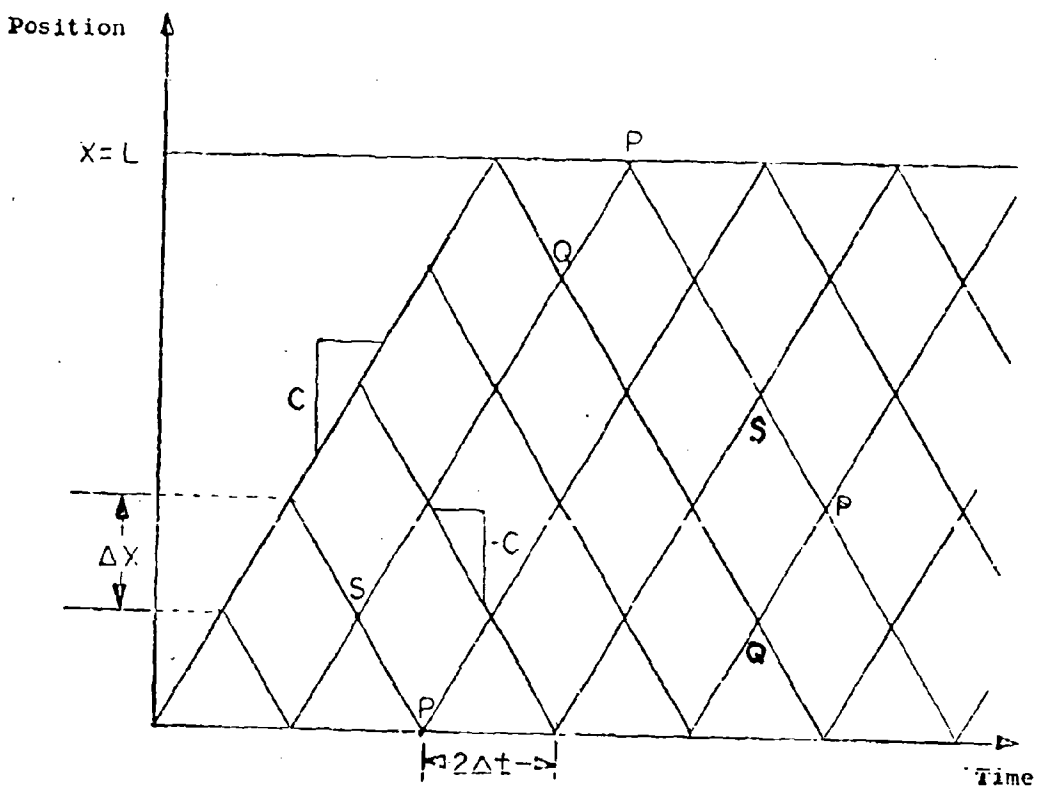

Figure 29. Characteristic Plane.

on a digital computer.

There is one important deficiency in the theory as applied to this problem. This is the fact that the theory is based on a perfectly elastic material, and consequently will not account for losses. When a disturbance propagates through a real material, there will be an attenuation of the disturbance due to internal friction. This will cause a decay of the amplitude of the disturbance with time. The results from this study will not show this decay.

3 - PROCEDURE

The equations were solved for three types of forcing functions. One was the ramp function as shown in Figure 30. This function was used to determine the effect of rise time on the measured force. In this study, τ, was the rise time, and solutions were obtained for rise times varying from 1.0 L/c to 30.0 L/c. The quantity (L/c) represents the time required for the disturbance to travel one length of the force link.

Another forcing function used was a half sine pulse as shown in Figure 31. This was used to determine the response for a transient representative of what might be encountered in use. The pulse duration here is Γ, and computations were made for this pulse for Γ from 1.0 L/c to 20 L/c.

The last type of excitation used was a steady state sinusoidal pulse. This was used to obtain information related to what would be considered the frequency response of the force link. The time parameter used to define these pulses was the time required for one complete period of the pulse, and the symbol used for this was also Γ.

In performing the computations, 11 grid points were used along the length of the force link, which gave information on the strain distribution along the force link in increments of 0.1 L. The time increment, Δt, was then determined from the slope of the characteristic lines.

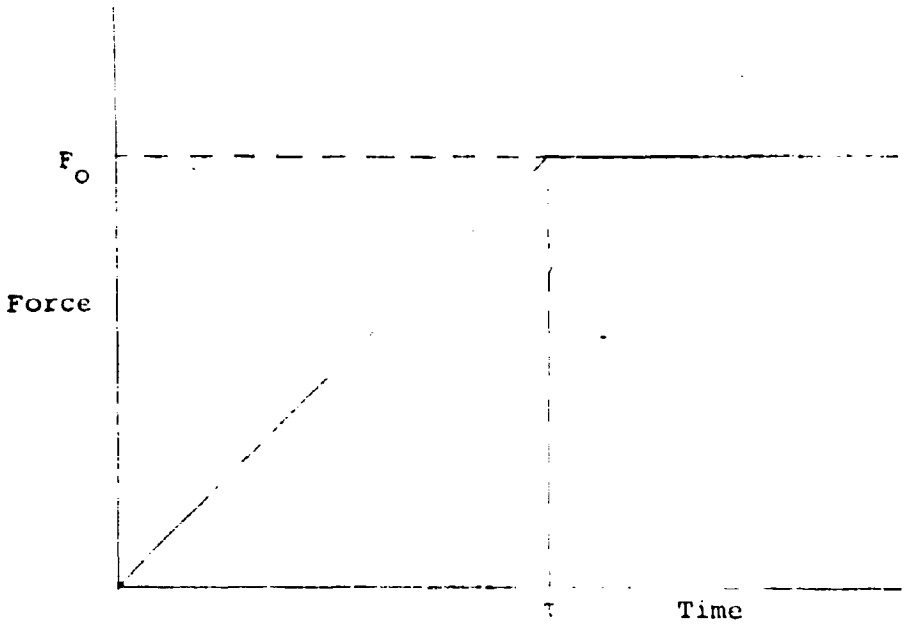

Figure 30. Ramp Function Pulse

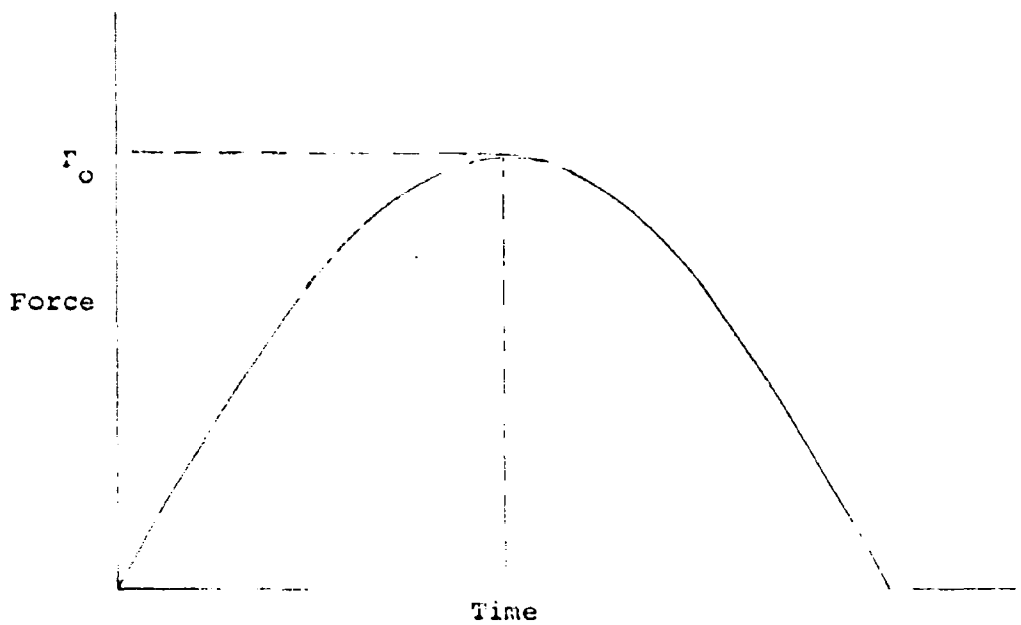

Figure 31. Half Sine Pulse

The numerical values of the material properties used in the computations were those of steel, but since all results were presented in nondimensional form, this was not restrictive on the applicability of the results.

In the computation of the force as would be measured by the transducer from the strain in the link, it was assumed that the strain indicated by a gage having a finite length would be the same as for a zero length gage located at the desired position. Use was then made of the relation,

$$F = \varepsilon EA \qquad (5.2.12)$$

to determine the force from the strain values.

4 - RESULTS

The results of this work indicate that the fidelity of the measured pulse is dependent upon both the position of the strain gages on the bar and the time parameter used in defining the inputs. The effect of these parameters on the measured pulse is most easily seen through a study of typical results. Figures 32 through 34 show results for the ramp function, Figures 35 through 39 show similar plots for the half sine pulse. The results for the harmonic excitation are shown in Figures 40 through 44.

The results for the half sine pulse and harmonic forcing are significant enough for further discussion. For the half sine pulse, it is noted that there is a considerable amount of "ringing" of the transducer for the shorter pulses. In this case, "ringing" is used to mean that the signal does not go to zero after the applied force does, but continues to oscillate. This phenomenon may explain the appearance of some of the data obtained with force transducers during sled runs. In addition to the ringing, these results also show considerable amplitude and phase distortion. For the longest pulse runs, i.e., $\tau = 20L/c$, it is noted that fairing of the data would tend to eliminate both the phase and amplitude distortion, but if this was not done, the peak measured force could be off by as much as 15%.

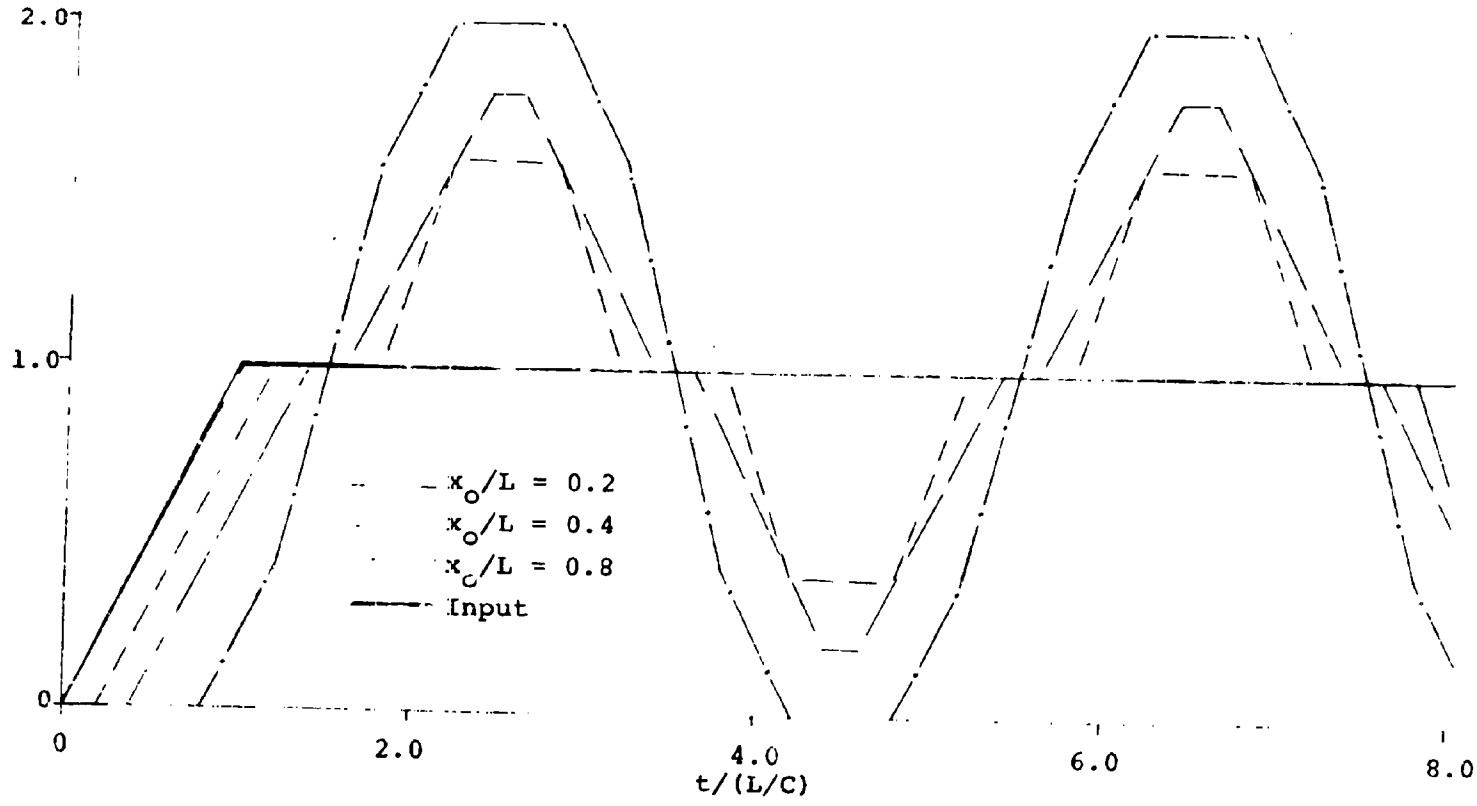

Figure 32. Ramp Function Results: = 1.0 L/C

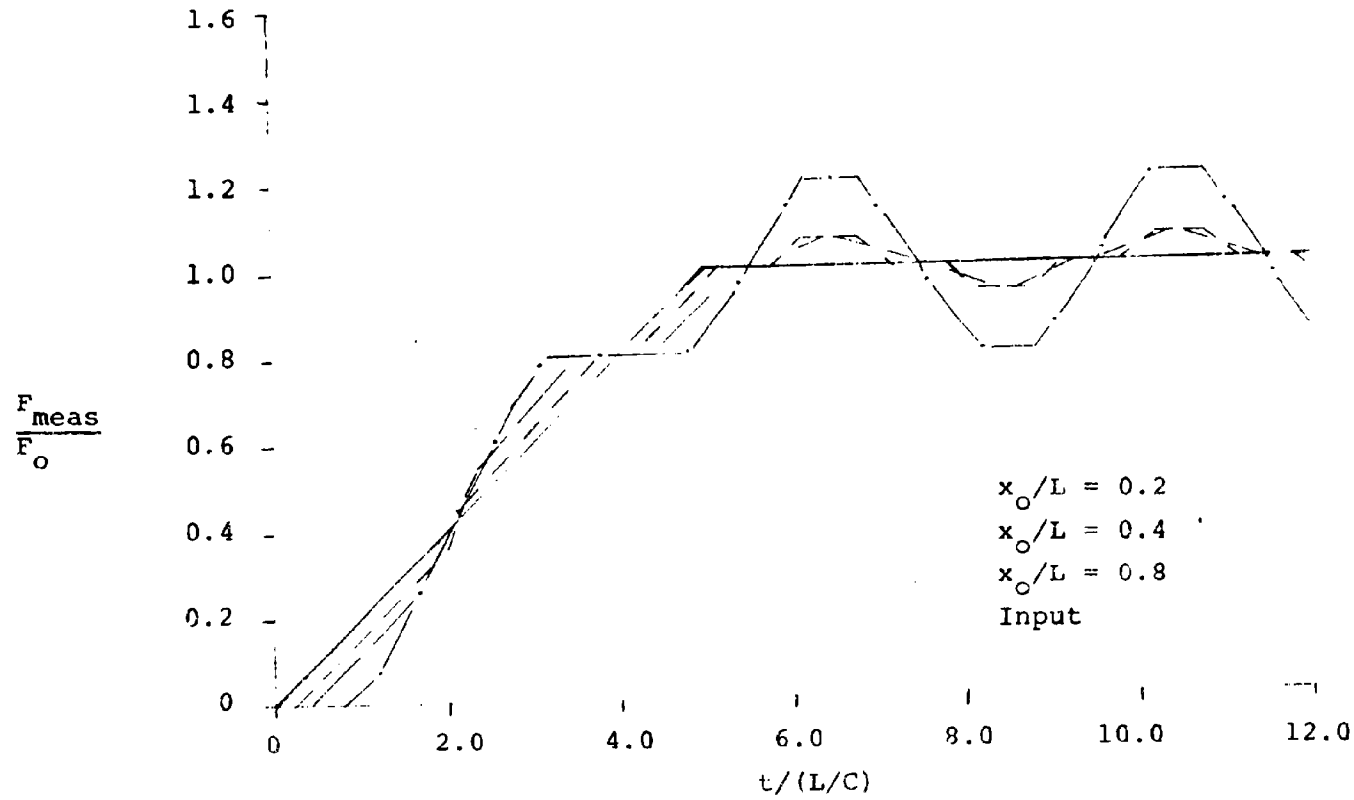

Figure 33. Ramp Function Results: = 5.0 L/C

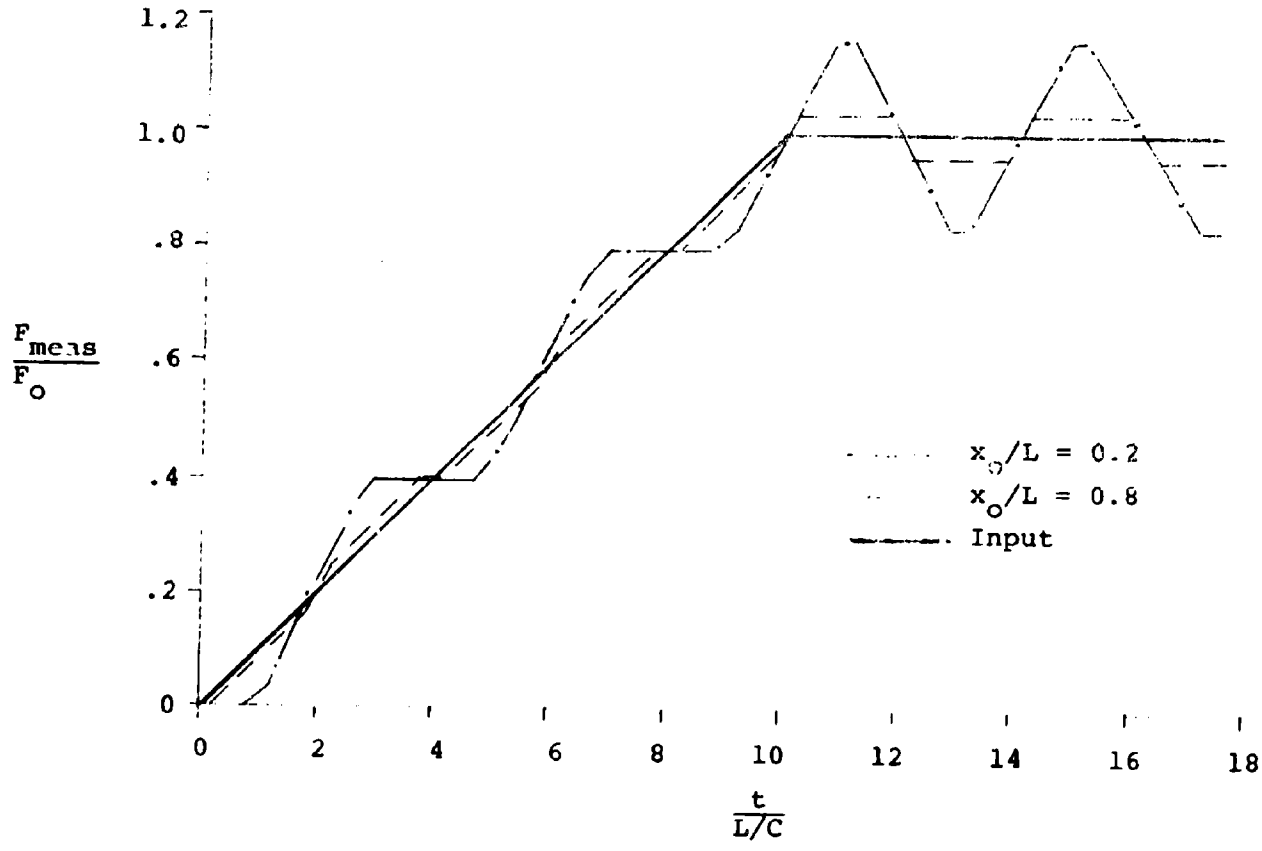

Figure 34. Ramp Function Results: = 10.0 L/C

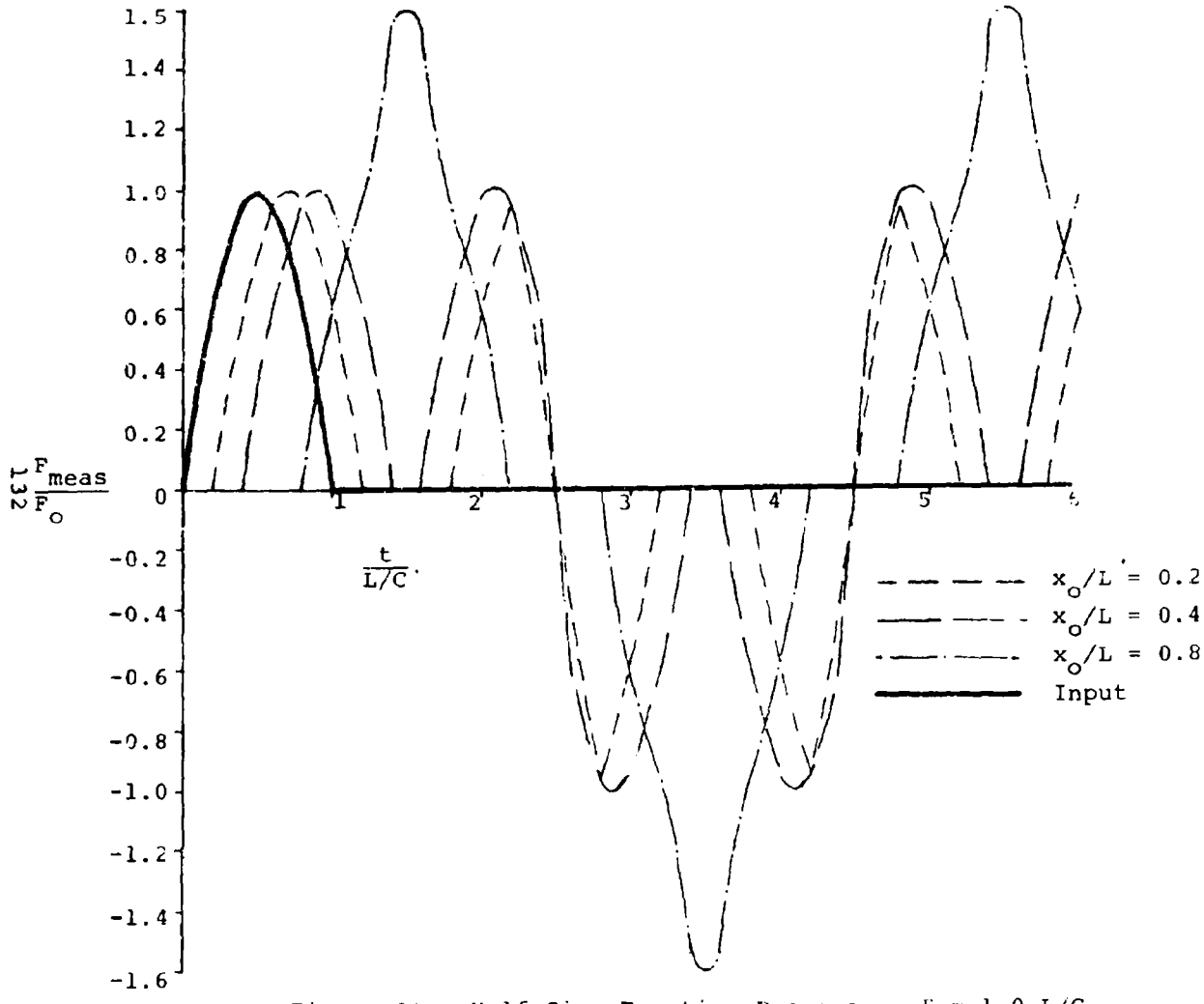

Figure 35. Half Sine Function Response: $\Gamma = 1.0$ L/C

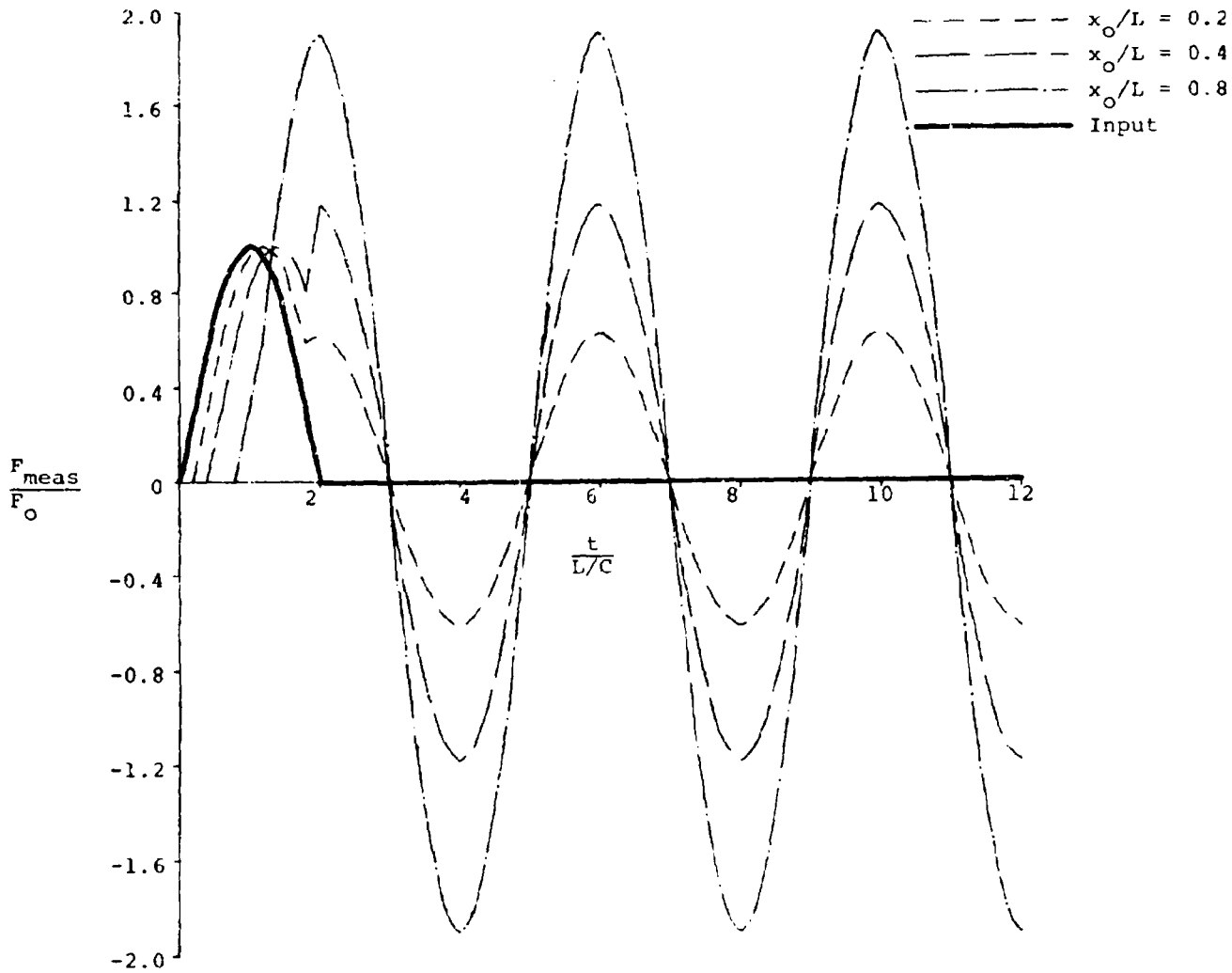

Figure 36. Half Sine Function Response: $\Gamma = 2.0L/C$

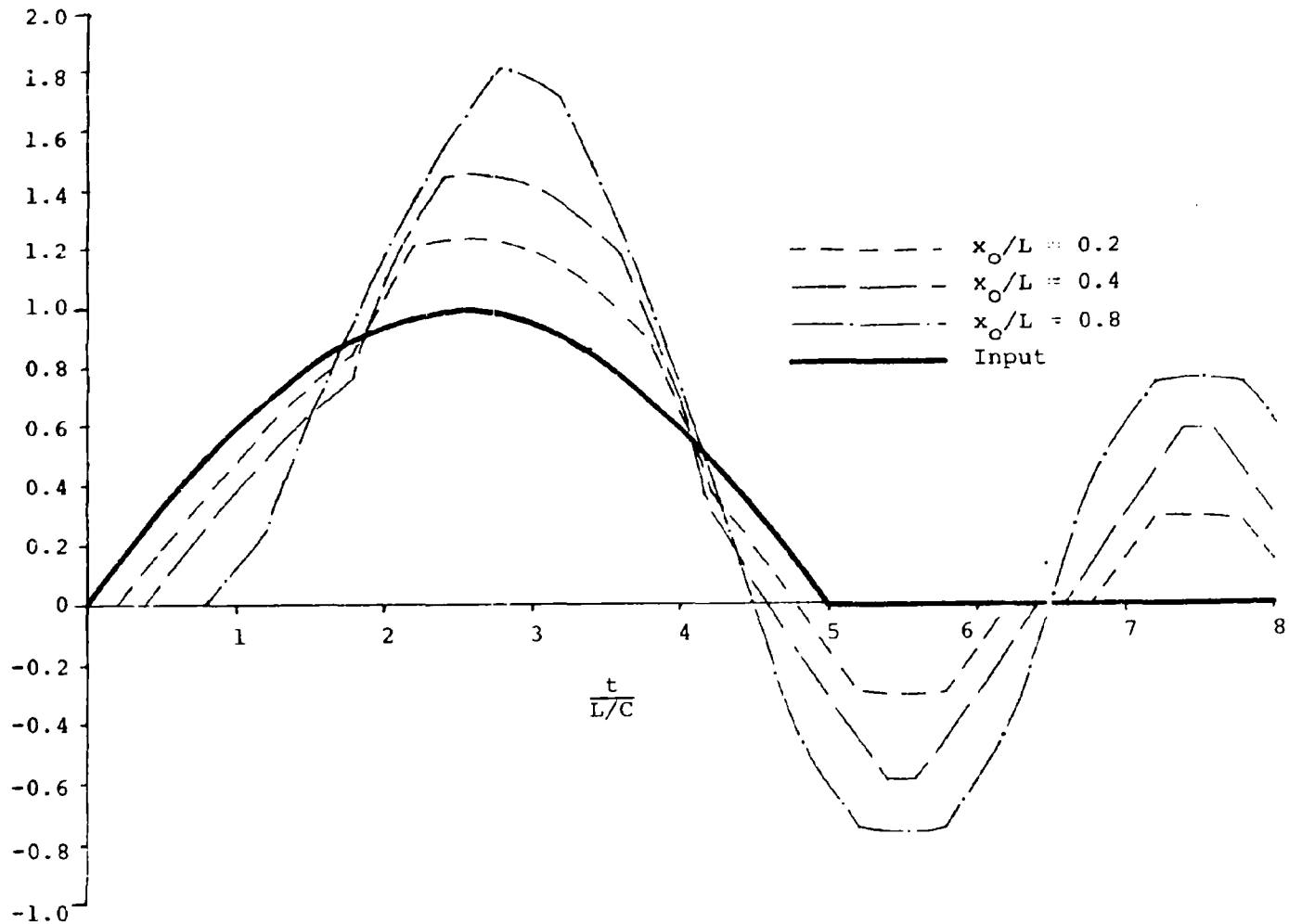

Figure 37. Half Sine Function Response: Γ = 5.0 L/C

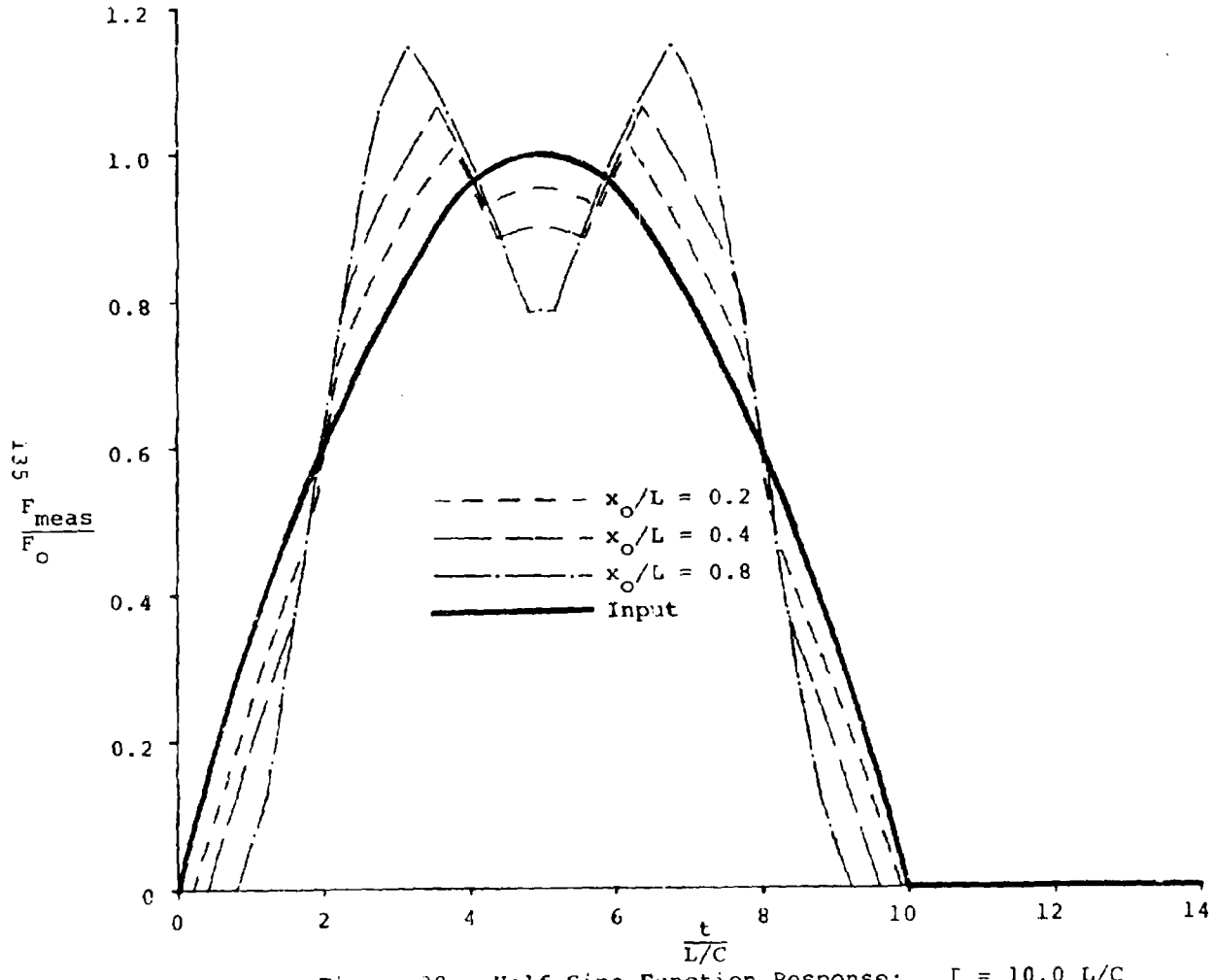

Figure 38. Half Sine Function Response: $\Gamma = 10.0$ L/C

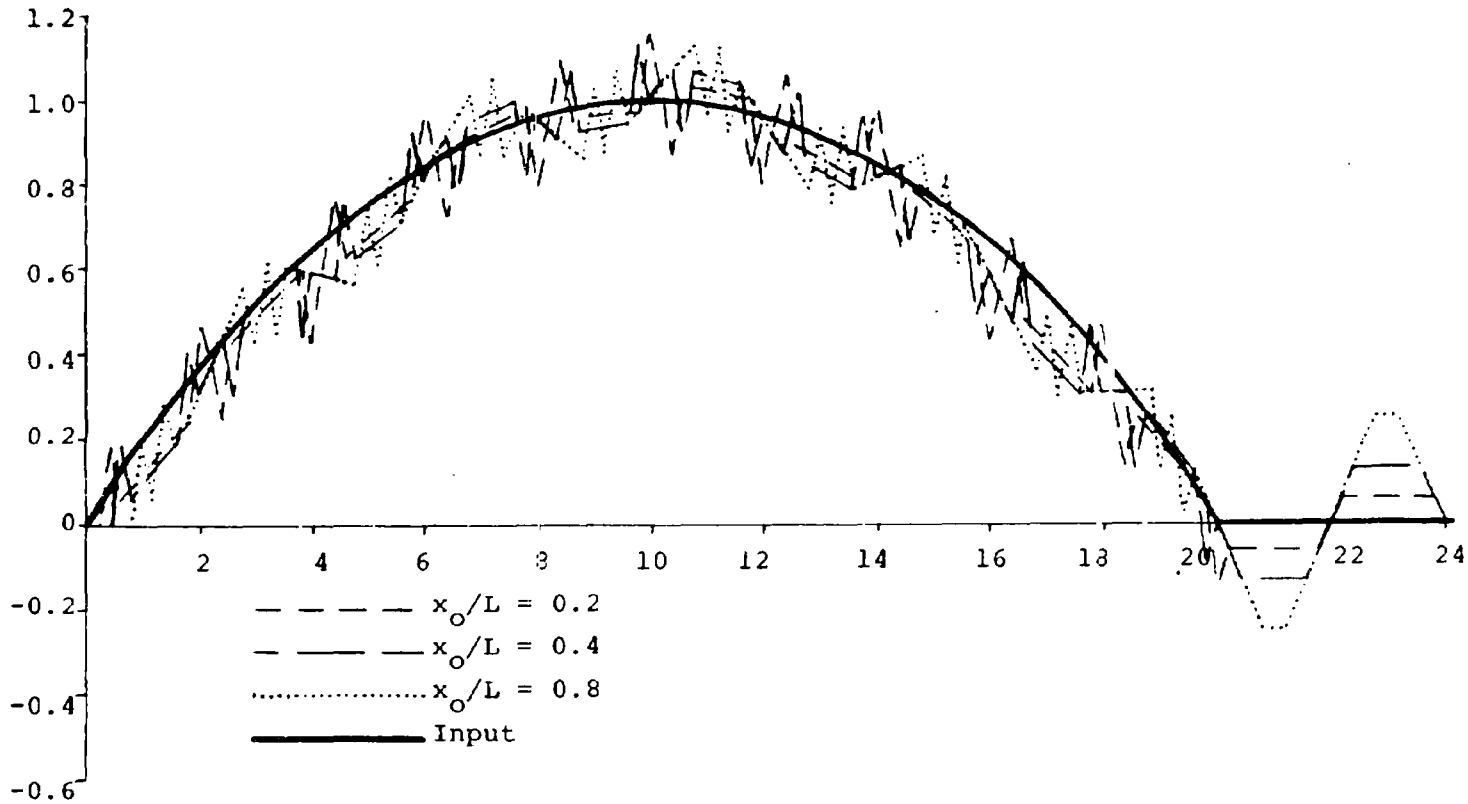

Figure 39. Half Sine Function Response: $\Gamma = 20.0$ L/C

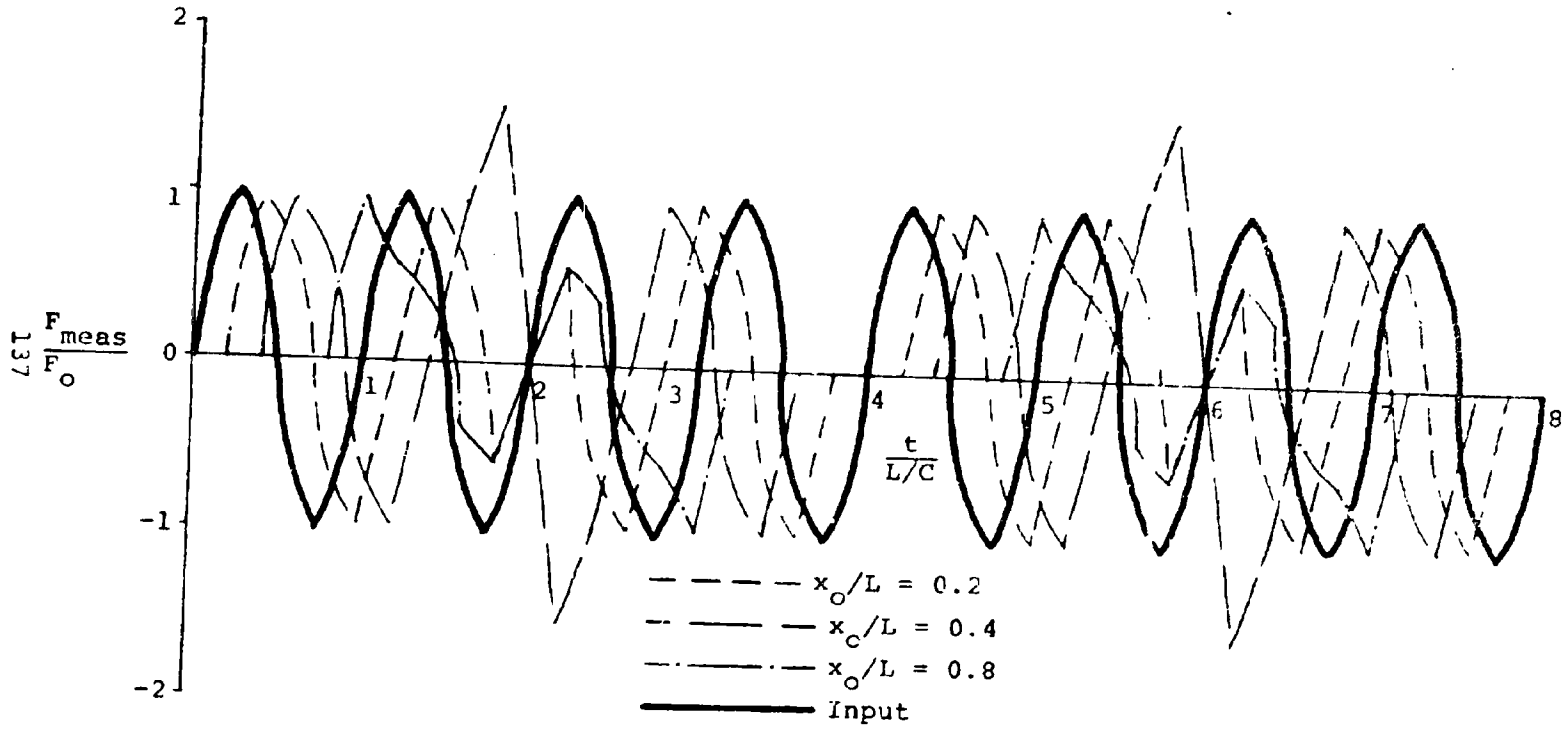

Figure 40. Harmonic Forcing Function Response: $\Gamma = 1.0$ L/C

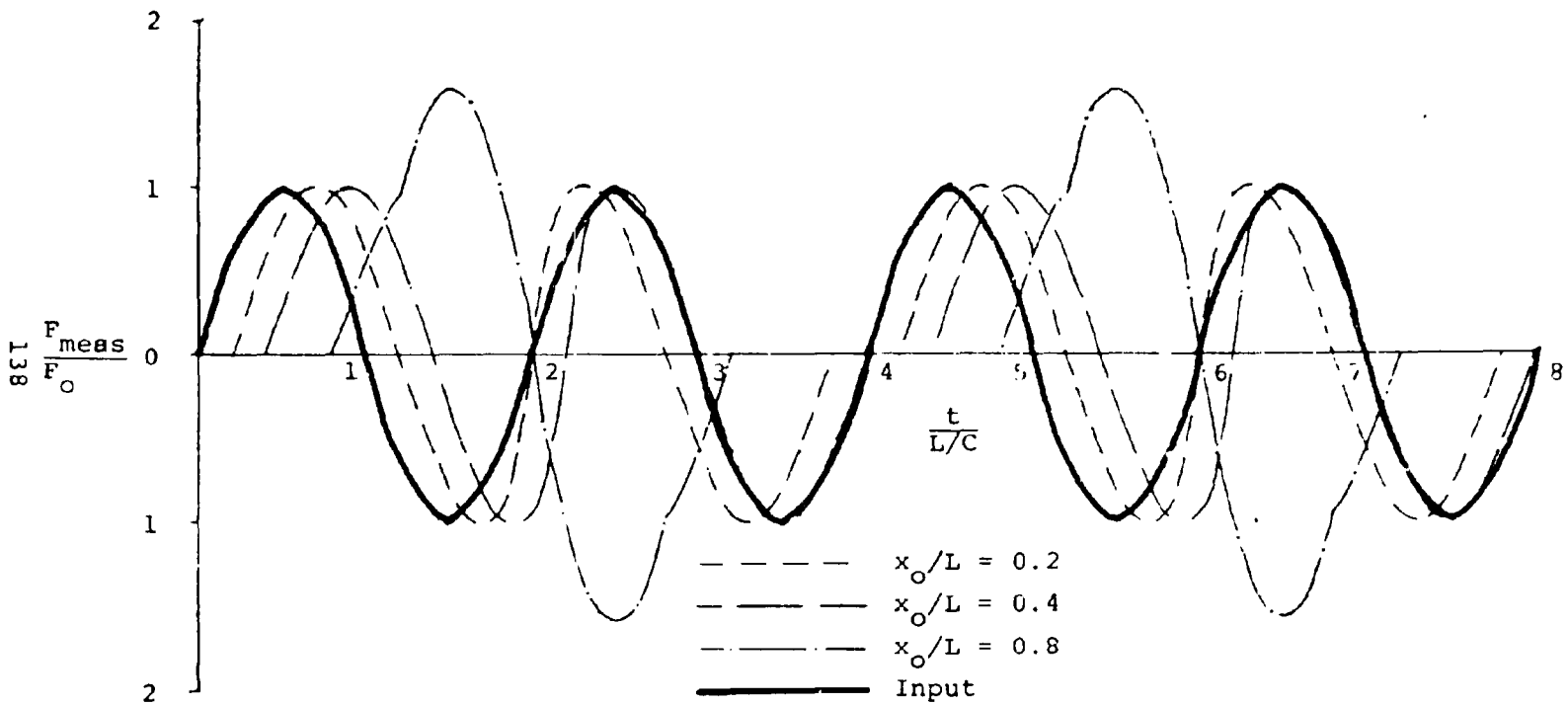

Figure 41. Harmonic Forcing Function Response. $\Gamma = 2.0$ L/C

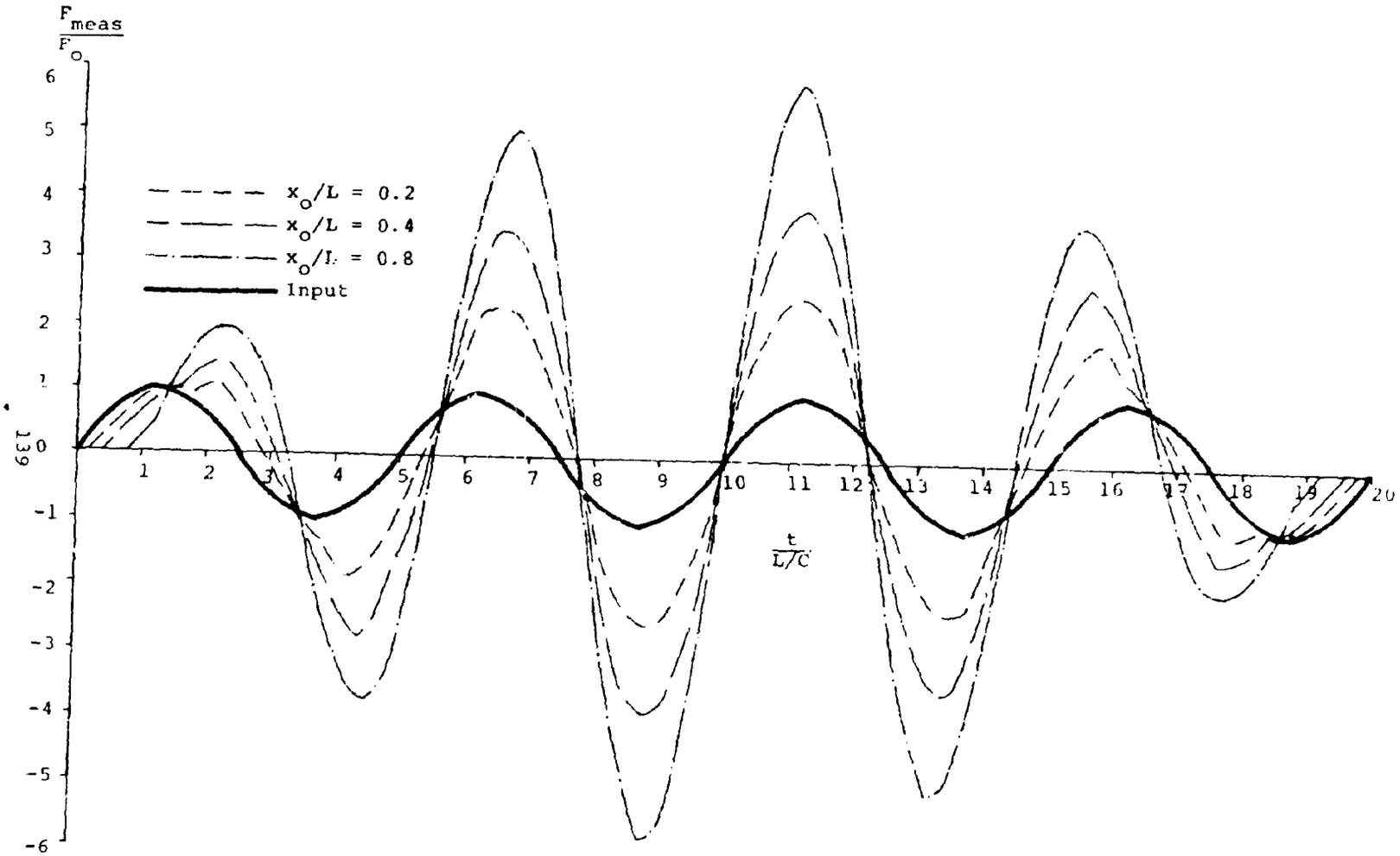

Figure 12. Harmonic Forcing Function: $\Gamma = 5.0$ L/C

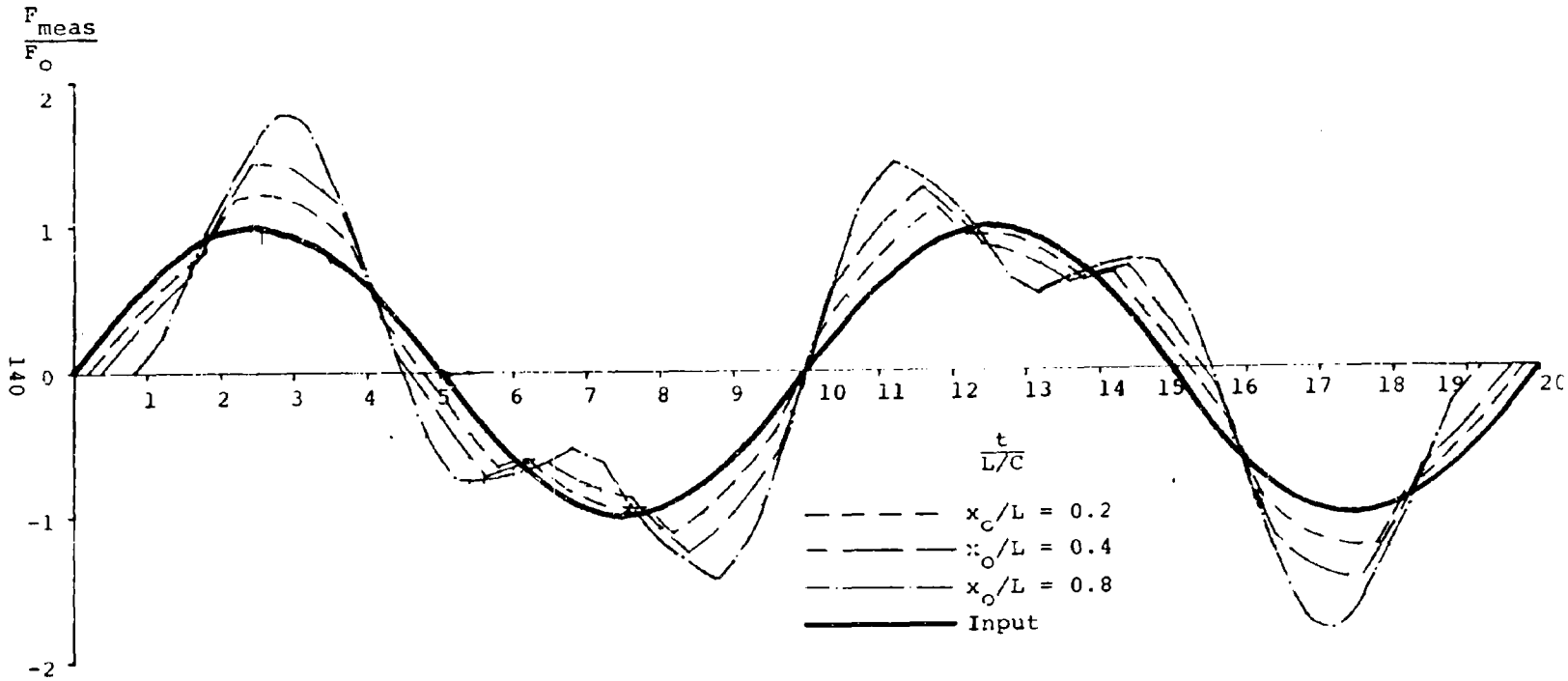

Figure 43. Harmonic Forcing Function Response : Γ = 10.0 L/C

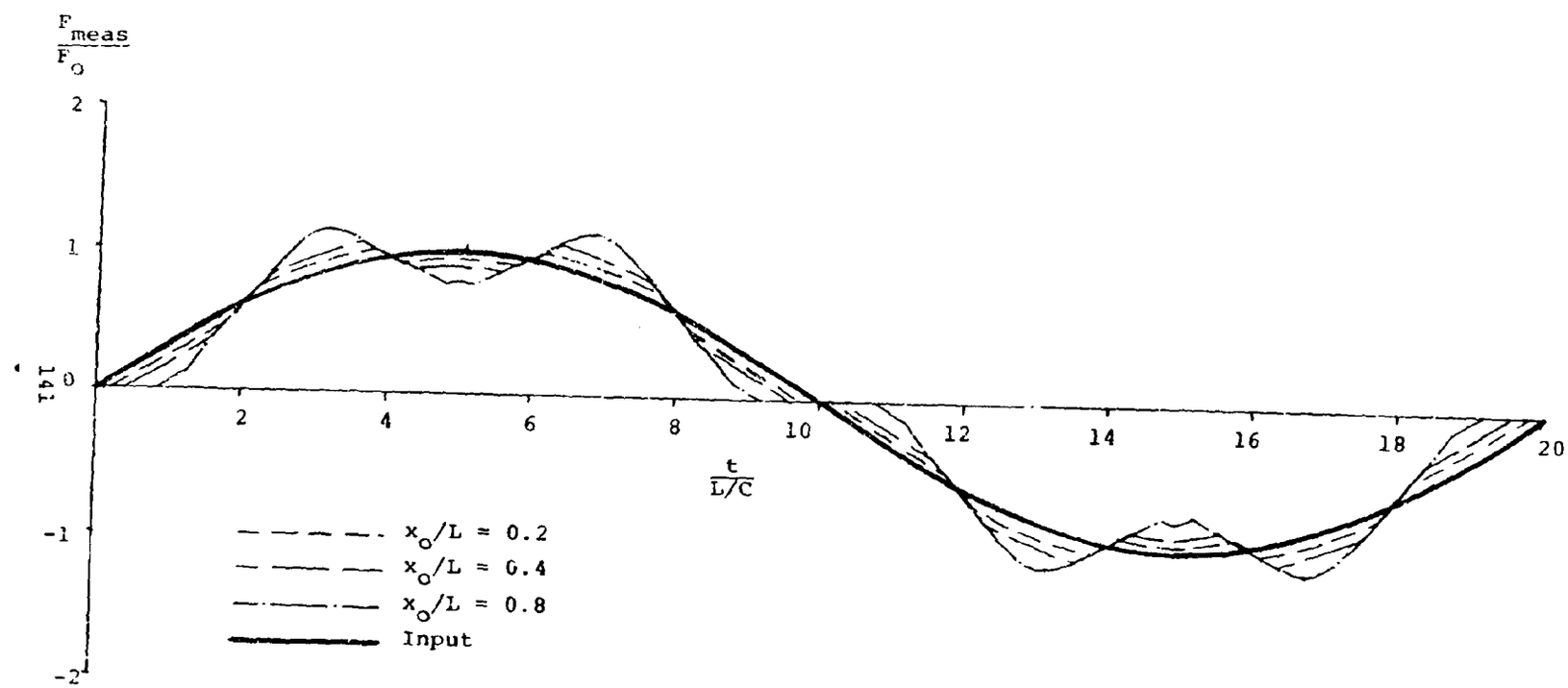

Figure 44. Harmonic Forcing Function Response: $\Gamma = 20.0$ L/C

A study of the results for the case of harmonic forcing also shows that significant distortion in the measured pulse can be introduced. Even for the lowest frequency pulse used in the work ($\Gamma = 20L/c$), the pulse signature is distorted, particularly for the gage location at $x/L = 0.8$. Also, a beat phenomenon with amplification for all gage positions is observed for $\Gamma = 5L/c$.

5 - CONCLUSIONS

The following conclusions can be drawn from the results of this study:

1. A force transducer composed of a gaged bar will not give a signal representative of the applied force if the rise time or pulse duration is too short. There may be significant difference in both the shape of pulse signature and the indicated peak force.
2. The degree of difference in the applied and measured quantities increases as the distance between the strain gages and the end to which the force is applied increases.
3. When accuracy of the peak force is the criterion for comparison, the rise time of a ramp function must be greater than 5L/c for approximately 5% accuracy. For similar accuracy with a half sine pulse, the duration of the pulse should be greater than 15L/c. Accuracy is increased as the rise time or pulse duration increases.

Certain idealizations have been made in this study which need to be emphasized, since they affect the applicability of these results to real situations. A discussion of two of these here is pertinent.

It has been assumed that one end of the force link is fixed, meaning no motion occurs. In any actual application

of force transducers, this cannot be accomplished. The supporting end will always undergo some deformation. The effect of this deformation on the measured signal has not been investigated.

The second idealization which is not achieved in practice is the assumption that the force applied is uniformly distributed across the end. This assumption results in the work showing that if strain gages were applied at this end, the force link would be valid for all pulses. However, in practice, the applied force will in general not be uniformly distributed. Therefore, if the gages were located very near the end of excitation, the nonuniform distribution could introduce significant error which could not be evaluated. Experience dictates that the effect of nonuniform distribution at both ends of the transducer can be minimized by locating the gages at the center. This has been done for all transducers developed for track use.

A comparison of the system investigated and a sled with a transducer between the slipper and sled body shows that there is considerable difference. Further studies of this particular problem using a similar technique with a more representative model for a sled could prove to be of value in understanding the measurements made. The results given here are those from the initial investigation, and further work is required for checking and expansion of the investigation.

VI A NUMERICAL DIFFERENTIATION TECHNIQUE

In the previous contract from the Air Force Missle Development Center to the University of New Mexico, a technique was developed for compensation of accelerometer data using digital techniques in order that the frequency range of accelerometers could be extended. In the process of developing this technique, it was necessary to develop a method of numerical differentiation which was highly accurate. Since this was not the main purpose of the initial study, the steps necessary for using this new process for numerical differentiation were not described in detail in the report. During the course of this contract, a small amount of time has been expended in order to do this.

This section of the report does not give the theory behind the technique, since this was given in the final report of the previous contract, number F29600-67-C-0017. This section only states how to use the method.

This work was considered pertinent to this contract since there are many instances where differentiation of test data is required, and most methods of accomplishing this are highly unreliable. Experience has shown this to be substantially better than others studied.

This technique obtains a value for the first and second derivative at every data point. An array of values is generated for each data point and the mean of this array is taken to be the derivative at that point. The array is

generated by fitting all possible polynomials of specified order to all possible segments of the data curve that contain the data point as an interior point. The polytable technique is used to fit the polynomials to the segments.

Table XVIII on the following page is a FORTRAN IV listing of the technique. This program requires data in the following order and form:

1) Read in the polytable row by row using the format 5E14.7.
2) Read in NDPTS, NTNTI, DIGINC by the format 2I5, E14.7, where: NDPTS is the number of data points, NTNTI is the number of different independent variable calculating increments, and DIGINC is the independent variable digitizing increment.
3) Read in the values of the dependent variable at each data point by the format 5E14.7.
4) Read in NTDINC, MINORD, NORDMX by the format 3I5, where: NTDINC is the number of digitizing increments, MINORD is the minimum order of the polynomial to be fit, and NORDMX is the maximum order of the polynomial to be fit for the first calculating increment.
5) Read in NTDINC, MINORD, MAXORD for the second calculating increments.

Table XVII. Program to Find the First and Second Derivative of Digitized Graphical Data.

```
      DIMENSION POYTAB(9,9),DATA( 500),X( 90,9),DIFTAB(9,9),
     1          YMEN( 500),YPMEN( 500),YPPMEN( 500),YSTD( 500),
     2          YPSTD( 500),YPPSTD( 500),NY( 500),NYP( 500),
     3          XD( 500),COF(9,9),NYPP( 500)
      READ(5,999) ((POYTAB(I,J),J=1,9),I=1,9)
      READ(5,998) NDPTS,NTNTI,DIGINC
      READ(5,999) (DATA(N),N=1,NDPTS)
      DO 200 NTIMES=1,NTNTI
      READ(5,997) NTDINC,MINORD,NORDMX
      DO 10 NDPT=1,NDPTS
      YMEN(NDPT)=0.0
      YPMEN(NDPT)=0.0
      YPPMEN(NDPT)=0.0
      YSTD(NDPT)=0.0
      YPSTD(NDPT)=0.0
      YPPSTD(NDPT)=0.0
      NY(NDPT)=0
      NYP(NDPT)=0
10    NYPP(NDPT)=0
      NAXFN=NDPTS-MINORD*NTDINC-1
      MINP1=MINORD&1
      INTPTS=NORDMX*NTDINC-1
      FNTINC=NTDINC
      DO 20 INTPT=1,INTPTS
      FINT=INTPT
      XBASE=FINT/FNTINC
      DO 20 NPOW=1,NORDMX
20    X(INTPT,NPOW)=XBASE**NPOW
      DO 140 NAXST=1,NTDINC
      MAXORD=NORDMX
      MAXM1=MAXORD-1
      DO 30 NP=1,MAXM1
      NPT1=(NP-1)*NTDINC&NAXST
      NPT2=NPT1&NTDINC
30    DIFTAB(NP&1,1)=DATA(NPT2)-DATA(NPT1)
      DO 40 J=2,MAXM1
      IFINAL=MAXORD&1-J
      DO 40 I=2,IFINAL
40    DIFTAB(I,J)=DIFTAB(I&1,J-1)-DIFTAB(I,J-1)
      DO 140 NAXIS=NAXST,NAXFN,NTDINC
      NPTNXT=NAXIS&MAXORD*NTDINC
      NPTLST=NPTNXT-NTDINC
      DO 50 J=1,MAXM1
      IFINAL=MAXORD-J
      DO 50 I=1,IFINAL
50    DIFTAB(I,J)=DIFTAB(I&1,J)
      IF(NDPTS-NPTNXT) 65,55,55
55    DIFTAB(MAXORD,1)=DATA(NPTNXT)-DATA(NPTLST)
```

Table XVIII. (continued)

```
      DO 60 J=2,MAXCRD
      I=MAXORD&1-J
 60   DIFTAB(I,J)=DIFTAB(I&1,J-1)-DIFTAB(I,J-1)
      GO TO 67
 65   MAXCRD=MAXORD-1
      MAXM1=MAXORD-1
 67   DO 70 NCOF=1,MINORD
      COF(NCOF,MINORD)=0.0
      DO 70 NTERM=NCOF,MINORD
 70   COF(NCOF,MINORD)=COF(NCOF,MINORD)&POYTAB(NCOF,NTERM)
     1                 *DIFTAB(1,NTERM)
      DO 80 NORD=MINP1,MAXORD
      COF(NORD,NORD-1)=0.0
      DO 80 NCOF=1,NORD
 80   COF(NCOF,NORD)=COF(NCOF,NORD-1)&POYTAB(NCOF,NORD)*
     1                DIFTAB(1,NORD)
      MIN=MINORD
      NXPTMX=NTDINC*MAXORD-1
      NXPTMN=NTDINC*MINORD-1
      DO 140 NXPT=1,NXPTMX
      IF(NXPT-NXPTMN) 100,100,90
 90   MIN=1&NXPT/NTDINC
100   NDPT=NXPT&NAXIS
      DO 140 NORD=MIN,MAXORD
      Y=DATA(NAXIS)
      YP=COF(1,NORD)
      YPP=2.*COF(2,NORD)
      DO 130 NPOW=1,NORD
      IF(NPOW-2) 130,120,110
110   FP=NPOW*(NPOW-1)
      YPP=YPP&FP*COF(NPOW,NORD)*X(NXPT,NPOW-2)
120   FP=NPOW
      YP=YP&FP*COF(NPOW,NORD)*X(NXPT,NPOW-1)
130   Y=Y&COF(NPOW,NORD)*X(NXPT,NPOW)
      IF(NORD-2) 137,135,133
133   NYPP(NDPT)=NYPP(NDPT)&1
      YPPMEN(NDPT)=YPPMEN(NDPT)&YPP/(FNTINC*DIGINC)**2
      YPPSTD(NDPT)=YPPSTD(NDPT)&(YPP/(FNTINC*DIGINC)**2)**2
135   NYP(NDPT)=NYP(NDPT)&1
      YPMEN(NDPT)=YPMEN(NDPT)&YP/(FNTINC*DIGINC)
      YPSTD(NDPT)=YPSTD(NDPT)&(YP/(FNTINC*DIGINC))**2
137   NY(NDPT)=NY(NDPT)&1
      YMEN(NDPT)=YMEN(NDPT)&Y
140   YSTD(NDPT)=YSTD(NDPT)&Y**2
      WRITE(6,996) NTDINC,DIGINC,MINORD,NORDMX
      DO 180 NDPT=1,NDPTS
      XN=NDPT-1
      IF(NY(NDPT)) 180,180,150
150   DEN=NY(NDPT)
      ARG=(YSTD(NDPT)-YMEN(NDPT)**2/DEN)/DEN
      IF(ARG) 152,152,154
152   YSTD(NDPT)=0.0
      GO TO 155
154   YSTD(NDPT)=SQRT(ARG)
155   YMEN(NDPT)=YMEN(NDPT)/DEN
      IF(NYP(NDPT)) 180,180,160
```

Table XVIII. (continued)

```
160   DEN=NYP(NDPT)
      ARG=(YPSTD(NDPT)-YPMEN(NDPT)**2/DEN)/DEN
      IF(ARG) 162,162,164
162   YPSTD(NDPT)=0.0
      GO TO 165
164   YPSTD(NDPT)=SQRT(ARG)
165   YPMEN(NDPT)=YPMEN(NDPT)/DEN
      IF(NYPP(NDPT)) 180,180,170
170   DEN=NYPP(NDPT)
      ARG=(YPPSTD(NDPT)-YPPMEN(NDPT)**2/DEN)/DEN
      IF(ARG) 172,172,174
172   YPPSTD(NDPT)=0.0
      GO TO 175
174   YPPSTD(NDPT)=SQRT(ARG)
175   YPPMEN(NDPT)=YPPMEN(NDPT)/DEN
180   XD(NDPT)=XN*DIGINC
      WRITE(6,995) (N,XD(N),DATA(N),YMEN(N),YSTD(N),NY(N),
     1              N=1,NDPTS)
      WRITE(6,993)
      WRITE(6,994) (N,YPMEN(N),YPSTD(N),NYP(N),YPPMEN(N),
     1             YPPSTD(N),NYPP(N),N=1,NDPTS)
200   CONTINUE
995   FORMAT(5E14.7)
998   FORMAT(2I5,E14.7)
997   FORMAT(3I5)
996   FORMAT(1H1,25X,'THE COMPUTING INCREMENT WAS',I5,' TIMES '
     1 ,'THE',/18X,'DIGITIZING INCREMENT WHICH WAS',E16.7,
     2 ' , AND THE',/18X,'MAXIMUM AND MINIMUM ORDER POLYNOMIALS'
     3 ,' USED WERE',I3,' AND',I3,////18X,'N',7X,'X',12X,'Y',
     4 11X,'YMEN',9X,'YSTD',6X,'NY'//)
995   FORMAT(15X,I5,4E13.5,I5)
994   FORMAT(15X,I5,2E12.4,I5,2E12.4,I5)
993   FORMAT(1H1,18X,'N',5X,'YPMEN',7X,'YPSTD',4X,'NYP',4X,
     1 'YPPMEN',6X,'YPPSTD',4X,'NYPP'//)
      CALL EXIT
      END
```

The variable names used in the output are defined as follows:

N = the number of the data point

X = the value of the independent variable

Y = the value of the dependent variable

YMEN = the mean value of the array representing Y

YSTD = the standard deviation of the array representing Y

NY = the number of elements in the array representing Y

YPMEN = the mean value of the array representing the first derivative

YPSTD = the standard deviation of the array representing the first derivative

NYP = the number of elements in the array representing the first derivative

YPPMEN = the mean value of the array representing the second derivative

YPPSTD = the standard deviation of the array representing the second derivative

NYPP = the number of elements in the array representing the second derivative.

The polytable required to use this technique is given in Table XIX.

Examples of the output obtained from this program are given in Tables XX, XXI, and XXII.

The function used in generating these tables was y = sin x. Different digitizing increments were used in generating each of these tables to show the effect of this parameter.

It has been found that when the technique is used on

TABLE XIX POLYTABLE FOR CURVE FITTING

P_{11} = 1.000	P_{12} = -0.5000000	P_{13} = +0.3333333E 00
P_{21} = 0.0	P_{22} = +0.5000000	P_{23} = -0.5000000E 00
P_{31} = 0.0	P_{32} = 0.0	P_{33} = 0.1666666E 00
P_{41} = 0.0	P_{42} = 0.0	P_{43} = 0.0
P_{51} = 0.0	P_{52} = 0.0	P_{53} = 0.0
P_{61} = 0.0	P_{62} = 0.0	P_{63} = 0.0
P_{71} = 0.0	P_{72} = 0.0	P_{73} = 0.0
P_{81} = 0.0	P_{82} = 0.0	P_{83} = 0.0
P_{91} = 0.0	P_{92} = 0.0	P_{93} = 0.0

P_{14} = -0.2500000E 00	P_{15} = +0.2000000E 00
P_{24} = +0.4583330E 00	P_{25} = -0.4166664E 00
P_{34} = -0.2500000E 00	P_{35} = +0.2916664E 00
P_{44} = 0.4166664E 00	P_{45} = -0.8333331E 00
P_{54} = 0.0	P_{55} = 0.8333329E 00
P_{64} = 0.0	P_{65} = 0.0
P_{74} = 0.0	P_{75} = 0.0
P_{84} = 0.0	P_{85} = 0.0
P_{94} = 0.0	P_{95} = 0.0

TABLE XIX (continued)

P_{16} = -0.1666666E 00	P_{17} = +0.1428571E 00
P_{26} = +0.3805555E 00	P_{27} = -0.3500000E 00
P_{36} = -0.3125000E 00	P_{37} = +0.3222220E 00
P_{46} = +0.1180555E 00	P_{47} = -0.1458331E 00
P_{56} = -0.2083333E 00	P_{57} = +0.3472221E-01
P_{66} = 0.1388889E 00	P_{67} = -0.4166663E-02
P_{76} = 0.0	P_{77} = 0.1984125E-03
P_{86} = 0.0	P_{87} = 0.0
P_{96} = 0.0	P_{97} = 0.0

P_{18} = -0.1250000E 00	P_{19} = +0.1111111E 00
P_{28} = +0.3241069E 00	P_{29} = -0.3019839E 00
P_{38} = -0.3256944E 00	P_{39} = +0.3255180E 00
P_{48} = +0.1678321E 00	P_{49} = -0.1854166E 00
P_{58} = -0.4861110E-01	P_{59} = +0.6186341E-01
P_{68} = +0.7986106E-02	P_{69} = -0.1249999E-01
P_{78} = -0.6944439E-03	P_{79} = +0.1504628E-02
P_{88} = 0.2480159E-04	P_{89} = -0.9920634E-04
P_{98} = 0.0	P_{99} = 0.2755732E-05

Table XX. Example 1 on Use of Numerical Differentiation Technique.

THE COMPUTING INCREMENT WAS 1 TIMES THE DIGITIZING INCREMENT WHICH WAS 0.3141593E 00 , AND THE MAXIMUM AND MINIMUM ORDER POLYNOMIALS USED WERE 1 AND 9

N	X	Y	YMEN	YSTD	NY
1	0.0	0.0	0.0	0.0	0
2	0.31416E 00	0.30902E 00	0.30902E 00	0.41396E-03	8
3	0.62832E 00	0.58779E 00	0.58778E 00	0.0	15
4	0.94248E 00	0.80902E 00	0.80902E 00	0.15804E-02	21
5	0.12566E 01	0.95106E 00	0.95105E 00	0.10834E-02	26
6	0.15708E 01	0.10000E 01	0.99999E 00	0.28527E-02	30
7	0.18850E 01	0.95106E 00	0.95105E 00	0.96165E-03	33
8	0.21991E 01	0.80902E 00	0.80901E 00	0.20880E-02	35
9	0.25133E 01	0.58779E 00	0.58778E 00	0.87649E-03	36
10	0.28274E 01	0.30902E 00	0.30902E 00	0.0	36
11	0.31416E 01	0.65539E-06	-0.70937E-06	0.43577E-05	36
12	0.34558E 01	-0.30902E 00	-0.30902E 00	0.0	36
13	0.37699E 01	-0.58778E 00	-0.58778E 00	0.56342E-03	36
14	0.40841E 01	-0.80902E 00	-0.80901E 00	0.20588E-02	36
15	0.43982E 01	-0.95106E 00	-0.95105E 00	0.92071E-03	36
16	0.47124E 01	-0.10000E 01	-0.99999E 00	0.28378E-02	36
17	0.50265E 01	-0.95106E 00	-0.95105E 00	0.65104E-03	36
18	0.53407E 01	-0.80902E 00	-0.80901E 00	0.21593E-02	36
19	0.56549E 01	-0.58779E 00	-0.58778E 00	0.65104E-03	36
20	0.59690E 01	-0.30902E 00	-0.30902E 00	0.0	36
21	0.62832E 01	-0.32769E-06	0.88785E-06	0.39423E-05	36
22	0.65973E 01	0.30902E 00	0.30902E 00	0.0	36
23	0.69115E 01	0.58779E 00	0.58778E 00	0.67108E-03	36
24	0.72257E 01	0.80902E 00	0.80901E 00	0.20588E-02	36
25	0.75398E 01	0.95106E 00	0.95105E 00	0.92071E-03	36
26	0.78540E 01	0.10000E 01	0.99999E 00	0.29115E-02	36
27	0.81681E 01	0.95106E 00	0.95105E 00	0.92071E-03	36
28	0.84823E 01	0.80902E 00	0.80901E 00	0.20588E-02	36
29	0.87965E 01	0.58779E 00	0.58778E 00	0.84573E-03	36
30	0.91106E 01	0.30902E 00	0.30901E 00	0.36394E-03	36
31	0.94248E 01	-0.23772E-07	-0.12931E-05	0.44271E-05	36
32	0.97389E 01	-0.30902E 00	-0.30902E 00	0.0	36
33	0.10053E 02	-0.58779E 00	-0.58778E 00	0.87346E-03	35
34	0.10367E 02	-0.80902E 00	-0.80901E 00	0.21503E-02	33
35	0.10681E 02	-0.95106E 00	-0.95105E 00	0.10086E-02	30
36	0.10996E 02	-0.10000E 01	-0.99999E 00	0.24226E-02	26
37	0.11310E 02	-0.95106E 00	-0.95105E 00	0.14764E-02	21
38	0.11624E 02	-0.80902E 00	-0.80901E 00	0.50429E-03	15
39	0.11938E 02	-0.58779E 00	-0.58778E 00	0.59802E-03	8
40	0.12252E 02	-0.30902E 00	0.0	0.0	0

Table XX. (continued)

N	YPMEN	YPSTD	NYP	YPPMEN	YPPSTD	NYPP
1	0.0	0.0	0	0.0	0.0	0
2	0.9490E 00	0.5213E-02	8	-0.3090E 00	0.1353E-02	7
3	0.8081E 00	0.3383E-02	15	-0.5872E 00	0.1864E-02	14
4	0.5873E 00	0.2152E-02	21	-0.8083E 00	0.2227E-02	20
5	0.3088E 00	0.1165E-02	26	-0.9504E 00	0.2817E-02	25
6	-0.8587E-06	0.6576E-03	30	-0.9994E 00	0.3077E-02	29
7	-0.3089E 00	0.9912E-03	33	-0.9506E 00	0.3164E-02	32
8	-0.5875E 00	0.2281E-02	35	-0.8086E 00	0.2415E-02	34
9	-0.8086E 00	0.3122E-02	36	-0.5875E 00	0.1974E-02	35
10	-0.9506E 00	0.3320E-02	36	-0.3089E 00	0.7382E-03	35
11	-0.9995E 00	0.3906E-02	36	-0.7501E-05	0.6023E-03	35
12	-0.9506E 00	0.3189E-02	36	0.3089E 00	0.7916E-03	35
13	-0.8086E 00	0.2912E-02	36	0.5875E 00	0.1960E-02	35
14	-0.5875E 00	0.2387E-02	36	0.8086E 00	0.2287E-02	35
15	-0.3089E 00	0.9766E-03	36	0.9506E 00	0.3167E-02	35
16	0.2751E-05	0.6003E-03	36	0.9995E 00	0.3026E-02	35
17	0.3089E 00	0.9766E-03	36	0.9506E 00	0.2801E-02	35
18	0.5875E 00	0.2184E-02	36	0.8086E 00	0.2471E-02	35
19	0.8086E 00	0.2912E-02	36	0.5875E 00	0.1557E-02	35
20	0.9506E 00	0.3189E-02	36	0.3089E 00	0.7195E-03	35
21	0.9995E 00	0.3960E-02	36	0.6012E-05	0.6020E-03	35
22	0.9506E 00	0.3320E-02	36	-0.3089E 00	0.7916E-03	35
23	0.8086E 00	0.2983E-02	36	-0.5875E 00	0.1904E-02	35
24	0.5875E 00	0.2171E-02	36	-0.8086E 00	0.2557E-02	35
25	0.3089E 00	0.9629E-03	36	-0.9506E 00	0.3097E-02	35
26	-0.1642E-05	0.6002E-03	36	-0.9995E 00	0.3026E-02	35
27	-0.3089E 00	0.9766E-03	36	-0.9506E 00	0.3167E-02	35
28	-0.5875E 00	0.2226E-02	36	-0.8086E 00	0.2557E-02	35
29	-0.8086E 00	0.2983E-02	36	-0.5875E 00	0.1522E-02	35
30	-0.9506E 00	0.3189E-02	36	-0.3089E 00	0.7742E-03	35
31	-0.9995E 00	0.3796E-02	36	-0.6200E-05	0.6019E-03	35
32	-0.9506E 00	0.3506E-02	36	0.3089E 00	0.7916E-03	35
33	-0.8086E 00	0.3097E-02	35	0.5875E 00	0.1765E-02	34
34	-0.5875E 00	0.2223E-02	33	0.8086E 00	0.2490E-02	32
35	-0.3088E 00	0.1099E-02	30	0.9505E 00	0.3162E-02	29
36	0.3380E-05	0.7064E-03	26	0.9993E 00	0.3026E-02	25
37	0.3088E 00	0.1296E-02	21	0.9502E 00	0.3026E-02	20
38	0.5871E 00	0.2509E-02	15	0.8082E 00	0.2462E-02	14
39	0.8072E 00	0.4395E-02	8	0.5874E 00	0.1988E-02	7
40	0.0	0.0	0	0.0	0.0	0

Table XXI. Example 2 on Use of Numerical Differentiation Technique.

THE COMPUTING INCREMENT WAS 2 TIMES THE DIGITIZING INCREMENT WHICH WAS 0.3141593E 00 , AND THE MAXIMUM AND MINIMUM ORDER POLYNOMIALS USED WERE 1 AND 9

N	X	Y	YMEN	YSTD	NY
1	0.0	0.0	0.0	0.0	0
2	0.31416E 00	0.30902E 00	0.30902E 00	0.68219E-02	9
3	0.62832E 00	0.58779E 00	0.58690E 00	0.74373E-02	17
4	0.94248E 00	0.80902E 00	0.80732E 00	0.85224E-02	25
5	0.12566E 01	0.95106E 00	0.94948E 00	0.85693E-02	32
6	0.15708E 01	0.10000E 01	0.99874E 00	0.82746E-02	39
7	0.18850E 01	0.95106E 00	0.95003E 00	0.74116E-02	45
8	0.21991E 01	0.80902E 00	0.80827E 00	0.62366E-02	51
9	0.25133E 01	0.58779E 00	0.58729E 00	0.48688E-02	56
10	0.28274E 01	0.30902E 00	0.30876E 00	0.34197E-02	61
11	0.31416E 01	0.65539E-06	-0.15847E-04	0.26678E-02	65
12	0.34558E 01	-0.30902E 00	-0.30882E 00	0.32580E-02	69
13	0.37699E 01	-0.58778E 00	-0.58741E 00	0.43185E-02	72
14	0.40841E 01	-0.80902E 00	-0.80851E 00	0.53179E-02	75
15	0.43982E 01	-0.95106E 00	-0.95047E 00	0.59224E-02	77
16	0.47124E 01	-0.10000E 01	-0.99939E 00	0.62308E-02	79
17	0.50265E 01	-0.95106E 00	-0.95044E 00	0.58918E-02	80
18	0.53407E 01	-0.80902E 00	-0.80845E 00	0.51902E-02	81
19	0.56549E 01	-0.58779E 00	-0.58727E 00	0.41175E-02	81
20	0.59690E 01	-0.30902E 00	-0.30859E 00	0.32023E-02	81
21	0.62832E 01	-0.32769E-06	0.28664E-03	0.24936E-02	81
22	0.65973E 01	0.30902E 00	0.30914E 00	0.32606E-02	81
23	0.69115E 01	0.58779E 00	0.58773E 00	0.42304E-02	81
24	0.72257E 01	0.80902E 00	0.80879E 00	0.53666E-02	80
25	0.75398E 01	0.95106E 00	0.95067E 00	0.59127E-02	79
26	0.78540E 01	0.10000E 01	0.99949E 00	0.62639E-02	77
27	0.81681E 01	0.95106E 00	0.95046E 00	0.60347E-02	75
28	0.84823E 01	0.80902E 00	0.80839E 00	0.53686E-02	72
29	0.87965E 01	0.58779E 00	0.58718E 00	0.44364E-02	69
30	0.91106E 01	0.30902E 00	0.30849E 00	0.33959E-02	65
31	0.94248E 01	-0.23772E-07	-0.38212E-03	0.28679E-02	61
32	0.97389E 01	-0.30902E 00	-0.30923E 00	0.36400E-02	56
33	0.10053E 02	-0.58779E 00	-0.58775E 00	0.52749E-02	51
34	0.10367E 02	-0.80902E 00	-0.80867E 00	0.67155E-02	45
35	0.10681E 02	-0.95106E 00	-0.95036E 00	0.81074E-02	39
36	0.10996E 02	-0.10000E 01	-0.99875E 00	0.91610E-02	32
37	0.11310E 02	-0.95106E 00	-0.94937E 00	0.96319E-02	25
38	0.11624E 02	-0.80902E 00	-0.80755E 00	0.97512E-02	17
39	0.11938E 02	-0.58779E 00	-0.58957E 00	0.36212E-02	8
40	0.12252E 02	-0.30902E 00	0.0	0.0	0

Table XXI. (continued)

N	YPMEN	YPSTD	NYP	YPPMEN	YPPSTD	NYPP
1	0.0	0.0	0	0.0	0.0	0
2	0.9489E 00	0.5757E-02	8	-0.3161E 00	0.3251E-01	7
3	0.8040E 00	0.1333E-01	16	-0.5933E 00	0.2811E-01	14
4	0.5844E 00	0.8689E-02	24	-0.8109E 00	0.2914E-01	21
5	0.3076E 00	0.6191E-02	31	-0.9507E 00	0.2707E-01	28
6	-0.1060E-03	0.5019E-02	38	-0.1002E 01	0.2855E-01	35
7	-0.3083E 00	0.5495E-02	44	-0.9523E 00	0.2575E-01	41
8	-0.5665E 00	0.6944E-02	50	-0.8106E 00	0.2208E-01	47
9	-0.8076E 00	0.8278E-02	55	-0.5891E 00	0.1814E-01	52
10	-0.9496E 00	0.8950E-02	60	-0.3095E 00	0.1493E-01	57
11	-0.9985E 00	0.8910E-02	64	0.2439E-04	0.1336E-01	61
12	-0.9497E 00	0.8407E-02	68	0.3094E 00	0.1400E-01	65
13	-0.8079E 00	0.7374E-02	71	0.5886E 00	0.1611E-01	68
14	-0.5870E 00	0.5868E-02	74	0.8100E 00	0.1820E-01	71
15	-0.3086E 00	0.4397E-02	76	0.9521E 00	0.1972E-01	73
16	0.2845E-04	0.3597E-02	78	0.1001E 01	0.2009E-01	75
17	0.3087E 00	0.4319E-02	79	0.9521E 00	0.1931E-01	76
18	0.5872E 00	0.5627E-02	80	0.8100E 00	0.1748E-01	77
19	0.8082E 00	0.7123E-02	80	0.5885E 00	0.1513E-01	77
20	0.9501E 00	0.7910E-02	80	0.3095E 00	0.1291E-01	77
21	0.9991E 00	0.8135E-02	80	0.1855E-03	0.1192E-01	77
22	0.9502E 00	0.7946E-02	80	-0.3092E 00	0.1293E-01	77
23	0.8083E 00	0.7029E-02	80	-0.5882E 00	0.1516E-01	77
24	0.5873E 00	0.5696E-02	79	-0.8098E 00	0.1757E-01	76
25	0.3088E 00	0.4423E-02	78	-0.9520E 00	0.1947E-01	75
26	0.6956E-04	0.3687E-02	76	-0.1001E 01	0.2037E-01	73
27	-0.3086E 00	0.4471E-02	74	-0.9522E 00	0.2000E-01	71
28	-0.5871E 00	0.6009E-02	71	-0.8101E 00	0.1858E-01	68
29	-0.8081E 00	0.7520E-02	68	-0.5887E 00	0.1644E-01	65
30	-0.9500E 00	0.8707E-02	64	-0.3097E 00	0.1443E-01	61
31	-0.9988E 00	0.9216E-02	60	-0.2599E-03	0.1383E-01	57
32	-0.9498E 00	0.9452E-02	55	0.3096E 00	0.1541E-01	52
33	-0.8078E 00	0.8735E-02	50	0.5887E 00	0.1908E-01	47
34	-0.5868E 00	0.7521E-02	44	0.8101E 00	0.2361E-01	41
35	-0.3086E 00	0.6049E-02	38	0.9524E 00	0.2789E-01	35
36	-0.7758E-03	0.5352E-02	31	0.9987E 00	0.2619E-01	28
37	0.3063E 00	0.5801E-02	24	0.9520E 00	0.3045E-01	21
38	0.5833E 00	0.1022E-01	16	0.8152E 00	0.3051E-01	14
39	0.8067E 00	0.5259E-02	8	0.5991E 00	0.3784E-01	7
40	0.0	0.0	0	0.0	0.0	0

Table XXII. Example 3 on Use of Numerical Differentiation Technique.

THE COMPUTING INCREMENT WAS 3 TIMES THE DIGITIZING INCREMENT WHICH WAS 0.3141593E 00 , AND THE MAXIMUM AND MINIMUM ORDER POLYNOMIALS USED WERE 1 AND 9

N	X	Y	YMEN	YSTD	NY
1	0.0	0.0	0.0	0.0	0
2	0.31416E 00	0.30902E 00	0.31053E 00	0.20431E-01	9
3	0.62832E 00	0.58779E 00	0.58636E 00	0.22722E-01	16
4	0.94248E 00	0.80902E 00	0.80577E 00	0.23236E-01	26
5	0.12566E 01	0.95106E 00	0.94612E 00	0.23245E-01	34
6	0.15708E 01	0.10000E 01	0.99448E 00	0.22105E-01	42
7	0.18850E 01	0.95106E 00	0.94641E 00	0.19824E-01	49
8	0.21991E 01	0.80902E 00	0.80581E 00	0.17186E-01	56
9	0.25133E 01	0.58779E 00	0.58618E 00	0.14723E-01	63
10	0.28274E 01	0.30902E 00	0.30847E 00	0.12242E-01	69
11	0.31416E 01	0.65539E-06	0.37363E-03	0.10945E-01	75
12	0.34556E 01	-0.30902E 00	-0.30795E 00	0.11336E-01	81
13	0.37699E 01	-0.58778E 00	-0.58614E 00	0.12637E-01	86
14	0.40841E 01	-0.80902E 00	-0.80700E 00	0.14144E-01	91
15	0.43982E 01	-0.95106E 00	-0.94876E 00	0.15102E-01	95
16	0.47124E 01	-0.10000E 01	-0.99744E 00	0.15394E-01	98
17	0.50265E 01	-0.95106E 00	-0.94832E 00	0.14811E-01	101
18	0.53407E 01	-0.80902E 00	-0.80618E 00	0.13733E-01	103
19	0.56549E 01	-0.58779E 00	-0.58498E 00	0.12418E-01	104
20	0.59690E 01	-0.30902E 00	-0.30628E 00	0.11761E-01	105
21	0.62832E 01	-0.32769E-06	0.26743E-02	0.12209E-01	105
22	0.65973E 01	0.30902E 00	0.31179E 00	0.14213E-01	104
23	0.69115E 01	0.58779E 00	0.59081E 00	0.16883E-01	103
24	0.72257E 01	0.80902E 00	0.81266E 00	0.20137E-01	101
25	0.75398E 01	0.95106E 00	0.95510E 00	0.23035E-01	98
26	0.78540E 01	0.10000E 01	0.10044E 01	0.25543E-01	95
27	0.81681E 01	0.95106E 00	0.95592E 00	0.27830E-01	91
28	0.84823E 01	0.80902E 00	0.81342E 00	0.28804E-01	86
29	0.87965E 01	0.58779E 00	0.59130E 00	0.28368E-01	81
30	0.91106E 01	0.30902E 00	0.31115E 00	0.27043E-01	75
31	0.94248E 01	-0.23772E-07	0.49016E-03	0.25140E-01	69
32	0.97389E 01	-0.30902E 00	-0.31027E 00	0.24012E-01	63
33	0.10053E 02	-0.58779E 00	-0.59043E 00	0.24372E-01	56
34	0.10367E 02	-0.80902E 00	-0.81314E 00	0.27474E-01	49
35	0.10681E 02	-0.95106E 00	-0.95695E 00	0.32649E-01	42
36	0.10996E 02	-0.10000E 01	-0.10087E 01	0.38693E-01	34
37	0.11310E 02	-0.95106E 00	-0.96292E 00	0.44194E-01	26
38	0.11624E 02	-0.80902E 00	-0.82822E 00	0.45750E-01	17
39	0.11938E 02	-0.58779E 00	-0.61725E 00	0.44537E-01	8
40	0.12252E 02	-0.30902E 00	0.0	0.0	0

Table XXII. (continued)

N	YPMEN	YPSTD	NYP	YPPMEN	YPPSTD	NYPP
1	0.0	0.0	0	0.0	0.0	0
2	0.9564E 00	0.9875E-02	8	-0.3412E 00	0.1534E 00	7
3	0.8044E 00	0.2357E-01	16	-0.6182E 00	0.1187E 00	14
4	0.5790E 00	0.2618E-01	24	-0.8321E 00	0.9997E-01	21
5	0.3013E 00	0.1993E-01	32	-0.9642E 00	0.8981E-01	28
6	-0.3019E-02	0.1760E-01	40	-0.1004E 01	0.8022E-01	35
7	-0.3085E 00	0.2008E-01	47	-0.9495E 00	0.6735E-01	42
8	-0.5845E 00	0.2329E-01	54	-0.8076E 00	0.5847E-01	49
9	-0.8050E 00	0.2500E-01	61	-0.5922E 00	0.7263E-01	56
10	-0.9466E 00	0.2595E-01	67	-0.3126E 00	0.6730E-01	62
11	-0.9959E 00	0.2573E-01	73	-0.2395E-02	0.6285E-01	68
12	-0.9476E 00	0.2420E-01	79	0.3096E 00	0.6213E-01	74
13	-0.8064E 00	0.2178E-01	84	0.5903E 00	0.6267E-01	79
14	-0.5861E 00	0.1877E-01	89	0.8139E 00	0.6353E-01	84
15	-0.3080E 00	0.1620E-01	93	0.9580E 00	0.6445E-01	88
16	0.4770E-03	0.1505E-01	96	0.1008E 01	0.6371E-01	91
17	0.3092E 00	0.1602E-01	99	0.9586E 00	0.6193E-01	94
18	0.5876E 00	0.1808E-01	101	0.8147E 00	0.6142E-01	96
19	0.8087E 00	0.2046E-01	102	0.5921E 00	0.5926E-01	97
20	0.9508E 00	0.2222E-01	103	0.3115E 00	0.5732E-01	98
21	0.9999E 00	0.2303E-01	103	0.1394E-02	0.5649E-01	98
22	0.9514E 00	0.2282E-01	102	-0.3097E 00	0.5768E-01	97
23	0.8099E 00	0.2162E-01	101	-0.5902E 00	0.5971E-01	96
24	0.5895E 00	0.2015E-01	99	-0.8136E 00	0.6096E-01	94
25	0.3113E 00	0.1914E-01	96	-0.9566E 00	0.6350E-01	91
26	0.3022E-02	0.1938E-01	93	-0.1006E 01	0.6525E-01	88
27	-0.3052E 00	0.2124E-01	89	-0.9558E 00	0.6591E-01	84
28	-0.5834E 00	0.2376E-01	84	-0.8123E 00	0.6559E-01	79
29	-0.8043E 00	0.2623E-01	79	-0.5898E 00	0.6462E-01	74
30	-0.9465E 00	0.2834E-01	73	-0.3077E 00	0.6207E-01	68
31	-0.9958E 00	0.2941E-01	67	0.2252E-02	0.6567E-01	62
32	-0.9481E 00	0.2948E-01	61	0.3114E 00	0.7077E-01	56
33	-0.8078E 00	0.2892E-01	54	0.5831E 00	0.5516E-01	49
34	-0.5906E 00	0.2654E-01	47	0.8023E 00	0.6062E-01	42
35	-0.3168E 00	0.2317E-01	40	0.9483E 00	0.7352E-01	35
36	-0.1395E-01	0.2244E-01	32	0.1006E 01	0.8454E-01	28
37	0.2915E 00	0.2659E-01	24	0.9699E 00	0.9656E-01	21
38	0.5718E 00	0.2831E-01	16	0.8403E 00	0.1190E 00	14
39	0.8008E 00	0.2566E-01	8	0.6282E 00	0.1605E 00	7
40	0.0	0.0	0	0.0	0.0	0

graphical data, the smallest digitizing increment is not necessarily the best. If the increment is too small relative to the precision of the input data, poor results are obtained. As yet, it has not been possible to develop a quantitative technique of identifying when this occurs. However, it has been found that a study of the results obtained with several digitizing increments, coupled with a general knowledge of the behavior of the quantity being determined (i.e., the derivative) permits good results to be obtained. The reader is referred to the previous contract report for a more detailed discussion of this.

UNCLASSIFIED
Security Classification

DOCUMENT CONTROL DATA - R & D

(Security classification of title, body of abstract and indexing annotation must be entered when the overall report is classified)

1. ORIGINATING ACTIVITY *(Corporate author)*
Department of Mechanical Engineering
The University of New Mexico

2a. REPORT SECURITY CLASSIFICATION
UNCLASSIFIED

2b. GROUP
NA

3. REPORT TITLE
Development of Measuring Techniques for Rocket Sleds

4. DESCRIPTIVE NOTES *(Type of report and inclusive dates)*
Final Report, December 1966 - October 1969

5. AUTHOR(S) *(First name, middle initial, last name)*
William E. Baker
John C. Gustafson

6. REPORT DATE
April 1970

7a. TOTAL NO. OF PAGES
171

7b. NO. OF REFS

8a. CONTRACT OR GRANT NO. AF29600-67-C-0017

b. PROJECT NO. 6876

c. Task 687655

d.

9a. ORIGINATOR'S REPORT NUMBER(S)
EE-166(69) HAFB-023

9b. OTHER REPORT NO(S) *(Any other numbers that may be assigned this report)*
MDC-TR-70-11

10. DISTRIBUTION STATEMENT
Distribution of this document is unlimited.

11. SUPPLEMENTARY NOTES
NA

12. SPONSORING MILITARY ACTIVITY
Air Force Missile Development Center
Air Force Systems Command
Holloman AFB, New Mexico

13. ABSTRACT

Work is described which was undertaken to develop and improve techniques for measuring forces acting on rocket sleds. Several specific projects have been completed. The Chaparral sled was instrumented and appropriate calibration made for measurement of vertical forces acting on the sled by the slipper. Resistance thermometers were also applied for measurement of temperature in the vicinity of the gage. A study of the accuracy of the Tech-2 sled transducer was made, and revised instrumentation applied in order to improve the accuracy. A force measuring system utilizing strain gages was developed for the modular monorail force transducer. Analytical studies of the response of a simple strain-gaged force link were made in order to better understand the behavior of the sled transducers under dynamic loading. The last area of work described is that of a highly accurate technique of differentiating analog data.

DD FORM NOV 65 1473

UNCLASSIFIED
Security Classification